

**FABRICATION OF CARBONNANOMATERIAL-
POLYMER COMPOSITE MICROELECTRODES FOR
ELECTROCHEMICAL SENSORS**

**A Thesis Submitted to
the Graduate School of
İzmir Institute of Technology
in Partial Fulfillment of the Requirements for the Degree of**

DOCTOR OF PHILOSOPHY

in Chemistry

**by
Ahmet ÖNDER**

**September 2024
İZMİR**

We approve the thesis of **Ahmet ÖNDER**

Examining Committee Members:

Assoc. Prof. Ümit Hakan YILDIZ

Department of Chemistry, İzmir Institute of Technology

Assoc. Prof. Engin KARABUDAK

Department of Chemistry, İzmir Institute of Technology

Assoc. Prof. Ümit TAYFUN

Department of Basic Sciences, Bartın University

Prof. Elif IŞGIN

Department of Chemistry, Dokuz Eylül University

Assist. Prof. Onur BÜYÜKÇAKIR

Department of Chemistry, İzmir Institute of Technology

20 September 2024

Assoc. Prof. Ümit Hakan YILDIZ

Supervisor, Department of Chemistry

İzmir Institute of Technology

Prof. Gülşah ŞANLI MOHAMED

Head of the Department of Chemistry

Prof. Mehtap EANES

Dean of the Graduate School

ABBREVIATIONS

CNT	Carbon Nanotubes
CVD	Chemical Vapor Deposition
DI	Distilled deionized
DOP	Diocetyl phthalate
DOS	Bis(2-ethylhexyl) sebecate
FIA	Flow-Injection Analysis
GF	Glass Fibers
ISE	Ion Selective Electrodes
ISME	Ion Selective Microelectrodes
IUPAC	International Union of Pure and Applied Chemistry
LOD	Limit of Detection
LRR	Linear Response Range
NMR	Nuclear Magnetic Resonance Spectroscopy
o-NPOE	o-Nitrophenyl octyl ether
PGE	Pencil Graphite Electrode
PPy	Polypyrrole
PVC	Polyvinyl chloride
RACNT	Radially Aligned Carbon Nanotubes
sccm	Standard cubic centimeters per minute
SEM	Scanning Electron Microscope
SPE	Screen Printed Electrodes
TDANO ₃	Tetradecylammonium nitrate
TDMAN	Tridodecylmethylammonium nitrate
THF	Tetrahydrofuran

ACKNOWLEDGEMENTS

I would like to thank my esteemed advisor, Assoc. Prof. Ümit Hakan YILDIZ, for his support at every moment of my work and for his great contributions to the subject of this research, directing the experimental studies, evaluating the results and writing them up.

I would like to thank Asst. Prof. Onur BÜYÜKÇAKIR and his research group and Dr. Alagappan Palaniappan for their great contributions to my experimental studies and writing stages.

I would like to thank the members of my study group Biomacros and Dr. Erman KIBRIS not only for this thesis but also for everything.

I feel it is my duty to express my gratitude and appreciation to my family, who have played a significant role in helping me reach this point and have always supported me in every moment of my life.

I am deeply and forever grateful to my life partner, Senanur ÖNDER, for her love, support, and encouragement throughout my life.

ABSTRACT

FABRICATION OF CARBONNANOMATERIAL-POLYMER COMPOSITE MICROELECTRODES FOR ELECTROCHEMICAL SENSORS

The detection of ions in low-volume samples presents significant challenges due to their small size, high mobility, and rapid diffusion. Potentiometric ion-selective electrodes (ISEs) have emerged as a reliable method for ion detection due to their cost-effectiveness, ease of use, and potential for miniaturization, making them suitable for microfluidic applications. In the first part of thesis, describes the fabrication of microelectrodes (r-ISE) using radially aligned carbon nanotubes (RACNT) grown on glass fibers (GF) via chemical vapor deposition as solid contact materials. The r-ISE fabricated with RACNT-GF as an interface material exhibited a limit of detection (LOD) of 7.5×10^{-6} M and a linear response range from 1.0×10^{-5} to 1.0×10^{-1} M. The use of RACNT-GF significantly improved the LOD, and detection selectivity compared to conventional solid-contact materials like graphite. The high surface area and mechanical durability of RACNT-GF enhanced the electrode's performance, providing stable and repeatable potentiometric responses even in confined microfluidic environments., In the second part of the thesis explores a systematic approach to a molecular cage as a synthetic ionophore for nitrate ions. By varying the molecular structure and therefore size of cage molecules, aimed to adjust the interaction between host-cage molecules and the guest- NO_3^- ions. Six synthetic molecular cage ionophores were evaluated for their nitrate-selective binding capabilities. The optimized CAGE ionophore-based ISE demonstrated a linear response from 1.0×10^{-5} to 1.0×10^{-1} M, with a high coefficient of determination ($R^2 = 0.9971$), a slope of -53.1 ± 1.4 mV/decade and LOD of 7.5×10^{-6} M for nitrate detection. In the last part of the thesis, the effect of droplet evaporation on the sensitivity in ion detection by screen printed electrode is explored. The results revealed that ion concentration lower than 1.0×10^{-5} M does not yield linear response and droplet evaporation methods is not preferable.

ÖZET

ELEKTROKİMYASAL SENSÖRLER İÇİN KARBONNANOMALZEME-POLİMER KOMPOZİT MİKROELEKTROTLARIN ÜRETİMİ

Düşük hacimli numunelerde iyonların tespiti, küçük boyutları, yüksek hareketlilikleri ve hızlı difüzyonları nedeniyle önemli zorluklar sunar. Potansiyometrik iyon seçici elektrotlar (ISE'ler), maliyet etkinlikleri, kullanım kolaylıkları ve minyatürleştirme potansiyelleri nedeniyle iyon tespiti için güvenilir bir yöntem olarak ortaya çıkmıştır ve bu da onları mikroakışkan uygulamalar için uygun hale getirmiştir. Tezin ilk bölümünde, katı kontak malzemeleri olarak kimyasal buhar biriktirme yoluyla doğrudan cam elyafı (GF) üzerinde büyütülen radyal olarak hizalanmış karbon nanotüpler (RACNT) kullanılarak mikroeletrotların (r-ISE) üretimi açıklanmaktadır. Bir arayüz malzemesi olarak RACNT-GF ile üretilen r-ISE, 7.5×10^{-6} M'lik bir tayin limiti (LOD) ve 1.0×10^{-6} ila 1.0×10^{-1} M arasında doğrusal bir yanıt sergilemiştir. RACNT-GF kullanımı, grafit gibi geleneksel katı kontak malzemelere kıyasla LOD'yi ve seçiciliği önemli ölçüde iyileştirmiştir. RACNT-GF'nin yüksek yüzey alanı ve mekanik dayanıklılığı, elektrotun performansını artırmış ve sınırlı mikroakışkan ortamlarda bile kararlı ve tekrarlanabilir potansiyometrik tepkiler sağlamıştır. Tezin ikinci bölümünde, nitrat iyonları için sentetik bir iyonofor olarak moleküler kafese sistematik bir yaklaşım araştırılmaktadır. Kafes moleküllerinin moleküler yapısını ve dolayısıyla boyutlarını değiştirerek, konak-kafes molekülleri ile misafir- NO_3^- iyonları arasındaki etkileşimi ayarlamayı amaçlamıştır. Altı sentetik moleküler kafes iyonoforu, nitrat seçici bağlanma yetenekleri açısından değerlendirilmiştir. Optimize edilmiş KAFES iyonoforuna dayalı ISE, yüksek bir belirleme katsayısı ($R^2 = 0.9971$), -53.1 ± 1.4 mV/on kat ve nitrat tespiti için 7.5×10^{-6} M LOD ile 1.0×10^{-5} ila 1.0×10^{-1} M arasında doğrusal bir yanıt göstermiştir. Tezin son bölümünde, yüzey baskılı elektrot ile iyon tespitinde damla buharlaşmasının duyarlılığa etkisi incelenmiştir. Sonuçlar, 1.0×10^{-5} M'den düşük iyon konsantrasyonlarının doğrusal yanıt vermediğini ve damla buharlaşma yönteminin tercih edilmediğini ortaya koymuştur.

TABLE OF CONTENTS

LIST OF FIGURES	ix
LIST OF TABLES	xii
CHAPTER 1 INTRODUCTION	1
CHAPTER 2 FOUNDATION	7
2.1. Potentiometry	7
2.2. Determination Principle in Potentiometric Methods	7
2.3. Reference Electrodes.....	9
2.4. Solid-Contact Ion Selective Electrodes.....	9
2.4.1. Conducting Polymers as Solid-Contacts.....	10
2.4.2. Carbon Materials as Solid-Contacts	12
2.4.3. Other Materials as Solid-Contacts	15
2.5. Sensor Materials.....	18
2.5.1. Membrane Materials	19
2.5.2. Ion-Exchange Membranes	21
2.5.3. Ionic Liquids	23
2.5.4. Molecular Imprinted Polymers	24
2.5.5. Ionophores	24
2.6. Miniaturized Ion-Selective Electrodes.....	25
CHAPTER 3 MATERIALS AND METHODS	29
3.1. Materials	29
3.2. Potentiometric Measurements.....	29
3.3. Fabrication of Electrodes	30
3.3.1. RACNT-GF Composite ISE	30
3.3.2. CAGE Incorporated ISE	32
3.4. Flow-Injection Set-Up and Fabrication of Microfluidic Cell	32
3.5. Growth of CNT on GF	34
3.6. Synthesis of Cage-based Ionophores	35

CHAPTER 4 RESULTS AND DISCUSSION.....	36
4.1. Morphological Characterization of r-ISE	37
4.2. Determination of Optimal Membrane Composition	38
4.2.1. Investigation of Plasticizer Effect.....	39
4.2.2. Investigation of The Percentage of Ionophores	40
4.2.3. Investigation of Polymer (PVC) Membrane Modification	42
4.3. Potentiometric Performance Characteristics of r-ISE.....	44
4.3.1. Forming the r-ISE Calibration Curve: Determining Slope, LOD, and LRR.....	45
4.3.2. Determination of r-ISE Selectivity	46
4.4. Comparison of r-ISE with Pencil Graphite Electrode.....	47
4.5. Comparison of the lifetime of r-ISE with PGE.....	49
4.6. Determination of ISME Assay Performance	51
4.7. Synthesis and Analysis of Cage-based Ionophores	53
4.8. Morphological Characterization of CAGE Incorporated ISE.....	54
4.9. Determination of Optimal CAGE and Composition.....	55
4.10. Potentiometric Performance Characteristics of CAGE Incorporated ISE	58
4.10.1. Forming the CAGE Incorporated ISE Calibration Curve: Determining Slope, LOD, and LRR.....	59
4.10.2. Determination of the Repeatability of CAGE Incorporated ISE.....	61
4.10.3. Determination of the Response Time of CAGE Incorporated ISE.....	62
4.10.4. Determination of the pH Range of CAGE Incorporated ISE ...	63
4.10.5. Determination of CAGE Incorporated ISE Selectivity.....	64
4.11. Morphological Characterization of NH ₄ ⁺ -SPE	67
4.12. Forming the NH ₄ ⁺ -SPE Calibration Curve: Determining Slope, LOD, and LRR.....	68
4.13. Improving the Detection Limit of the NH ₄ ⁺ -SPE	70
CHAPTER 5 CONCLUSION	74
REFERENCES	76

LIST OF FIGURES

<u>Figure</u>	<u>Page</u>
Figure 3.1 The RACNT dip-coated with an Fe catalyst (A). (B) illustrates an individual GF fiber displaying uniform RACNT growth. For the construction of the r-ISE, the radially oriented GF-CNT was attached to a copper wire (C) and then covered with an insulating material	30
Figure 3.2 The schematic illustrations of radial alignment of CNT on GF in PVC-COOH membrane incorporating nonactin for selective NH_4^+ detection.	31
Figure 3.3 Fabrication Steps of CAGE Incorporated ISE	32
Figure 3.4 Construction of microfluidic cell.....	33
Figure 3.5 Flow injection set-up.....	33
Figure 3.6 Preparation and CNT Growth on 10 cm x 10 cm GF Fabric: (A) Initial GF Fabric, (B) Dip-Coated with Fe Catalyst, (C) resulting CNT growth.....	34
Figure 3.7 Synthesis pathways of cage compound half-CAGE-1	35
Figure 3.8 Synthesis pathways of cage compound CAGE-1	35
Figure 4.1 GF with CNTs grown using Fe catalyst ratios of 1:2 (A) and 1:10 (C). Optical microscopy image of an individual GF Fiber post-CNT growth (B), and SEM image of a single GF filament post-CNT growth displaying radial CNT alignment (D).	38
Figure 4.2 Potentiometric response of r-ISE prepared with different plasticizers.....	40
Figure 4.3 Potentiometric response of PVC r-ISE prepared with different ionophore percentage	41
Figure 4.4 Potentiometric response of PVCCOOH r-ISE prepared with different ionophore percentage	42
Figure 4.5 Potentiometric Sensing mechanism of r-ISE.....	43
Figure 4.6 Potentiometric response of r-ISE in ammonium solutions at various concentrations	45
Figure 4.7 Linear calibration plot for NH_4^+ detection	46
Figure 4.8 Potentiometric response of r-ISE for varying concentrations of cations.....	48
Figure 4.9 Potentiometric response of pencil graphite electrode for varying concentrations of cations.....	48

<u>Figure</u>	<u>Page</u>
Figure 4.10 Change in the slope of the ammonium-selective electrodes with time	49
Figure 4.11 Change in the slope of the ammonium-selective electrodes with time (day)	50
Figure 4.12 Potentiometric response of r-ISE in the FIA system.....	51
Figure 4.13 Calibration curve of r-ISE in the FIA system.....	52
Figure 4.14 ¹ H NMR spectra of half-CAGE-1(A), ¹ H NMR spectra of CAGE-1 (B), and FT-IR spectra of cage molecules(C).	53
Figure 4.15 SEM Images of Electrodes Pre- (A) and Post- (B) CAGE Incorporation...	54
Figure 4.16 Potentiometric response of CAGE-incorporated-ISE in nitrate solutions at various concentrations.....	59
Figure 4.17 Linear calibration plot for NO ₃ ⁻ detection.....	60
Figure 4.18 Repeatability of the CAGE-incorporated ISE a:1.0×10 ⁻³ M; b:1.0×10 ⁻² M; c:1.0×10 ⁻¹ M NO ₃ ⁻ (pH:7.0).....	61
Figure 4.19 Response time of the CAGE-incorporated ISE.....	62
Figure 4.20 Variation in the response of the nitrate-selective electrode with pH: (a) 1.0×10 ⁻³ M nitrate solution, (b) 1.0×10 ⁻² M nitrate solution.....	63
Figure 4.21 Potentiometric responses of NO ₃ ⁻ selective electrode CAGE incorporated ISE for varying concentrations of anions.....	65
Figure 4.22 Potentiometric responses of cage-free electrode for varying concentrations of anions.....	66
Figure 4.23 Screen-Printed Carbon Electrodes (A), SEM images of Screen-Printed Carbon Electrodes (B), 2x magnification (C).	67
Figure 4.24 PVC coated Screen-Printed Carbon Electrodes (E), SEM images of PVC coated Screen-Printed Carbon Electrodes (F), both conditions (bare and coated) (G).	68
Figure 4.25 Potentiometric response of SPE in water and ammonium solutions at various concentrations.....	69
Figure 4.26 Linear calibration plot of SPE for NH ₄ ⁺ detection	70
Figure 4.27 Contact angle measurements during evaporation at four different times(Source: De Angelis et al. 2011).	71

<u>Figure</u>	<u>Page</u>
Figure 4.28 Photographs of the Screen-Printed Carbon Electrodes (A), SPE with a reservoir that can hold a drop of 200 μL volume (B and C), and with a sample solution drop (D).	72
Figure 4.29 Potentiometric response of NH_4^+ -SPE until drop evaporated	73

LIST OF TABLES

<u>Table</u>	<u>Page</u>
Table 4.1 Potentiometric Performance Characteristics of r-ISEs Prepared with Various Plasticizers.....	39
Table 4.2 Impact of Ionophore Concentration on the Potentiometric Performance Characteristics of r-ISE with PVC membrane	40
Table 4.3 Impact of Ionophore Concentration on the Potentiometric Performance Characteristics of r-ISE with PVCCOOH membrane.....	41
Table 4.4 Selectivity coefficients of ammonium-selective r-ISE to various cationic species calculated using the separate solution method	47
Table 4.5 Impact of CAGE structure on the potentiometric performance characteristics of NO ₃ ⁻ selective electrodes	55
Table 4.6 Impact of coating cycle on the potentiometric performance characteristics of NO ₃ ⁻ selective electrodes	57
Table 4.7 Selectivity coefficients of nitrate-selective CAGE incorporated ISE to various anionic species calculated using the separate solution method.....	65

CHAPTER 1

INTRODUCTION

In recent years, there has been a growing emphasis on mitigating environmental pollutants, prompting increased attention towards the development and deployment of user-friendly sensor technologies tailored for detecting various ions in environmental settings.(E. Wang et al. 1997; Willner and Vikesland 2018) Ions play a critical role in numerous environmental and biological processes, highlighting their significance in applications such as wastewater treatment, agriculture, and water quality analysis. Accurate ion detection is crucial in these fields to manage resources effectively, sustain agricultural yields, and protect water supplies. The analysis of ions in environmental samples is essential for assessing pollution levels and the eutrophication status of natural water bodies. Precise ion measurements are indispensable for maintaining environmental integrity and public health, serving as reliable indicators of natural water purity and enzymatic byproducts essential to physiological functions. (Sadik and Wallace 1994; María Cuartero et al. 2020)

Nitrogen is a fundamental element crucial for the growth and reproduction of all living organisms and serves as a primary mineral nutrient essential for crop cultivation.(Cui et al. 2020; Karimi and Moradi 2018; C.-W. Liu et al. 2014) The supplementation of nitrogen in soil is essential to achieve high grain yields and sustain the production of food, feed, and fiber.(Colaço and Molin 2017; Hyusein and Tsakova 2023) Effective management of agricultural productivity depends on precise fertilizer application, including considerations of timing, location, quantity, and methods.(Dinnes et al. 2002) Elevated nitrate levels can lead to significant environmental issues such as groundwater contamination(Y. Li et al. 2018), soil acidification(Borrelli et al. 2016), and water eutrophication.(Cui et al. 2020) Consequently, there is an increasing demand for rapid, cost-effective, and real-time measurement of nitrate concentrations in both water and soil samples.

The monitoring of ammonium ion concentration has garnered significant interest among researchers across diverse disciplines due to its critical roles in environmental and biomedical contexts. Ammonium serves as a key parameter in assessing natural

water quality and acts as a potential biomarker indicating enzymatic byproducts essential to vital physiological processes. Its presence is widely acknowledged as a marker for water quality in natural ecosystems and as a biomarker reflecting enzymatic activity in fundamental biochemical reactions.(María Cuartero et al. 2020)

The main analytical techniques used for ion assays include spectroscopic measurements, capillary electrophoresis, and chromatographic analyses combined with mass spectrometry methods like HPLC and GC-MS.(Gallardo-Gonzalez et al. 2019; Alahi and Mukhopadhyay 2018; Akyüz and Ata 2009; Zuo, Wang, and Van 2006; Niedzielski, Kurzyca, and Siepak 2006) Although these methods offer excellent selectivity and sensitivity, they are limited by high costs and lengthy assay times. Moreover, these advanced instruments are often impractical for real-time or on-site analyses, emphasizing the necessity for developing assays that are user-friendly, affordable, and capable of delivering quick results. In this regard, considerable research has been directed towards creating potentiometric ion-selective electrodes (ISEs), due to their promising potential for miniaturization. Potentiometric ion-selective electrodes are widely used for measuring ion concentrations in various samples, providing a broad measurement range for both positively and negatively charged ions. Compared to traditional ISEs that use internal electrolytes, potentiometric solid contact ISEs offer several advantages, including ease of use, compactness, portability, quick response, and cost-effective production. These solid contact electrodes are typically made from polymer materials like epoxy and incorporate conducting substances such as graphite, macroporous carbon, spherical carbon, C60 fullerenes, carbon nanotubes (CNTs), carbon fiber, and highly ordered pyrolytic graphite.(Suriyaprakash et al. 2022; Takahashi et al. 2015; Faraji and Mohammadzadeh Aydisheh 2019; Xiong et al. 2017; Gallardo-Gonzalez et al. 2019) The conducting material ensures electrical contact between the sample solutions and the ISE's transduction elements, while the polymer materials provide durability.(Jiang et al. 2019; Ping et al. 2011; Crespo, Macho, and Rius 2008; Bomar, Owens, and Murray 2017; Onder, Topcu, and Coldur 2018; Topcu et al. 2018; Anupriya et al. 2022) Therefore, the performance of potentiometric ISEs is largely determined by the morphological and electrical properties of both the polymer and conducting materials used in their construction.

Among the various conducting materials assessed for ISE fabrication, carbon nanotubes stand out due to their high aspect ratio, large surface area, exceptional electrical conductivity, and thermal and electrochemical stability.(Dubey et al. 2021a)

These properties make CNTs highly attractive for use as solid contact materials in electrochemistry. CNTs have been widely reported to enhance the performance of various electrochemical devices, such as sensors, supercapacitors, fuel cells, lithium-ion batteries, and electrocatalysis. In the context of ISEs, CNTs facilitate modification and improve assay selectivity and sensitivity. (Lyu et al. 2020; Shao, Ying, and Ping 2020; Jordan et al. 2021) With respect to electrochemical assays, CNT possesses the potential to provide a stable and efficient ion-to-electron transduction interface while facilitating the charge transfer, owing to their high surface area. In this context, glass fiber (GF), a material that is robust and cohering of defined micron-sized GF filaments, could further improve the surface area for the deposition of CNT, potentially enabling the combination of GF and CNT to be an ideal composite for the fabrication of sensitive ISE. In the initial part of this thesis, CNTs are directly grown on GF using a chemical vapor deposition (CVD) method and assessed as an interface material for potentiometric ISE fabrication. This fabrication process results in a composite with CNTs radially aligned on individual GF filaments. The adopted fabrication protocol produced a composite with CNTs aligned radially on individual GF filaments. This configuration, combining the radial alignment of CNTs and the fibrous structure of GF, provides a high surface area, maximizing the accommodation of the PVC-based membrane, improving electrical contact, enhancing stability, and increasing durability.

The specificity and sensitivity of the RACNT-GF composite ion-selective electrode (r-ISE) were confirmed through the detection of ammonium ions (NH_4^+), a key target in ion assays. This was accomplished by incorporating RACNT with an NH_4^+ -selective nonactin ionophore within bis(2-ethylhexyl) sebacate (DOS) plasticized polyvinyl chloride (PVC) membranes. The steady-state potentiometric NH_4^+ assay responses using the nonactin-functionalized r-ISE showed a slope of 58.2 ± 0.6 mV/decade, a detection limit (LOD) of 7.5×10^{-6} M, and a linear response range (LRR) of 1.0×10^{-5} to 1.0×10^{-1} M. These findings illustrate the r-ISE's capability for selective and sensitive NH_4^+ detection. Control experiments using graphite instead of RACNT exhibited a one order of magnitude reduction in sensitivity and a less steep slope in the potentiometric response, highlighting that the high surface area of the RACNT-GF composite, due to the radial alignment of CNTs and the fibrous structure of GF, greatly enhances assay performance. Additionally, the use of r-ISE as an ion-selective microelectrode (ISME) was explored by conducting the assay in a microfluidic cell. The

ISME's compatibility with standard microfabrication techniques allows for the creation of low-cost, disposable sensors suitable for resource-limited environments, with applications in water quality monitoring, disease diagnosis, and agricultural soil health assessment. The potential for miniaturization and integration with handheld and smartphone-based devices could further increase the practicality and accessibility of the developed r-ISE/ISME. (A. Zhao et al. 2022; Y. Zhang et al. 2018; Hu et al. 2014; Xu et al. 2022; Triroj et al. 2020; Salve et al. 2022)

In the second part of this thesis, the use of a molecular cage as an ionophore for nitrate ions is explored. A key component of ion-selective electrodes is the ionophore, which allows for the selective and precise measurement of specific ions in a solution. Ionophores are organic molecules that specialize in selectively binding to specific ions and aiding their movement through the electrode membrane. The ionophores commonly used in the fabrication of solid-contact ion-selective electrodes for nitrate detection include TDMAN (tridodecylmethylammonium nitrate) (Thuy et al. 2022; Hjort et al. 2022; Paré et al. 2023), polypyrrole (PPy) doped with NO_3^- ions (L. Zhang, Wei, and Liu 2020; Fozia et al. 2023), Nitrate Ionophore VI (Fan et al. 2020; Yueling Liu et al. 2020; Baumbauer et al. 2022), cobalt(II) complex with 4,7-diphenyl-1,10-phenanthroline (Pietrzak, Wardak, and Łyszczek 2020), and TDANO3 (tetradecylammonium nitrate). (Kim et al. 2021) Specifically, the commercial nitrate ionophore VI demonstrates outstanding selectivity and reproducibility for nitrate measurement. However, many ionophores are derived from natural sources such as certain plants or microorganisms. These methods involve time-consuming and expensive processes for extraction, purification, and characterization.

Over the past few decades, organic molecular cages have attracted significant attention due to their unique structural characteristics, including inherent voids that can be tailored in terms of size and functionality. This adaptability makes them ideal for numerous applications such as gas sorption (Tian et al. 2022; Buyukcakir, Seo, and Coskun 2015), separation (M. Liu et al. 2019), sensing (Song et al. 2016), and catalysis (Bhandari and Mukherjee 2023). The precise customization of their internal cavities has allowed these molecules to serve as hosts for the selective recognition of specific molecules and ions. (Yun Liu et al. 2019; Kang et al. 2010; Jiao et al. 2017; Hasell et al. 2016)

Research into anion recognition via host-guest interactions has long been a focal point in supramolecular chemistry due to its significance in environmental and

biological contexts.(Evans and Beer 2014; Chen et al. 2020; Langton, Serpell, and Beer 2016) Organic cage compounds have shown considerable promise in this area, thanks to their high association constants (K_a) and selectivity, leading to substantial advancements in anion recognition. For instance, in 2021, Xie et al.(Xie et al. 2021) reported the synthesis of a hexapodal cage compound and studied its complexation with anions. Their results indicated that the hexapodal cage compound had a notable affinity for sulfate (SO_4^{2-}) and hydrogen phosphate (HPO_4^{2-}) anions over halides and carbonate (CO_3^{2-}) ions. The following year, Lauer et al.(Lauer et al. 2022) introduced a cage compound structurally similar to one previously published by Bisson and colleagues (Bisson et al. 1997a). Precise modifications to the cage structure for nitrate encapsulation have enhanced the strengths of hydrogen bonding and π -stacking interactions between the host and guest, significantly improving nitrate selectivity compared to chloride (Cl^-) and hydrogen sulfate (HSO_4^-) anions. The recognition studies involving cage structures primarily focus on secondary interactions, such as hydrogen bonding and π -stacking. However, recent research has also identified anion- π interactions as a viable non-covalent attractive force between neutral electron-deficient aromatic units and negatively charged ions.(D.-X. Wang and Wang 2020; Bisson et al. 1997b) For instance, Wang et al. examined interactions between halides and a structurally stable D_{3h} symmetric cage molecule known as "bis(tetraoxacalix[2]arene[2]triazine)," which features three V-shaped clefts with electron-deficient triazine rings.(D. Wang et al. 2010) This study notably demonstrated clear anion- π interactions between sulfonates and the electron-deficient triazine rings. The study notably demonstrated clear anion- π interactions between sulfonates and the electron-deficient triazine rings. Several other studies have utilized the same cage molecule as a platform for anion- π interactions in specific applications, such as anion- π catalysis(Luo et al. 2021b; 2021a), Perrhenate removal from aqueous solutions(Qin et al. 2023), and the formation of anion- π directed self-assemblies(X.-Y. Wang et al. 2019), highlighting the cage's versatility in anion- π motifs. Despite considerable advancements in understanding cage-based ion capture and recognition, examples of organic cage molecules in potentiometric ion sensing are scarce in the literature.(L. Li et al. 2022) To our knowledge, such cage compounds have not been previously used as ionophores in potentiometric sensors for the selective detection of nitrate in aqueous environments.

In the second part of this thesis, molecular cages were comprehensively investigated as selective ionophores for nitrate in potentiometric ion-selective electrodes. By fine-tuning the size and electronic structure of the cage molecules, we enhanced nitrate selectivity over other anions in aqueous analytes. The electrode (E4) prepared using CAGE-1 exhibited a linear response for NO_3^- ions within the concentration range of 1.0×10^{-5} to 1.0×10^{-1} M, with a high coefficient of determination ($R^2 = 0.9971$) and a slope of -53.1 ± 1.4 mV dec⁻¹. The calculated limit of detection for the NO_3^- selective electrode was determined to be 7.5×10^{-6} M. This study demonstrates the potential of cage molecules as ionophores for detecting nitrate ions in aqueous environments and offers new insights for the development of potentiometric ion-selective electrodes.

CHAPTER 2

FOUNDATION

2.1. Potentiometry

Potentiometry is a widely employed analytical technique in chemical analysis. This method involves measuring the voltage difference between two electrodes while ensuring that the electric current between them is maintained under a nearly zero-current condition. In the most prevalent forms of potentiometry, the potential of an indicator electrode varies as a function of the analyte concentration, whereas the potential of a second reference electrode remains ideally constant. (Telting-Diaz and Qin 2006)

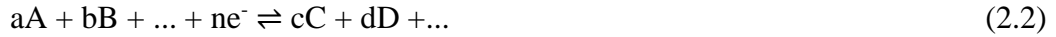
2.2. Determination Principle in Potentiometric Methods

The potential of an electrode is dependent on the activity of the ion or ions present in the solution it is immersed in. In a modern ion-selective electrode, the ion-selective membrane, internal standard solution, and the ions in the test solution are distinguished from one another. Simple ions, electrons, or charged or neutral complexes of the tested ion move towards the inner parts of the membrane in proportion to the composition of the internal standard solution. This movement results in the formation of an electrostatic potential (EMF) within the ion-selective electrode membrane. The resulting potential is calculated by combining the reference electrode half-cell with the membrane electrode half-cell.

$$E_{\text{cell}} = E_{\text{working electrode}} + E_{\text{reference electrode}} + E_{\text{liquid junction potential}} \quad (2.1)$$

In equation 2.1, the potential of the reference electrode is constant. In well-designed modern measurement systems, the liquid junction potential varies very slightly (a few mV), and this variation can be neglected. When the liquid junction potential is considered constant, the measured cell potential is directly related to the potential of the

working electrode. The relationship between concentration and electrode potential (E) is generally represented by the following reversible half-reaction:



Considering equation 2.2, the Nernst Equation can be expressed as:

$$E = E^0 - \frac{RT}{nF} \ln \frac{[C]^c [D]^d}{[A]^a [B]^b} \quad (2.3)$$

Where:

- E is the working electrode potential,
- E^0 is the standard electrode potential,
- R is the gas constant ($8.314 \text{ J}\cdot\text{mol}^{-1}\cdot\text{K}^{-1}$),
- T is the temperature in Kelvin (273.15 K for 0°C),
- F is the Faraday constant ($96486 \text{ J}\cdot\text{V}^{-1}$),
- $[A]$, $[B]$, $[C]$, and $[D]$ are the activities of the ions sensed by the electrode,
- a , b , c , and d are the stoichiometric coefficients of the species in the half-reaction,
- n is the number of electrons exchanged or the charge of the active ion in the membrane.

For a single ion activity, the equation is written as:

$$E = E^0 \pm \frac{RT}{nF} \ln a_i \quad (2.4)$$

In equation 2.4, the (\pm) sign represents (-) for anions and (+) for cations.

If the ion activity changes from a_1 to a_2 , the potential change is given by:

$$E = E^0 \pm \frac{RT}{nF} \ln \frac{a_2}{a_1} \quad (2.5)$$

According to the equation, the electrode response to an increase in ion activity in the solution is observed logarithmically:

$$E = E^0 \pm \frac{2,303RT}{nF} \log \frac{a_2}{a_1} \quad (2.6)$$

If measurements are taken at 25°C , substituting the constants transforms the Nernst Equation into:

$$E = E^0 \pm \frac{0,0592}{n} \log \frac{a_2}{a_1} \quad (2.7)$$

According to equation 2.7, the theoretical change in E-Log(a) relationship for every tenfold difference in activity at 25°C is $59.2/n$ mV for ions with charge n .

This change is generally positive for cations and negative for anions. According to the Nernst equation, the theoretical change for a tenfold difference in activity for singly, doubly, and triply charged ions is 59.2, 29.6, and 19.8 mV, respectively. (Bard 2001; Y. Umezawa, Umezawa, and Sato 1995; Bobacka, Ivaska, and Lewenstam 2008a; Hulanicki, Glab, and Ingman 1991a; "Noticeboard" 2006)

2.3. Reference Electrodes

In many electroanalytical applications, it is desirable for the potential of one of the electrodes to be known, constant, and unaffected by the composition of the surrounding solution. Electrodes that meet these criteria are called reference electrodes or standard electrodes. The electrode potential of these reference electrodes is precisely known. The potential of reference electrodes is independent of the solution in which they are used. Changes in the activity of the analyte or other ions present in the solution being studied do not affect the potential of the reference electrodes. The commonly used reference electrodes are calomel electrodes and silver/silver chloride electrodes. (Kharton and Tsipis 2013; Volkov and Markin 2002; Buck and Lindner 1994a)

2.4. Solid-Contact Ion Selective Electrodes

Solid contact ion-selective electrodes (SC-ISEs) represent a distinct class of ion-selective electrodes characterized by the utilization of a solid contact layer to facilitate ion-to-electron transduction between the ion-selective membrane and the electronic conductor. In contrast to conventional ion-selective electrodes, which typically depend on an internal liquid electrolyte, SC-ISEs present several advantages, including enhanced mechanical stability, reduced maintenance requirements, and greater potential for miniaturization. (Zdrachek and Bakker 2019; Bakker 2016) The solid contact layer plays a pivotal role in converting the ionic signal from the membrane into an electronic signal. Materials commonly employed for this layer encompass conducting polymers (such as polypyrrole and polyaniline), carbon nanotubes, and other nanomaterials known for their high conductivity and stability. The ion-to-electron transduction in SC-ISEs is achieved through capacitive or redox mechanisms facilitated by the solid contact layer. (Zdrachek and Bakker 2019; Bakker 2016) Upon interaction of the ion-selective

membrane with the target ions in the sample solution, a potential difference is generated across the membrane. This potential difference is subsequently transferred to the solid contact layer, which translates it into an electronic signal measurable by a potentiometer. This efficient transduction mechanism underpins the functionality and efficacy of SC-ISEs in various analytical applications.(Patel, Sharma, and Prasad 2008; Priego-López and Luque de Castro 2004; C. Zhao et al. 2008)

2.4.1. Conducting Polymers as Solid-Contacts

The conducting polymers poly(3,4-ethylenedioxythiophene) (PEDOT), polypyrrole, and poly(3-octylthiophene) (POT) are among the earliest solid-contact materials used in this field.(Zdrachek and Bakker 2019) The study by Guzinski et al. (2017) investigates the role of poly(3,4-ethylenedioxythiophene): polystyrenesulfonate (PEDOT(PSS)) as a solid contact (SC) material in ion-selective electrodes (ISEs). Specifically, the research focuses on how the thickness of the PEDOT(PSS) film affects the equilibration times of these electrodes.(Guzinski et al. 2017)

Jarvis et al. (2017) conducted a study to elucidate the differences in poly(3,4-ethylenedioxythiophene)-poly(styrenesulfonate) (PEDOT(PSS)) films when electrochemically deposited on gold (Au) and platinum (Pt) substrate electrodes. The research employed a Quartz Crystal Microbalance (QCM) to monitor the deposition process and analyze the characteristics of the resulting films. The research finding that the differences in film properties directly affected the equilibration times and standard potentials of solid-contact ion-selective electrodes (SC-ISEs) utilizing PEDOT(PSS).

The article by Pławińska, Michalska, and Maksymiuk (2016) addresses the optimization of the capacitance of conducting polymer solid contacts in ion-selective electrodes (ISEs). The primary goal is to enhance the analytical performance of ISEs, particularly under polarization conditions, by improving the stability and efficiency of ion-to-electron transduction through increased capacitance. The study emphasizes the importance of ion mobility within the polymer and membrane. (Pławińska, Michalska, and Maksymiuk 2016)

Ning He et al. (2017) aims to improve the potential reproducibility and stability of solid-contact ion-selective electrodes (SC-ISEs) by using pre-polarized hydrophobic conducting polymer films. The study utilized polypyrrole (PPy) doped with

perfluorooctanesulfonate (PFOS⁻) as the solid contact material. PFOS⁻ imparts hydrophobic properties to the polymer, helping prevent aqueous layer formation. K⁺-selective SC-ISEs were fabricated by depositing the ISM on pre-polarized PPy-PFOS films. The findings suggest that using pre-polarized hydrophobic conducting polymers as solid contacts can enhance the performance of SC-ISEs, making them more suitable for single-use and disposable applications in various analytical fields.(He et al. 2017)

The article by Jennifer M. Jarvis et al. (2016) investigates the use of poly(3-octylthiophene) (POT) as a solid contact material in ion-selective electrodes (ISEs), focusing on the contradictory performance characteristics reported in the literature. The authors aim to understand the sources of these contradictions and propose methods to enhance the potential stability and reproducibility of POT-based solid contact ISEs (SC-ISEs). POT films were deposited on gold (Au), platinum (Pt), and glassy carbon (GC) electrodes using drop-casting techniques. Some POT films were loaded with 7,7,8,8-tetracyanoquinodimethane (TCNQ) to create a redox-active layer. Potassium (K⁺)-selective membranes were coated over the POT or POT+TCNQ films to fabricate K⁺-selective SC-ISEs. The study suggests further exploration into incorporating salts like K⁺TCNQ⁻ into POT films to enhance the interfacial potential stability and overall performance of SC-ISEs.(Jarvis et al. 2016)

The study by Chenchen Liu et al. (2017) explores the development of a solid-contact lead(II) ion-selective electrode (Pb²⁺-ISE) using electrospun polyaniline (PANI) microfibers as the ion-to-electron transducer. The research aims to improve the potential stability, capacitance, and overall performance of solid-contact ISEs by utilizing a novel transducer material. The GC electrodes were coated with electrospun PANI/PMMA microfibers (s-PANI) and compared with drop-cast PANI/PMMA coatings (d-PANI). The Pb²⁺-selective membrane was then applied to the coated electrodes. The s-PANI electrodes showed a Nernstian slope of 28.4 mV/decade and a low detection limit of 6.31×10⁻¹⁰ M in the linear range of 10⁻⁹ to 10⁻³ M Pb(NO₃)₂. The response time for s-PANI electrodes was under 10 seconds, significantly faster than d-PANI and bare GC electrodes. The study demonstrates that electrospun PANI microfibers significantly enhance the performance of solid-contact Pb²⁺-ISEs by improving potential stability, capacitance, and response time. The elimination of the interfacial water layer and the high capacitance of the s-PANI transducer are key factors contributing to these improvements. The research suggests that the electrospinning technique can be

effectively used to develop advanced solid-contact ISEs for heavy metal detection.(C. Liu et al. 2017)

2.4.2. Carbon Materials as Solid-Contacts

Carbon materials like graphene, graphene oxide, and carbon nanotubes (CNTs) are commonly utilized as solid contact materials in potentiometric sensors due to their significant lipophilicity and high capacitance.(Zdrachek and Bakker 2019) Among the conducting materials assessed for the fabrication of ISE, CNTs are particularly attractive for use as solid contact materials in electrochemistry due to their high aspect ratio, large surface area, excellent electrical conductivity, and thermal and electrochemical stability.(Dubey et al. 2021b)

"Evidence of double layer/capacitive charging in carbon nanomaterial-based solid contact polymeric ion-selective electrodes" by Cuartero et al. provides significant insights into the charging mechanisms in solid contact ion-selective electrodes (SC-ISEs) utilizing carbon nanomaterials. This study marks the first direct spectroscopic evidence supporting the presence of double layer or capacitive charging within these materials, achieved through synchrotron radiation-X-ray photoelectron spectroscopy (SR-XPS) and synchrotron radiation valence band (SR-VB) spectroscopy. The findings revealed that the electrical double layer charging is indeed responsible for the high capacitance observed in f-MWCNT-based SC-ISEs. This was evidenced by the adsorption and enrichment of ions at the buried interfaces within the nanostructured material. The study demonstrated that capacitive charging in these electrodes is facilitated by the formation of an electrical double layer involving the adsorption/absorption of lipophilic anions into the f-MWCNT film.(Maria Cuartero et al. 2016)

Ewa Jaworska, et al. (2016) examines different dispersing agents for carbon nanotubes (CNTs) used in the creation of ion-selective electrodes (ISEs), with a particular focus on introducing carboxymethylcellulose (CMC) as a new dispersing agent for CNT-based solid contacts. The research highlights the importance of achieving uniform dispersion of CNTs in solvents, which is crucial for their use in electrochemical sensors. It compares traditional surfactants like sodium dodecylbenzenesulfonate (NaDBS) and cetyltrimethylammonium chloride (CTAC) to

CMC, evaluating their effects on the physical properties and performance of the resulting CNT layers. The study concludes that CMC is an effective and promising dispersing agent for CNTs in the fabrication of solid-contact ion-selective electrodes, offering enhanced sensor stability and performance. The results indicate potential applications for CMC-dispersed CNTs in various electrochemical sensing technologies. (Jaworska, Maksymiuk, and Michalska 2016)

Enguang Lv et al. (2018) introduce an innovative potentiometric aptasensing platform for the detection of small molecules, with bisphenol A (BPA) serving as the model target. The proposed sensor relies on surface charge changes, utilizing carboxylated multiwall carbon nanotubes (CNTs), poly(diallyldimethylammonium chloride) (PDDA), and an aptamer. This configuration is designed to achieve high sensitivity and selectivity in small molecule detection. The aptamer employed possesses a high binding affinity for BPA. The electrode preparation involved a layer-by-layer assembly technique, wherein CNTs, PDDA, and the aptamer were sequentially modified onto the electrode surface. Potentiometric measurements were carried out using a double-junction Ag/AgCl reference electrode. The electrodes were incubated with various concentrations of BPA, and the corresponding potential responses were recorded. The sensor demonstrated a linear response to BPA concentrations ranging from 3.2×10^{-8} to 1.0×10^{-6} M, with a detection limit of 1.0×10^{-8} M. Control experiments confirmed the sensor's selectivity for BPA over structurally similar molecules. The article showcases a potentiometric aptasensing platform for small molecules, highlighting the enhancement in sensor sensitivity due to the inclusion of polyions like PDDA. The proposed methodology is versatile and can be extended to detect other small molecules, bacteria, proteins, and metal ions. This work underscores the potential of aptamer-based sensors for the sensitive and selective detection of various analytes. (Lv, Ding, and Qin 2018)

Tanji Yin, Jinghui Li, and Wei Qin (2017) present the development of an innovative all-solid-state calcium ion (Ca^{2+})-selective electrode (ISE) utilizing a polymeric membrane. This study's unique contribution is the incorporation of hydrophobic octadecylamine-functionalized graphene oxide (GO-ODA) as a crucial component. The significance of this research lies in addressing the limitations of traditional ISEs, such as inadequate potential stability caused by the presence of an undesired water layer at the interface between the electronic conductor and the ion-selective membrane. The hydrophobic composite, GO-ODA, was synthesized by

functionalizing graphene oxide (GO) with octadecylamine (ODA). This functionalization process aimed to enhance both the hydrophobicity and electrical conductivity of GO, making it suitable for use in the ion-selective membrane. The ion-selective membrane (ISM) was prepared with a combination of calcium ionophore, sodium tetraphenylborate, poly(vinyl chloride) (PVC), and 2-nitrophenyl octyl ether (o-NPOE), along with the GO-ODA composite. The developed all-solid-state Ca^{2+} ISEs demonstrated stable potential responses over a wide linear range of Ca^{2+} concentrations (3.0×10^{-7} to 1.0×10^{-3} M), with detection limits as low as 1.6×10^{-7} M. The presence of the GO-ODA composite significantly improved potential stability by preventing the formation of a water layer at the ISM-GC interface. This study successfully developed a novel all-solid-state Ca^{2+} selective electrode utilizing a hydrophobic alkyl-chain-functionalized graphene oxide composite. The inclusion of GO-ODA in the ion-selective membrane not only enhanced potential stability and selectivity but also prevented the formation of undesirable water layers. This work offers a simple, efficient, and cost-effective approach for fabricating robust and stable all-solid-state ISEs, with potential applications in various fields requiring precise ion detection. (Yin, Li, and Qin 2017)

Beata Paczosa-Bator et al. (2018) investigate the application of a graphene layer supporting platinum nanoparticles (PtNPs-GR) in electrochemical sensors designed for both potentiometric and voltammetric detection. The study's objective is to enhance the performance of electrochemical sensors by leveraging the distinctive properties of PtNPs-GR. For potentiometric sensors, the PtNPs-GR layer was coated with a potassium ion-selective membrane incorporating valinomycin as the ion carrier. For voltammetric sensors, the PtNPs-GR modified electrodes were utilized to detect paracetamol. The potassium-selective electrodes exhibited a Nernstian response with a slope of 59.10 mV/pK, demonstrating high stability and minimal potential drift. The inclusion of the PtNPs-GR layer significantly improved the detection limit and long-term stability of these sensors. The voltammetric sensors showed a linear response to paracetamol concentrations ranging from 20 nM to 2.2 μM , with a detection limit of 8 nM. The presence of the PtNPs-GR layer enhanced both the sensitivity and detection capabilities of the sensors. The study conclusively demonstrates that the incorporation of a graphene layer supporting platinum nanoparticles markedly enhances the performance of electrochemical sensors. The PtNPs-GR layer improves the stability, sensitivity, and detection limits of both potentiometric and voltammetric sensors. This

work provides a straightforward and effective approach for developing high-performance electrochemical sensors suitable for a variety of analytical applications.(Paczosa-Bator et al. 2018)

2.4.3.Other Materials as Solid-Contacts

Magdalena Piek et al. (2016) presents an innovative all-solid-state nitrate-selective electrode that utilizes a nanocomposite of graphene and tetrathiafulvalene (GR-TTF/TTF+) as the solid-contact material. This study addresses the limitations of traditional ion-selective electrodes (ISEs) by leveraging the high redox and double layer capacitance properties of the nanocomposite to enhance the performance of nitrate-selective sensors. The electrodes were fabricated by drop-casting a suspension of graphene and tetrathiafulvalene onto a glassy carbon disc, followed by coating with a nitrate-selective membrane. The incorporation of the GR-TTF/TTF+ nanocomposite was intended to improve the electrode's potential stability, reduce potential drift, and eliminate the formation of an undesirable aqueous layer at the interface between the ion-selective membrane and the solid contact. The modified electrodes demonstrated a good Nernstian response with a slope of -59.14 mV/decade over a concentration range of 10^{-6} to 10^{-1} M nitrate ions, indicating high sensitivity and a wide linear detection range. The study concludes that the graphene-tetrathiafulvalene nanocomposite is an effective solid-contact material for nitrate-selective electrodes, providing a simple and efficient approach to developing robust and stable all-solid-state ISEs.(Pięk, Piech, and Paczosa-Bator 2016)

Magdalena Piek et al. (2018) investigates the application of a tetrathiafulvalene-tetracyanoquinodimethane (TTF-TCNQ) solid contact layer in all-solid-state ion-selective electrodes (ISEs) for the detection of potassium (K^+) and nitrate (NO_3^-) ions. TTF-TCNQ, a well-known charge transfer salt, is valued for its unique electrical properties and potential applications across various fields. This study represents the first instance of utilizing TTF-TCNQ as an ion-to-electron transducer in ISEs. The electrodes were fabricated by drop-casting a TTF-TCNQ suspension in either acetonitrile (ACN) or dimethylformamide (DMF) onto glassy carbon discs (GCD). Potassium-selective membranes were formulated using valinomycin, while nitrate-selective membranes incorporated nitrate ionophore V. The potassium-selective

electrodes demonstrated a Nernstian response with a slope of 58.52 mV/decade over a concentration range of 10^{-6} to 10^{-1} M K^+ . Similarly, the nitrate-selective electrodes exhibited a sensitivity of -58.47 mV/decade for concentrations ranging from 10^{-5} to 10^{-1} M NO_3^- . The study confirms the effectiveness of TTF-TCNQ as a solid contact layer in all-solid-state ISEs for potassium and nitrate detection. The TTF-TCNQ layer significantly enhances the potential stability, sensitivity, and overall performance of the electrodes. This research presents a novel and efficient approach to developing high-performance, stable ISEs with considerable potential for various analytical applications.(Pięk, Piech, and Paczosa-Bator 2018)

The article by Ewa Jaworska et al. (2017) introduces an innovative method to enhance the performance and reproducibility of all-solid-state ion-selective electrodes (ISEs) through the incorporation of cobalt(II) porphyrin and cobalt(III) corrole as transducers. This study addresses the prevalent issue of potential stability in ISEs by utilizing these porphyrinoids, which are characterized by their high stability and lipophilicity. Cobalt(II) porphyrin and cobalt(III) corrole were synthesized and combined with multi-walled carbon nanotubes (MWCNTs) to create the transducer layers. The electrodes were fabricated by drop-casting this mixture onto glassy carbon electrodes, followed by coating them with potassium-selective PVC membranes. The potassium-selective electrodes demonstrated nearly Nernstian responses with slopes close to 59 mV/decade, indicating high sensitivity and a broad linear detection range. This study conclusively demonstrates that incorporating cobalt(II) porphyrin and cobalt(III) corrole in the transducer phase significantly enhances the performance of all-solid-state ISEs. The improvements in stability, sensitivity, and reproducibility make these sensors highly suitable for various analytical applications. The novel use of porphyrinoids presents a promising alternative to existing transducer systems for potentiometric sensors, paving the way for the development of high-performance, stable, and reproducible ISEs.(Jaworska et al. 2017)

Shinichi Komaba et al. (2017) investigates the development of all-solid-state ion-selective electrodes (ISEs) for lithium, sodium, and potassium ions. These electrodes utilize redox-active insertion materials, specifically Li_xFePO_4 for lithium, $Na_{0.33}MnO_2$ for sodium, and $K_xMnO_2 \cdot nH_2O$ for potassium, as inner solid-contact layers to enhance the performance of the sensors. The study addresses common issues in traditional ISEs, such as potential instability and the presence of an undesired aqueous

layer at the membrane/electrode interface. The incorporation of these insertion materials aims to improve the stability, sensitivity, and reproducibility of the electrodes. The electrodes were constructed by installing a composite layer containing the insertion materials onto a glassy carbon disc, followed by coating with a plasticized poly(vinyl chloride) (PVC)-based ion-sensitive membrane containing the corresponding ionophores for Li^+ , Na^+ , and K^+ ions. These double-layer ISEs exhibited quick potential responses (less than 5 seconds) and nearly Nernstian slopes of calibration curves (approximately 59 mV per decade) for each ion. Overall, the article demonstrates that the integration of redox-active insertion materials in all-solid-state ISEs provides a simple, effective, and high-performance approach for ion detection, with potential applications in various fields requiring precise ion analysis. (Komaba et al. 2017)

Klink, Ishige, and Schuhmann (2017) presents a study on the development of solid-contact ion-selective electrodes (SC-ISEs) utilizing Prussian Blue Analogues (PBAs) as a versatile framework for tuning electrode potentials. SC-ISEs are crucial for point-of-care sensors and other analytical applications due to their simplicity, predictability, and reproducibility. The authors synthesized PBAs, including potassium copper (K-CuHCF), potassium nickel (K-NiHCF), and potassium iron (K-FeHCF) hexacyanoferrate, using a co-precipitation method. These PBAs were employed as the solid-contact layer in SC-ISEs, which were constructed by applying the PBA material onto a glassy carbon electrode, followed by coating it with an ion-selective membrane (ISM) specific for Na^+ , K^+ , or Ca^{2+} ions. The SC-ISEs exhibited nearly Nernstian responses with slopes close to 59 mV/decade for potassium ions, indicating high sensitivity and a wide linear detection range. The study effectively demonstrates that incorporating Prussian Blue Analogues as transducers significantly enhances the performance of all-solid-state ion-selective electrodes. The improved stability, sensitivity, and reproducibility render these sensors suitable for various analytical applications. The versatility of PBAs in tuning electrode potentials offers a promising alternative to existing transducer systems, paving the way for the development of high-performance, stable, and reproducible SC-ISEs. (Klink, Ishige, and Schuhmann 2017)

Xianzhong Zeng and Wei Qin (2017) investigate the development of a solid-contact potassium-selective electrode (SC-ISE) utilizing MoO_2 microspheres as the ion-to-electron transducer. The objective is to address common issues in conventional ion-selective electrodes, such as potential instability, maintenance challenges, and poor portability, by employing a solid contact that provides stable and reproducible

potentiometric measurements. Glassy carbon (GC) electrodes were polished and cleaned before being coated with a dispersion of MoO₂ microspheres to form the solid contact layer. A potassium-selective membrane containing valinomycin, NaTFPB, PVC, and o-NPOE was then applied onto the MoO₂-coated GC electrodes. The SC-ISEs exhibited a near-Nernstian response with a slope of 55 mV/decade for potassium ion concentrations ranging from 10⁻⁵ to 10⁻³ M, and a detection limit of 10⁻⁵ M. The electrode showed rapid and stable potential responses even at lower concentrations. The SC-ISEs were used to determine potassium concentrations in seawater samples, showing good agreement with results obtained by inductively coupled plasma atomic emission spectrometry (ICP-AES). The study demonstrates that MoO₂ microspheres can serve as effective ion-to-electron transducers in solid-contact potassium-selective electrodes. The enhanced stability, sensitivity, and reproducibility of the SC-ISEs make them suitable for various analytical applications. The use of MoO₂ microspheres as a metallic analogue provides a promising and cost-effective alternative to noble metal-based transducers. (Zeng and Qin 2017)

2.5.Sensor Materials

Ion-selective electrodes (ISEs) are fundamental in analytical chemistry for the selective and sensitive detection of specific ions within diverse and complex matrices. The performance and reliability of these electrodes are heavily influenced by the materials used in their construction, particularly the sensor materials. These materials are essential as they determine the selectivity, sensitivity, and overall response characteristics of the ISEs. The selection of sensor materials is critical in the design and functionality of ISEs. Each material offers distinct advantages and limitations, affecting factors such as ion selectivity, response time, and operational stability. Continuous research and development in sensor materials aim to address existing limitations, improve electrode performance, and broaden the applicability of ISEs across various scientific and industrial domains. (Hulanicki, Glab, and Ingman 1991b; Bobacka, Ivaska, and Lewenstam 2008b)

2.5.1. Membrane Materials

The efficacy of Ion-selective electrodes is profoundly influenced by the characteristics of the membrane materials utilized. The membrane functions as a selective barrier, permitting only the target ion to interact with the electrode, thus producing a measurable potential difference. A fundamental component of ISEs is the ion-selective membrane, which can be fabricated from various materials, including glass, crystalline, or polymeric substances. Each type of membrane material possesses distinctive properties that render it suitable for applications. (Bobacka, Ivaska, and Lewenstam 2008b)

Glass membranes, typically used in pH electrodes, are made of silicate glass. These membranes are highly selective for hydrogen ions due to their ability to exchange cations. The high chemical stability and robustness of glass make it an ideal material for various industrial and laboratory applications. (Bakker and Telting-Diaz 2002)

Crystalline membranes are made from single or polycrystalline materials, such as lanthanum fluoride for fluoride-selective electrodes. These membranes exhibit high selectivity and sensitivity due to their well-defined crystalline structure, which allows for specific ion exchange.

Polymeric membranes are among the most versatile and widely used in ISEs. These membranes are typically composed of polyvinyl chloride (PVC) doped with plasticizers and ionophores. The ionophore is a crucial component that imparts selectivity to the membrane by complexing specifically with the target ion. The plasticizer ensures the membrane remains flexible and mechanically stable. (Hulanicki, Glab, and Ingman 1991b)

Lugert-Thom, E. C., et al. (2017) examines the stability and performance of pH-selective ionophore-doped fluororous membranes subjected to cleaning-in-place (CIP) treatments, which are prevalent in industrial processes. The study specifically evaluates membranes composed of Teflon AF2400, plasticized with a linear perfluoropolyether, and doped with ionic sites and two types of H⁺ ionophores: tris[3-(perfluorooctyl)propyl]amine (ionophore 1) and tris[3-(perfluorooctyl)pentyl]amine (ionophore 2). The researchers subjected the membranes to a 3.0% NaOH solution at 90°C for 30 minutes, simulating typical CIP conditions. The findings revealed that membranes doped with ionophore 1 exhibited decreased potentiometric response slopes

and increased resistances after a single exposure. Conversely, membranes doped with ionophore 2 retained their theoretical (Nernstian) response slope up to pH 12, even after ten exposures, totaling five hours in the hot NaOH solution. Furthermore, the incorporation of a fluorophilic electrolyte salt, methyltris[3-(perfluorooctyl)propyl] ammonium tetrakis[3,5-bis(perfluorohexyl)phenyl]borate, significantly reduced membrane resistance. The study concludes that ionophore 2 exhibits superior stability and performance under rigorous CIP conditions, whereas ionophore 1 is less robust due to its weaker H⁺ binding affinity. These findings underscore the potential of employing fluorous membranes with strongly binding ionophores for reliable pH sensing in industrial applications. (Lugert-Thom et al. 2018)

Carey et al. (2017) investigates the development and application of semifluorinated polymers for use in ion-selective electrode (ISE) membranes. The study aims to address the limitations of traditional ISE membranes, such as those made from plasticized polyvinyl chloride (PVC), by exploring semifluorinated polymers that offer improved selectivity and stability. The researchers synthesized semifluorinated polymers (P1 and P2) with perfluorohexyl and perfluorooligoether side chains, respectively. These polymers were specifically designed to avoid functional groups that could lower selectivity and to have glass transition temperatures (T_g) suitable for ISE operation. The performance of ionophore-doped membranes using the synthesized semifluorinated polymers was also investigated. Silver ion-selective electrodes (ISEs) were tested with various fluorophilic and lipophilic ionophores. The semifluorinated polymer-based membranes demonstrated good selectivity and stability, although they were slightly less selective than their fully fluorous counterparts. The study concludes that semifluorinated polymers, especially when cross-linked, present a promising alternative for ISE membranes, combining the benefits of fluorous properties with enhanced mechanical stability and thermal resilience. These advancements could lead to more reliable and versatile ion-selective electrodes for various industrial and environmental applications. (Carey et al. 2017)

Shogo Ogawara et al. (2016) investigate the performance of hydrophilic ion-exchanger membranes with high ion-exchange capacity in ion-selective electrodes (ISEs). The study focuses on these membranes' resistance to Donnan failure, a phenomenon that restricts the upper detection limit of ISEs due to the transfer of co-ions into the sensing membrane. The research demonstrated that HHCIE membranes maintained Nernstian responses even in the presence of high concentrations of

hydrophobic co-ions, whereas PVC/IE and PVC/ionophore membranes exhibited significant deviations from ideal behavior. Hydrophilic anion-exchanger membranes showed Nernstian responses for anions as large as 2.0 nm, indicating that their resistance to Donnan failure is not due to size exclusion but rather to the high activity of exchangeable ions in the ion exchanger phase. The research concludes that hydrophilic high-capacity ion-exchanger membranes provide a substantial advantage in resisting Donnan failure, primarily because of their high ion-exchange capacity. This makes them particularly suitable for use in ISEs, especially in applications involving biological samples or environments with high concentrations of hydrophobic co-ions. The study underscores the potential for these membranes to enhance the performance and reliability of ISEs across various applications.(Ogawara et al. 2016)

2.5.2.Ion-Exchange Membranes

Nanopores have long been recognized as a versatile sensing platform. Their functionality relies on the selective alteration of ion flux through preconditioned pores, influenced by the chemical and physical properties of the interior pore surface. Traditionally, most nanopore-based sensors utilize ionic current as an analytical signal. However, a potentiometric readout mode has recently garnered attention due to its simpler instrumentation and higher signal-to-noise ratio. The potentiometric response of nanopores can be explained using the concept of permselectivity, analogous to conventional polymer membrane ion-selective electrodes (ISEs).(Zdrachek and Bakker 2019)

István Makra et al. (2016) introduce an innovative method for the selective detection of nucleic acids using potentiometric sensing. This technique employs nanopores modified with positively charged peptide-nucleic acid (PNA) to achieve high selectivity and sensitivity. The nanopores demonstrated remarkable sensitivity, with significant potential responses observed at miRNA concentrations as low as 0.1 nM. The study revealed that the location and surface density of the PNA layer within the nanopores were critical factors influencing the response, with smaller nanopores (26 nm diameter) showing superior performance compared to larger ones. The research validated the feasibility of real-time, label-free detection of miRNA by directly adding nucleic acid samples to the sample compartment. By monitoring the potential changes

over time, the kinetics of the binding process were elucidated, and kinetic parameters such as association and dissociation rate constants were determined from the potential-time traces. The estimated limit of detection (LOD), based on the standard deviation of the potential signal in the blank solution, was approximately 100 pM, which closely matched the experimentally detected miRNA concentrations. The study supports the viability of potentiometric transduction for the selective detection of nucleic acids by leveraging charge inversion in PNA-modified nanopores. The findings suggest that this method provides a straightforward and effective alternative to conventional sensing techniques, with potential applications in various fields requiring sensitive and selective nucleic acid detection. The theoretical and experimental insights offer a solid foundation for further optimization and development of nanopore-based potentiometric sensors. (Makra et al. 2017)

Soma Papp et al. (2018) report on the synthesis and analytical application of Cu^{2+} -selective synthetic ion channels using peptide-modified gold nanopores. This research tackles the challenge of incorporating hydrophilic ligands into ion-selective membranes (ISMs), a process traditionally hindered by the hydrophobic nature of conventional ISMs. The study investigated the use of a ternary mixture of functional thiols to modify the nanopores, optimizing the proportions of hydrophilic peptide ionophores, mercaptodecanesulfonate (MDSA), and alkanethiols with different chain lengths. The optimal modification achieved involved a 6:3:1 molar ratio of the Cu^{2+} -selective peptide, hexadecanethiol (HDT), and MDSA, which created a hydrophobic environment within the nanopores essential for potentiometric ion-selectivity. The peptide-modified nanopores exhibited near-Nernstian behavior for Cu^{2+} detection, with a sub-micromolar limit of detection. The electrodes demonstrated fast, drift-free responses and significant selectivity over other cations, including alkali and alkaline earth metals. Selectivity coefficients indicated that the peptide-modified nanopores outperformed conventional plasticized PVC membranes that use standard Cu^{2+} ionophores. The study illustrates that hydrophilic ionophores, when incorporated into a hydrophobic nanoporous environment, can provide superior ion-selective properties. This method offers substantial advantages in selectivity, stability, and suppression of component leaching, making it a promising alternative for constructing high-performance ISEs. While the concept appears broadly applicable, ligands containing thiols or disulfides in their binding sites may require the use of alternative nanoporous

materials and surface chemistries. The findings have potential applications beyond chemical sensing, including in desalination and energy harvesting devices.(Papp, Jágerszki, and Gyurcsányi 2018)

2.5.3.Ionic Liquids

Room temperature ionic liquids (ILs) are considered promising materials for potentiometric sensors. Despite their potential, their role in these sensors is not yet fully comprehended. ILs have been proposed to function as inert plasticizers, nonspecific ion exchangers, and even as ionophores.(Zdrachek and Bakker 2019)

Lukasz Mendecki et al. investigate the impact of incorporating trihexyl(tetradecyl)phosphonium-based ionic liquids (ILs) on the selectivity of ion-exchange membranes employed in potentiometric sensors. The membranes were fabricated using a variety of ILs as well as traditional plasticizers, such as DOS and NPOE. Ionophore-free membranes were produced by blending PVC with the selected IL or plasticizer. The findings demonstrate that phosphonium-based ILs can effectively modulate the selectivity of ion-exchange membranes, thereby presenting significant potential for tailored sensor applications.(Mendecki et al. 2016)

B. Schazmann et al. presents a study on the development of robust, single-layer ion-selective electrodes (ISEs) utilizing Ag/AgCl electrodes as solid supports without intermediate polymer layers. Hybrid materials (PVC-1 and PVC-2) were synthesized using click chemistry to combine imidazolium ionic liquids (ILs) with poly(vinyl chloride) (PVC). The electrodes were prepared by coating Ag/AgCl wires or planar screen-printed carbon electrodes with the synthesized membrane cocktails. These electrodes exhibited the expected selectivity patterns according to the Hofmeister series, with enhanced selectivity for perchlorate ions attributed to the presence of ILs. This study highlights the potential of PVC-IL hybrid materials in creating simple, robust ISEs with significantly reduced handling requirements, offering substantial advantages for practical sensing applications.(Schazmann et al. 2018)

2.5.4.Molecular Imprinted Polymers

Molecularly imprinted polymers (MIPs) are custom-designed materials that exhibit selective recognition properties for specific target compounds. The synthesis of MIPs involves the polymerization of a functional monomer with a template molecule in the presence of a cross-linking agent, followed by the removal of the template molecule prior to use. MIPs have proven valuable in various analytical applications and have recently gained popularity as recognition elements incorporated into the polymer membranes of ion-selective electrodes (ISEs).(Zdrachek and Bakker 2019)

Molecularly imprinted polymers (MIPs) have demonstrated utility in various analytical applications and have recently gained popularity as recognition elements incorporated into the polymer membranes of ion-selective electrodes (ISEs).(Zdrachek and Bakker 2019) They have been employed for the potentiometric detection of several compounds, including the insecticide dinotefuran (Abdel-Ghany, Hussein, and El Azab 2017), 1-hexyl-3-methylimidazolium (Zhuo et al. 2016), acetylcholine (Sacramento et al. 2017), lactic acid (Alizadeh, Nayeri, and Mirzaee 2019), 2-naphthoic acid (P. Li et al. 2018), taurine (Kupis-Rozmystowicz et al. 2016), bisphenol S (C. Wang et al. 2022), and bisphenol AF (H. Zhang et al. 2018).

2.5.5.Ionophores

Ionophores are essential components in the design of potentiometric ion-selective electrodes, which are extensively employed for the selective detection of specific ions across a range of analytical applications. These chemical compounds facilitate the selective binding and transport of target ions across a membrane. In potentiometric ISEs, ionophores are embedded within the ion-selective membrane, conferring selectivity to the electrode for a particular ion. This selectivity is achieved through the ionophore's ability to form stable complexes with the target ion, thereby enabling its selective transport or binding. When an ionophore within the ion-selective membrane selectively binds to the target ion from the sample solution, this binding event alters the membrane potential. The change in potential is measured by the ISE and is directly related to the concentration of the target ion in the solution, thus allowing for

quantitative analysis.(Bakker and Pretsch 2005; Bakker, Bühlmann, and Pretsch 1997; Bobacka, Ivaska, and Lewenstam 2008c)

2.6. Miniaturized Ion-Selective Electrodes

Jinbo Hu et al. (2016) presents the development and characterization of an innovative ion-sensing platform. This platform incorporates a potentiometric cell into a paper substrate, resulting in a cost-effective, disposable, and highly efficient tool for ion detection. The fabrication process involves the use of a polyurethane-based hydrophobic barrier to create microfluidic channels, facilitating scalability and ease of production. The sensing membrane can be customized for different ions through the incorporation of specific ionophore-doped ion-selective electrode (ISE) membranes or hydrophilic high-capacity ion-exchange membranes. The platform was evaluated for the detection of chloride (Cl^-) and potassium (K^+) ions in both aqueous and biological samples, exhibiting high reproducibility and a linear response within the clinically relevant concentration range. The devices demonstrated a Nernstian response, underscoring their theoretical predictability and practical reliability. This disposable planar paper-based ion-sensing platform signifies a substantial advancement in ion detection technology. Its simplicity, affordability, and high reproducibility position it as a promising tool for clinical and environmental analyses, especially for point-of-care and in-field applications. The study underscores the potential for further development and optimization to enhance the device's performance and expand the range of detectable ions.(Hu, Stein, and Bühlmann 2016)

T. Fayose, et al. (2017) presents a straightforward, cost-effective method for creating ion-selective electrodes using common household materials. Graphite from a household pencil is applied onto a modified acetate sheet via mechanical abrasion to create a conductive substrate. This graphite layer is then covered with ion-selective membranes to create functional ISEs. The entire setup is insulated with simple adhesive tape, leaving only the required areas exposed for membrane application. The electrodes were tested for the detection of biologically and environmentally important ions (NH_4^+ , Na^+ , and NO_3^-), demonstrating near-Nernstian response slopes and selectivity. The study presents a highly accessible and inexpensive approach to fabricating ISEs using commonly available materials. The electrodes produced by this method making this

technique a promising alternative for developing simple, low-cost sensing devices for various applications.(Fayose et al. 2017)

Wang et al. (2017) developed a wearable sweatband sensor platform utilizing a gold nanodendrite (AuND) array as an efficient solid contact for ion-selective electrodes (ISEs). The platform integrates an all-solid-state ISE and reference electrode (RE), featuring a poly(vinyl acetate)/inorganic salt (PVA/KCl) membrane-coated all-solid-state RE. The AuND array was fabricated using a simple, one-step electrodeposition process on a microwell patterned chip, enhancing the surface area and hydrophobicity of the electrodes. The study investigated the relationship between the surface area of AuND electrodes and their performance characteristics, demonstrating that electrodes with larger surface areas exhibited improved potential stability. The PVA/KCl membrane coated RE also showed high potential stability after prolonged storage. The wearable sweatband platform was tested for real-time sweat sodium analysis during indoor exercise, demonstrating effective sweat collection and analysis. The platform showed promise for use in portable and wearable devices for healthcare, sports, clinical diagnostics, and environmental monitoring. The study highlights the platform's simplicity, stability, and potential for further development, making it a significant advancement in wearable sensor technology.(S. Wang et al. 2017)

Parrilla et al. (2016) presents the development of wearable potentiometric sensors based on commercial carbon fibers (CCF) for real-time monitoring of sodium levels in sweat during exercise. The study highlights the advantageous properties of CCF, such as good electrical conductivity, chemical inertness, flexibility, and mechanical resilience, making them suitable for wearable electrochemical sensors. The sensors, incorporating CCF and solid-contact reference electrodes, demonstrated near-Nernstian response and good stability. The wearable patch, integrating the potentiometric cell, exhibited reliable performance in detecting sodium levels from 10^{-3} M to 10^{-1} M in artificial sweat, within the physiological range. The sensors showed low noise levels and stability (± 0.4 mV \cdot h $^{-1}$). To enhance usability, a calibration-free approach was explored, improving reproducibility and reducing the need for frequent calibration. The study underscores the potential of CCF-based sensors for generating personalized physiological data, with applications in sports, nutrition, and healthcare. The sensors' performance was validated through on-body tests, demonstrating their robustness and stability under physical stress during exercise. The research presents a

promising direction for the development of accessible, low-cost wearable sensors with significant implications for real-time health monitoring.(Parrilla et al. 2016)

Uria et al. (2016) present the development and application of miniaturized metal oxide pH sensors for detecting bacterial growth, specifically focusing on *Escherichia coli* (*E. coli*). The study addresses the limitations of conventional glass pH electrodes, such as bulkiness, fragility, and high cost, which hinder their use in miniaturized systems. Two types of metal oxide sensors, iridium oxide (IrO_x) and tantalum pentoxide (Ta_2O_5), were fabricated on silicon chips with platinum contacts, using electrodeposition and e-beam sputtering methods, respectively. These sensors were integrated with an Ag/AgCl pseudo-reference electrode, enabling operation in small sample volumes. The sensors were calibrated in phosphate-buffered saline (PBS) and Luria-Bertani (LB) medium supplemented with glucose, demonstrating linear responses in the pH range of 3 to 8. The IrO_x sensors exhibited super-Nernstian behavior, while the Ta_2O_5 sensors showed Nernstian response. Stability tests confirmed the sensors' performance after overnight incubation in LB-glucose medium. The sensors were applied to monitor *E. coli* growth, detecting viable cells in concentrations as low as 102 colony-forming units per milliliter (cfu/mL) within 5 hours. The results were comparable to those obtained using a conventional glass pH electrode but required significantly smaller sample volumes. This study highlights the potential of these miniaturized sensors for rapid, sensitive, and cost-effective bacterial detection in various applications, including water quality monitoring and medical diagnostics.(Uria et al. 2016)

Toczyłowska-Mamińska et al. (2016) describe the design and characterization of a novel all-solid-state potentiometric sensor array dedicated to physiological measurements. The sensor array, constructed on epoxy-glass laminate, integrates ion-selective electrodes for potassium, sodium, chloride, and pH, along with a reference electrode. These ISEs are based on plasticized polyurethane membranes and are coated directly onto the transducer's surface, following the coated wire electrode approach. The sensor array demonstrated high sensitivity (55.271 mV/dec for sodium, 56.372 mV/dec for potassium, 58.471 mV/dec for chloride, and 53.571 mV/pH for pH-selective electrodes) within the physiologically relevant concentration range (10^{-5} to 10^{-1} M for primary ions). It also exhibited low response time ($t_{95} < 10$ s), high potential stability (± 2 mV over 28 hours), and excellent potential reproducibility (± 1 mV). The system

was validated through the simultaneous determination of K^+ , Na^+ , Cl^- , and pH in a model physiological solution, with results showing high accuracy and repeatability. Additionally, the sensor array was applied to measure ion fluxes in human colon epithelium Caco-2 cell monolayers. The system effectively monitored chloride ion transport, demonstrating its applicability for real-time, non-invasive physiological measurements. The study highlights the potential of this all-solid-state sensor array for various applications in biology and medicine, offering a reliable and efficient tool for ion flux studies in living cells and tissues. (Toczyłowska-Mamińska et al. 2016)

CHAPTER 3

MATERIALS AND METHODS

3.1. Materials

Analytical grade tetrahydrofuran (THF), nonactin, high molecular weight PVC, carboxylated PVC (PVC-COOH), o-nitrophenyl octyl ether (NPOE), dioctyl phthalate (DOP), DOS, aluminum nitrate ($\text{Al}(\text{NO}_3)_3$), iron nitrate ($\text{Fe}(\text{NO}_3)_3$), and all reagents for CNT synthesis were obtained from Sigma-Aldrich. Distilled deionized (DI) water was used in all experiments. The gases for CNT growth were sourced from National Oxygen in Singapore. Starting materials, reagents, and solvents, including 4'-Hydroxyacetophenone, Cyanuric chloride, N,N-dimethylamine solution (40 wt. % in H_2O), and CDCl_3 , were sourced from Sigma Aldrich Chemical Co. Silicon tetrachloride, N,N-Diisopropylethylamine, and Phloroglucinol were obtained from Tokyo Chemical Industry Co.-TCI, while acetonitrile, acetone, THF, DMF, toluene, methanol, and ethanol were purchased from Carlo Erba Reagents. All chemicals, along with sodium and potassium salts of anions and nitrate, chloride salts of cations, were supplied by Sigma-Aldrich.

3.2. Potentiometric Measurements

Potentiometric measurements were carried out using the $\mu\text{Stat-i}$ 400s instrument, a Metrohm Potentiostat/Galvanostat. In these measurements, the RACNT-GF composite ion-selective electrode (r-ISE) and the CAGE Incorporated ISE served as the working electrodes, while an Ag/AgCl reference electrode (provided by Gamry) was used. Both the working and reference electrodes were submerged to an equal depth in a 30 mL assay solution, with continuous stirring at a constant rate to ensure uniformity. Before each measurement sequence, both the reference and working electrodes were thoroughly rinsed with deionized (DI) water and carefully dried with a soft absorbent tissue to prevent any contamination. The RACNT-GF composite ISE was conditioned by soaking it in a 0.01 M NH_4NO_3 solution, while the CAGE Incorporated ISE was

conditioned by soaking it in a 0.01 M NaNO₃ solution for 4 hours. This conditioning step is essential for ensuring the stability and reliability of the electrode's responses. Following the conditioning process, the potentiometric responses of the ISEs were recorded. Measurements were taken for the target ions as well as for other anionic and cationic species. To evaluate the response of the sensors, they were immersed in standard solutions with concentrations ranging from 1.0×10⁻⁶ to 1.0×10⁻¹ M. This procedure helps in determining the sensitivity and selectivity of the ISEs towards various ions across a broad concentration spectrum.

3.3.Fabrication of Electrodes

3.3.1.RACNT-GF Composite ISE

Individual glass fibers (GF) from the GF fabric coated with carbon nanotubes (CNT) are separated for the construction of the r-ISE (Figure 3.1 B). Each fiber in the fabric is made up of a specific number of GF filaments: 816 filaments with diameters of 9 μm in the vertical direction and 204 filaments with diameters of 7 μm in the horizontal direction, sourced from Hexcel 1543 fabric (as shown in Figure 3.1 A).

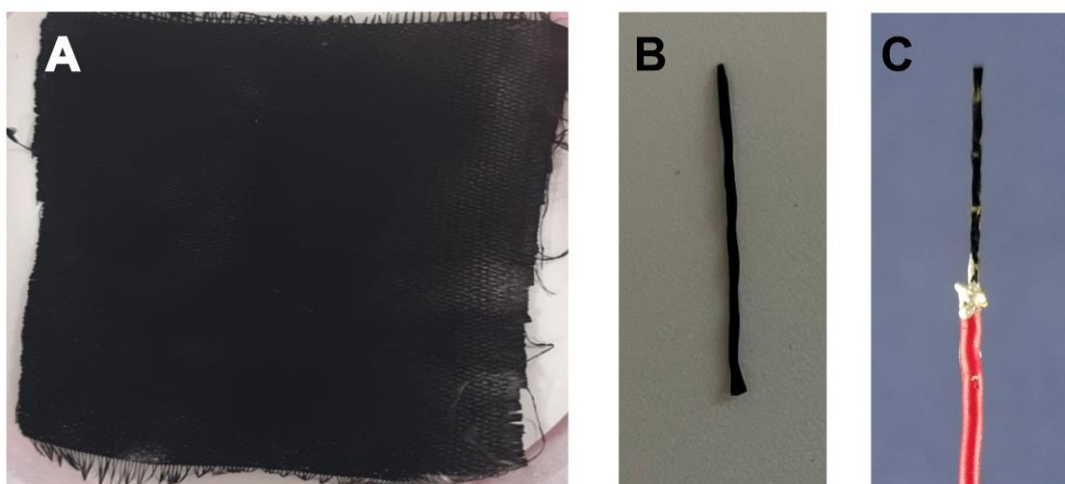


Figure 3.1 The RACNT dip-coated with an Fe catalyst (A). (B) illustrates an individual GF fiber displaying uniform RACNT growth. For the construction of the r-ISE, the radially oriented GF-CNT was attached to a copper wire (C) and then covered with an insulating material

The individual RACNT-GF composite fiber is then dip-coated using a tetrahydrofuran (THF) solution containing 100 mg of PVC/PVC-COOH, plasticizers, and nonactin in varying stoichiometric ratios (depicted in Figure 3.1 C).

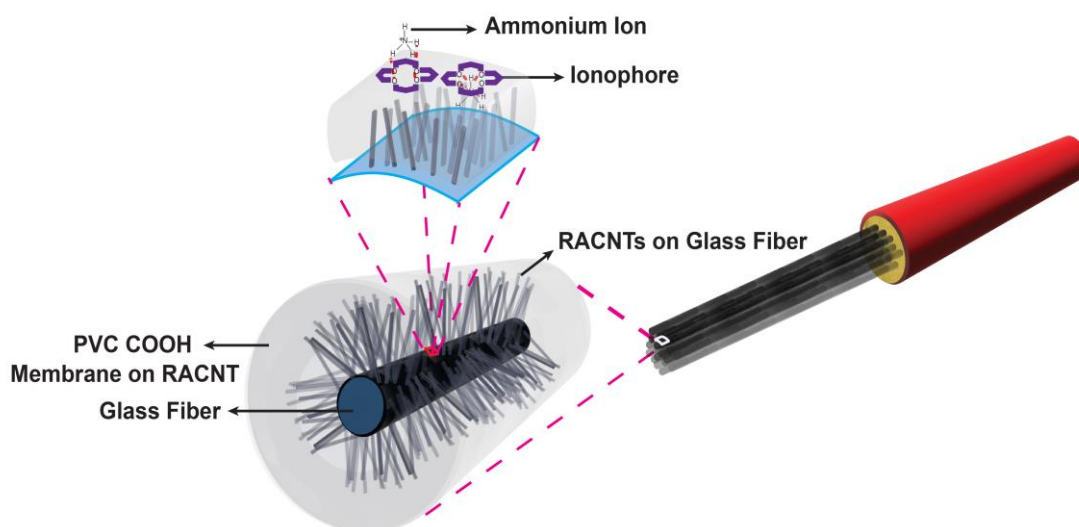


Figure 3.2 The schematic illustrations of radial alignment of CNT on GF in PVC-COOH membrane incorporating nonactin for selective NH_4^+ detection.

The r-ISE is illustrated schematically in Figure 3.2, showing how the surface area is enhanced through the radial alignment of CNT on the fibrous GF. This alignment maximizes the incorporation of nonactin, resulting in the selective and sensitive detection of NH_4^+ . For control experiments, pencil graphite electrodes (PGE) with a diameter of 0.7 mm were used. These PGEs were treated as described in previous studies (Annu et al. 2020; Santiago and Kubota 2013) and then dip-coated with a THF solution containing 100 mg of PVC/PVC-COOH, plasticizers, and nonactin in varying stoichiometric ratios. The PGE, with the same mass equivalent as the r-ISE, was used to compare the responses of these two electrodes, which differ in their planar and radially aligned carbon morphologies. The total carbon content of both the r-ISE and the PGE was standardized gravimetrically for all control experiments to ensure accurate comparisons.

3.3.2.CAGE Incorporated ISE

To create solid contact electrodes, a 1:1 ratio of graphite and epoxy was dispersed in the appropriate amount of tetrahydrofuran (THF) and mixed until it achieved a thick consistency. A 10 cm long copper wire with a 0.5 mm radius was prepared, and its open end was repeatedly dipped into this mixture to achieve a solid-state contact with a coating thickness of approximately 0.2 mm. The coated wires were then dried in an oven at 50 °C for 24 hours. Next, cage solutions were prepared by dissolving 10 mg of each cage molecule in 400 μL of THF and sonicated for 10 minutes to ensure complete dissolution. These ion-selective electrodes were then created by drop-casting the prepared cage solutions onto the surface of the coated electrodes. The electrodes were subsequently dried in an oven at 50 °C for another 24 hours to ensure proper adhesion and functionality. The detailed fabrication steps of the ion-selective electrodes (ISE) are illustrated in Figure 3.3.

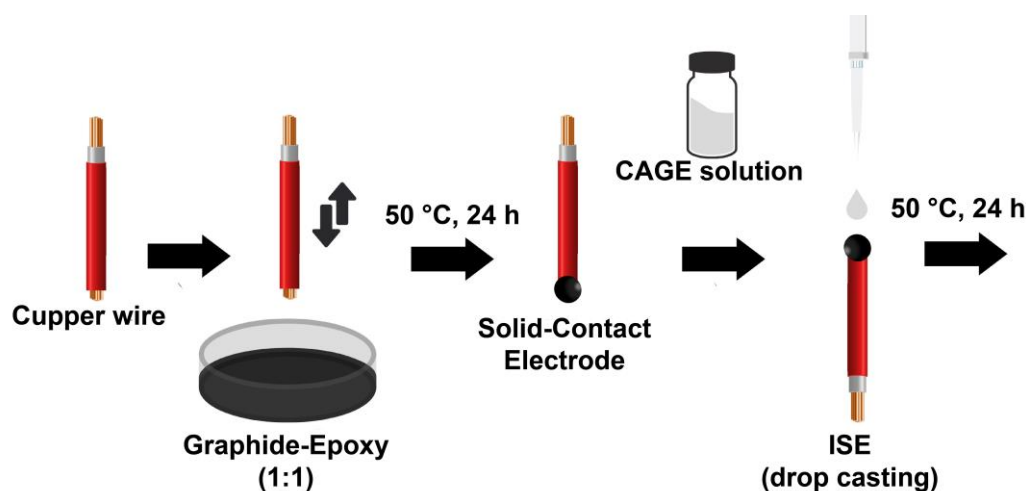


Figure 3.3 Fabrication Steps of CAGE Incorporated ISE

3.4.Flow-Injection Set-Up and Fabrication of Microfluidic Cell

A flow-injection analysis (FIA) system was employed for the quantification of NH_4^+ . This setup comprised a microfluidic cell, a syringe pump, and a valve (figure 3.5). The microfluidic cell was designed using a laser cutter to create precise channels and grooves, which housed the RAVNT-GF composite on PMMA substrates. Each PMMA substrate measured 2 cm x 2 cm with a thickness of 3 mm. The reference

electrode and the r-ISE (working electrode) were placed into designated slots on the PMMA substrate, as shown in Figure 3.4.

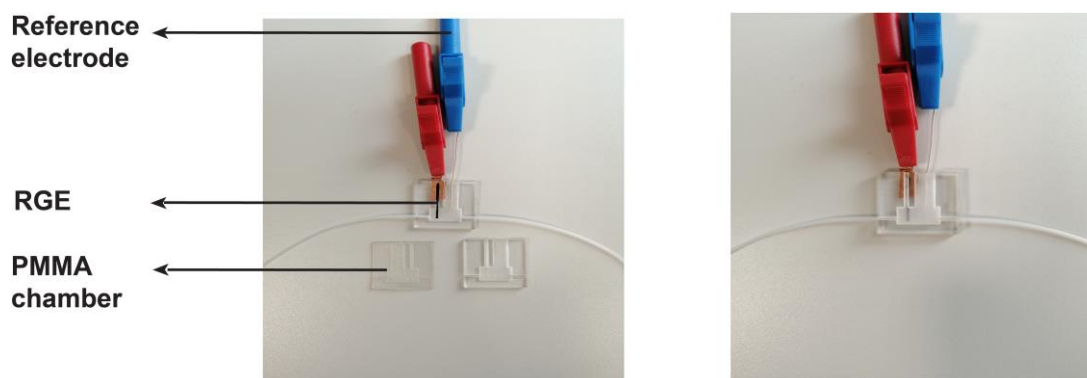


Figure 3.4 Construction of microfluidic cell

To complete the cell assembly, another PMMA substrate was used to seal the structure, secured with double-sided tape to ensure a tight and reliable bond. A standard ammonium solution (60 μL) with a carrier solution of 1 mM NaNO_3 was injected into the system at a flow rate of 0.5 ml/min through an injection loop. The potentiometric responses were monitored using a Metrohm Potentiostat/Galvanostat, and data was recorded and analyzed via the DropView software. This configuration allowed for accurate and efficient measurement of ammonium ion concentrations.

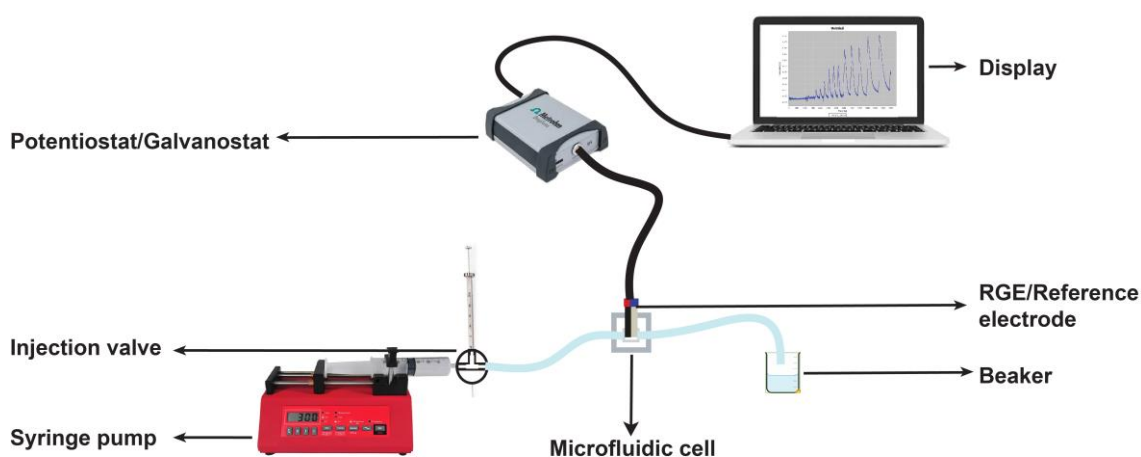


Figure 3.5 Flow injection set-up

3.5. Growth of CNT on GF

Glass fiber (GF) fabric, sourced from Hexcel (Hexforce 1543), was cut into 10 cm x 10 cm pieces (Figure 3.6. A). For the deposition of the CNT growth catalyst, aluminum nitrate ($\text{Al}(\text{NO}_3)_3$) and iron nitrate ($\text{Fe}(\text{NO}_3)_3$) were selected due to their water solubility. A solution was prepared by dissolving the salts in 100 ml of deionized (DI) water, using different Fe ratios (1:2, 1:10, and 1:50). The GF fabric pieces were then dip-coated in these catalyst solutions (Figure 3.6. B).



Figure 3.6 Preparation and CNT Growth on 10 cm x 10 cm GF Fabric: (A) Initial GF Fabric, (B) Dip-Coated with Fe Catalyst, (C) resulting CNT growth

Following the dip-coating, a chemical vapor deposition (CVD) process was used to grow CNTs on the GF fabric. The catalyst-coated GF fabric was placed inside a CVD furnace. Argon (200 sccm (standard cubic centimeters per minute)) and hydrogen (50 sccm) gases were introduced into the furnace. The temperature was gradually increased to 1035 °C over 45 minutes to eliminate any oxides present on the GF surface. Subsequently, methane, serving as the carbon precursor, was introduced into the growth chamber at a flow rate of 30 sccm for 10 minutes. After this growth period, the chamber was allowed to cool down to room temperature. The hydrogen flow was ceased once the temperature decreased to 700 °C. The GF fabric, now coated with radially aligned carbon nanotubes (RACNT), was removed from the furnace after it had cooled completely (Figure 3.6. C).

3.6.Synthesis of Cage-based Ionophores

A mixture of 1,3,5-Tris(4-hydroxyphenyl) benzene (3.5 g, 10 mmol) and DIPEA (5.0 g, 7.8 mL, 39 mmol) was gradually added to a solution of cyanuric chloride (8.3 g, 45 mmol) at 0 °C over a period of 1.5 hours. The resulting suspension was stirred continuously at 0 °C for an additional 6 hours. Upon completion of the reaction, the precipitate was filtered off, and the filtrate was concentrated under reduced pressure. The crude product was then washed three times with a DCM/hexane (1:10) mixture (20 mL each) to obtain the pure product, half-CAGE-1, as a white solid (5.7 g, 72%).

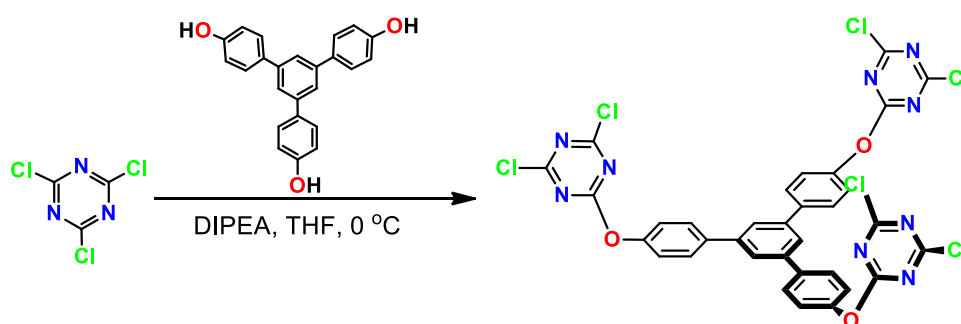


Figure 3.7 Synthesis pathways of cage compound half-CAGE-1

To a suspension of finely ground K_2CO_3 (620.0 mg, 4.5 mmol) in acetone (250 mL), a solution of Half-CAGE-1 (1.0 g, 1.3 mmol) in acetone (150 mL) and 1,3,5-Tris(4-hydroxyphenyl) benzene (445.0 mg, 1.3 mmol) in acetone (150 mL) were added simultaneously over a period of 6 hours at room temperature. The resulting mixture was then stirred continuously at room temperature for three days. Upon completion of the reaction, the solution was filtered, and the filtrate was concentrated under reduced pressure. The crude product was purified by column chromatography on silica gel using a DCM/EtOAc (100:2) eluent to yield the pure product, CAGE-1, as a white solid (271.2 mg, 25%).

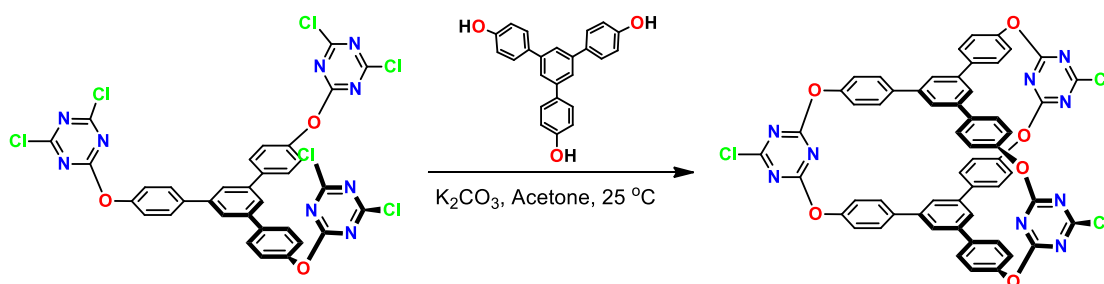


Figure 3.8 Synthesis pathways of cage compound CAGE-1

CHAPTER 4

RESULTS AND DISCUSSION

The findings in the thesis are presented under three main headings. In first study, radially aligned carbon nanotubes (RACNT) grown directly on glass fiber (GF) through the chemical vapor deposition method were explored as interface materials for the fabrication of ammonium-selective electrodes, incorporating nonactin ionophore into a PVC membrane. Initially, the optimal membrane composition was determined by examining the most suitable types of plasticizers and ionophore ratios. For the electrode prepared with the optimal membrane composition, several potentiometric performance characteristics were evaluated. These included the linear operating ranges of the electrodes, detection limits, sensitivity, response times, repeatability, and selectivity coefficient commonly used cations. Lastly, the practicality of using the prepared r-ISE as ion-selective microelectrodes (ISME) was demonstrated through assays conducted in a microfluidic cell.

In the second study, the use of a molecular cage as an ionophore for the detection of nitrate ions was thoroughly investigated. The interaction between the cage molecules and nitrate ions in a competitive environment was assessed by modifying the size and electronic structure of the cage molecules. After identifying the optimal cage structure and coating thickness, various potentiometric performance properties of the prepared electrode were evaluated. These properties included the linear ranges, detection limits, sensitivity, response times, repeatability, pH range, and selectivity coefficient commonly used anions.

In the third study, efforts were made to enhance the detection limit of ammonium electrodes prepared using Screen Printed Carbon Electrodes (SPE) by employing the drop evaporation method, without altering the electrode material or membrane composition. To achieve this, potentiometric measurements were conducted on SPEs that were modified with a chamber capable of holding a 200 μL drop. This modification aimed to improve the electrode's performance by optimizing the conditions under which the measurements were taken.

4.1. Morphological Characterization of r-ISE

As shown in Figure 4.1-A, pristine glass fiber (GF) fabric was dip-coated with Fe catalyst solutions at varying ratios (1:2, 1:10, and 1:50). The number of dip-coating cycles and the withdrawal rate were optimized to achieve a uniform catalyst coating, indicated by the consistent pale-yellow color observed in Figure 4.1-C. Subsequently, carbon nanotubes (CNTs) were directly grown on the GF fabric using a chemical vapor deposition (CVD) protocol, with all growth parameters, including growth time and temperature, optimized to ensure a homogeneous CNT distribution. The different catalyst ratios produced three distinct CNT morphologies, as revealed by scanning electron microscopy (SEM): radially aligned and non-homogeneous (Figure 4.1-A), radially aligned and homogeneous (Figure 4.1-C), and randomly oriented and non-homogeneous. The enhanced homogeneity and radial alignment of CNTs with the 1:10 Fe catalyst ratio is attributed to the optimal proportion of aluminum salts, which prevents the aggregation of large Fe nanoparticles and ensures optimal Fe distribution on the GF fabric, thereby promoting CNT growth. (Sakurai et al. 2012) It is hypothesized that either insufficient or excessive aluminum salts lead to non-homogeneous Fe nucleation sites on the GF fabric or hinder CNT growth by blocking the carbon precursor from reaching the Fe nucleation sites. Figure 4.1-B shows an optical microscopy image of individual GFs within the GF fabric (highlighted in the blue box in Figure 4.1-A), displaying cohered GF filaments uniformly coated with CNTs. High-resolution SEM analysis of a single GF filament (highlighted in the red box in Figure 4.1-C) reveals a darker core and a lighter shell (Figure 4.1-D), corresponding to the GF filament and radially aligned CNTs (RACNT), respectively. This observation further confirms the radial alignment and uniform growth of CNTs on the GF filaments. The diameter of the individual fiber is approximately 10 μm , consistent with the specifications of the original GF fabric.

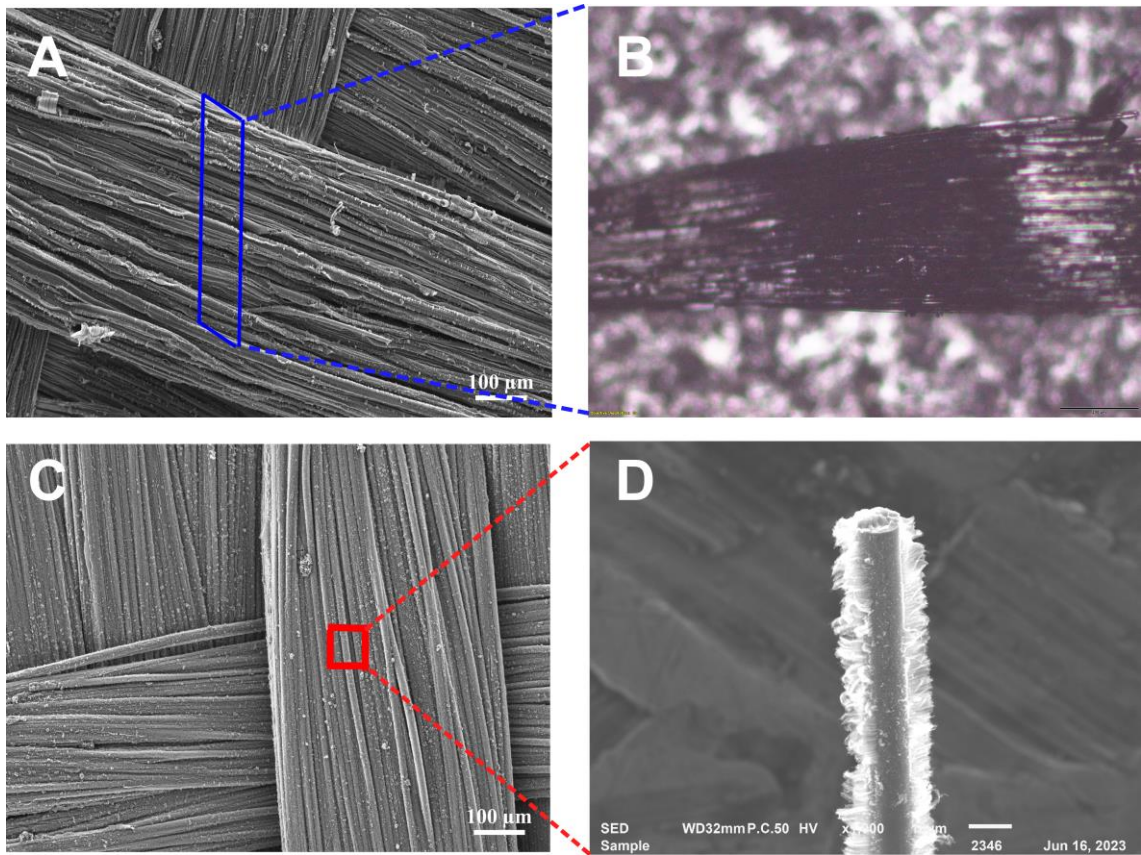


Figure 4.1 GF with CNTs grown using Fe catalyst ratios of 1:2 (A) and 1:10 (C). Optical microscopy image of an individual GF Fiber post-CNT growth (B), and SEM image of a single GF filament post-CNT growth displaying radial CNT alignment (D).

4.2.Determination of Optimal Membrane Composition

In PVC membrane ion-selective electrodes, the ratios of PVC, ionophore, plasticizer, and ionizer, as well as the types of plasticizers and ionizer, are critical parameters influencing the potentiometric performance of the electrode.(Shamsipur et al. 2001) To identify the electrode with optimal potentiometric performance, various membrane compositions were prepared by altering these parameters. The potentiometric performance properties slope, detection limit, linear range, and R^2 value for the calibration curve of the electrodes fabricated using these membranes were systematically investigated.

4.2.1. Investigation of Plasticizer Effect

The impact of various plasticizers (o-NPOE, DOP, and DOS) on the performance of the prepared electrodes was evaluated. The membrane composition was formulated with 3.0% (w/w) ionophore, 30.0% (w/w) PVC, and 67.0% (w/w) plasticizer, based on a total mass of 100 mg.

Table 4.1 Potentiometric Performance Characteristics of r-ISEs Prepared with Various Plasticizers

Plasticizers	Slope, mV dec ⁻¹	LOD, M	LRR, M	R ²
o-NPOE	12.6	1.0×10 ⁻⁵	1.0×10 ⁻⁴ -1.0×10 ⁻¹	0.939
DOS	45.9	1.0×10⁻⁵	1.0×10⁻⁵-1.0×10⁻¹	0.999
DOP	19.1	1.0×10 ⁻⁵	1.0×10 ⁻⁵ -1.0×10 ⁻²	0.864

Table 4.1 demonstrates that the PVC membrane electrode prepared with DOS, among the plasticizers studied, exhibits superior slope, linear working range, and detection limit values compared to membranes prepared with other plasticizers. The slope of the membrane with the DOS plasticizer was significantly better than those prepared with other plasticizers and showed behavior more consistent with the Nernstian response (Figure 4.2). Based on these findings, DOS was determined to be the most suitable plasticizer for membrane preparation.

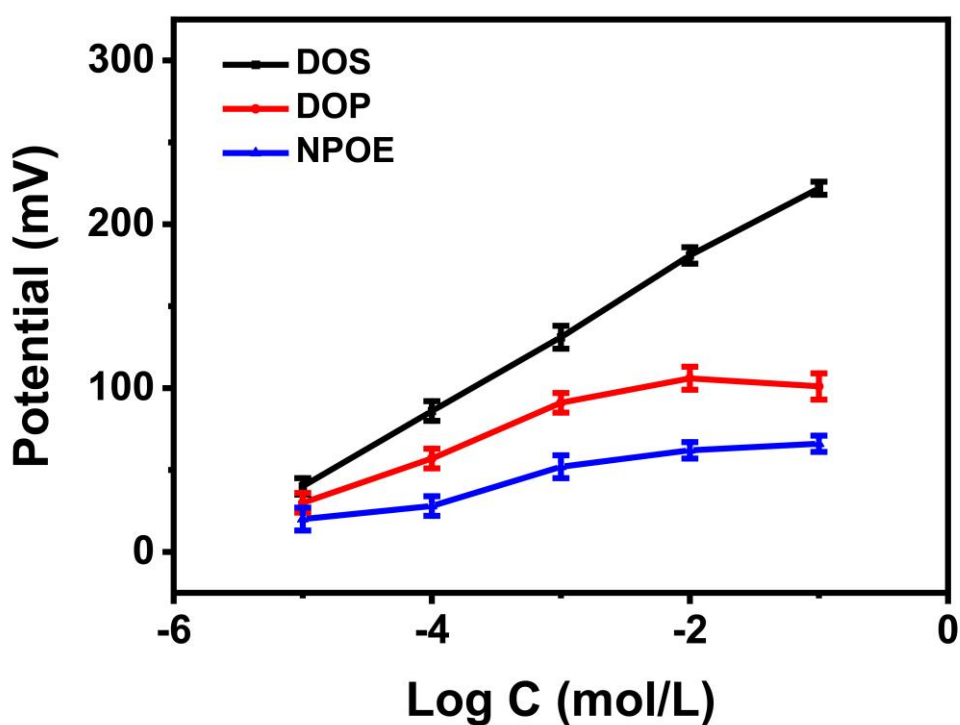


Figure 4.2 Potentiometric response of r-ISE prepared with different plasticizers

4.2.2. Investigation of The Percentage of Ionophores

This study examined the potentiometric performance properties of r-ISEs, which were prepared by incorporating ionophores at increasing concentrations from 0.8% to 3.5% (w/w) into membranes composed of both PVC and PVCCOOH.

Table 4.2 Impact of Ionophore Concentration on the Potentiometric Performance Characteristics of r-ISE with PVC membrane

Ionophore, % (w/w)	Slope, mV dec ⁻¹	LOD, M	LRR, M	R ²
0.8	26.4	1.0×10 ⁻⁵	1.0×10 ⁻⁵ -1.0×10 ⁻²	0.955
1.4	34.5	1.0×10 ⁻⁵	1.0×10 ⁻⁵ -1.0×10 ⁻¹	0.954
2.0	24.3	1.0×10 ⁻⁵	1.0×10 ⁻⁵ -1.0×10 ⁻¹	0.947
3.0	45.9	1.0×10⁻⁵	1.0×10⁻⁵-1.0×10⁻¹	0.999
3.5	15.6	1.0×10 ⁻⁵	1.0×10 ⁻⁴ -1.0×10 ⁻¹	0.932

Table 4.2 reveals that increasing the ionophore percentage in the membrane enhances the electrode's performance. However, when the ionophore concentration exceeds 3%, there is a noticeable decline in the slope and a reduction in the linear range. Experimentally, the PVC membrane composition containing 3.0% ionophore was determined to possess the optimal properties among the compositions tested.

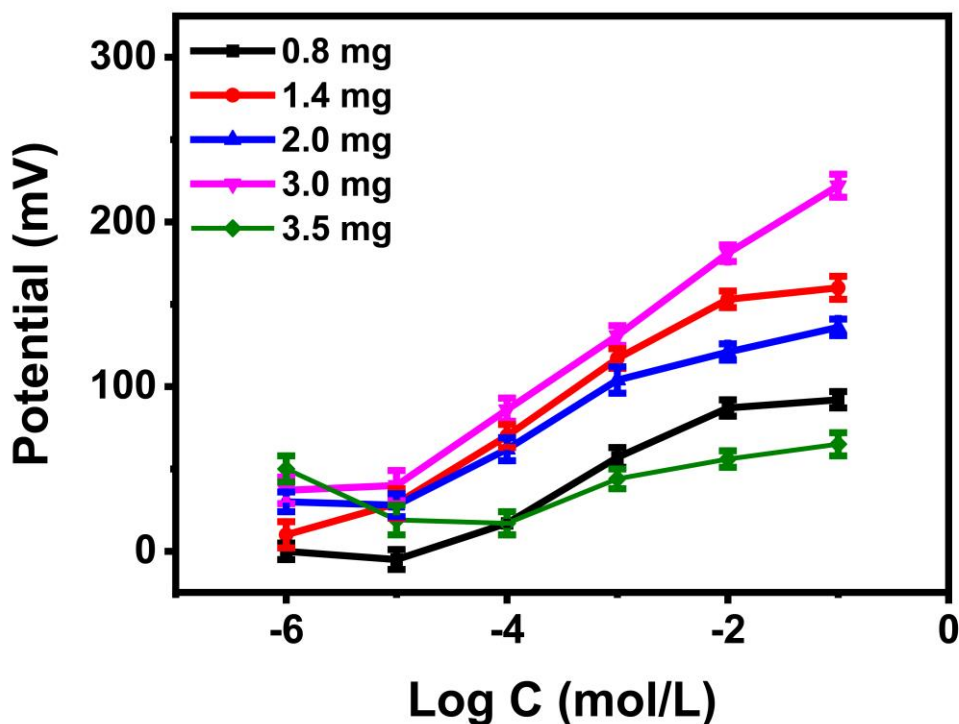


Figure 4.3 Potentiometric response of PVC r-ISE prepared with different ionophore percentage

Table 4.3 Impact of Ionophore Concentration on the Potentiometric Performance Characteristics of r-ISE with PVCCOOH membrane

Ionophore, % (w/w)	Slope, mV dec ⁻¹	LOD, M	LRR, M	R ²
0.8	44.1	1.0×10 ⁻⁵	1.0×10 ⁻⁵ -1.0×10 ⁻¹	0.998
2.0	35.6	1.0×10 ⁻⁵	1.0×10 ⁻⁵ -1.0×10 ⁻¹	0.990
2.2	32.6	5.0×10 ⁻⁶	1.0×10 ⁻⁵ -1.0×10 ⁻¹	0.987
3.0	58.2	7.5×10⁻⁶	1.0×10⁻⁵-1.0×10⁻¹	0.998
3.5	43.9	1.0×10 ⁻⁵	2.5×10 ⁻⁵ -1.0×10 ⁻¹	0.996

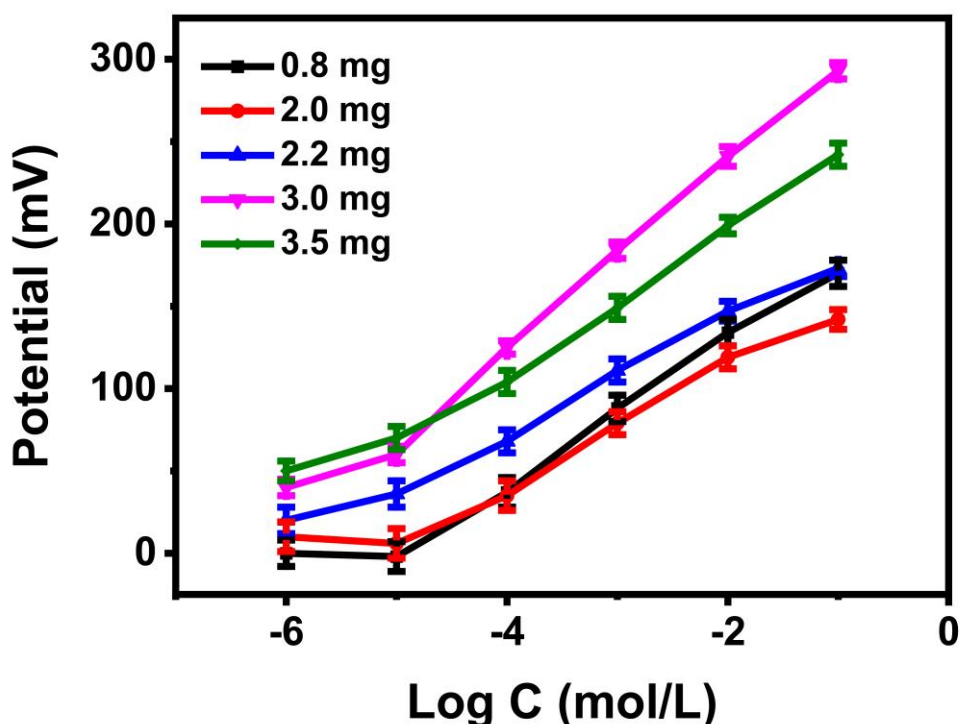


Figure 4.4 Potentiometric response of PVCCOOH r-ISE prepared with different ionophore percentage

The influence of membrane composition was examined using PVC-COOH with DOS as the plasticizer at different nonactin concentrations. Table 4.3 and Figure 4.4 indicate that the PVC-COOH membrane with a nonactin concentration of approximately 3% exhibits the most favorable potentiometric characteristics in terms of linear range and slope.

4.2.3. Investigation of Polymer (PVC) Membrane Modification

As shown in Table 4.3, the PVC-COOH membrane with approximately 3% nonactin delivers the most favorable potentiometric performance in terms of linear range and slope. The enhanced response is likely due to the presence of COOH/COO groups, which facilitate Donnan anion exclusion. With the membrane's fixed negative charges, cations can move through more easily than anions, allowing for efficient nonactin-NH₄⁺ interactions. According to Table 4.3, the ideal combination for sensitive NH₄⁺ detection on r-ISE consists of around 30% PVC-COOH, 67% DOS, and 3%

nonactin (ratios highlighted in bold). With the correct nonactin concentration and a suitable plasticizer, the r-ISE demonstrates high sensitivity, providing a clear, proportional response to varying NH_4^+ ion concentrations.

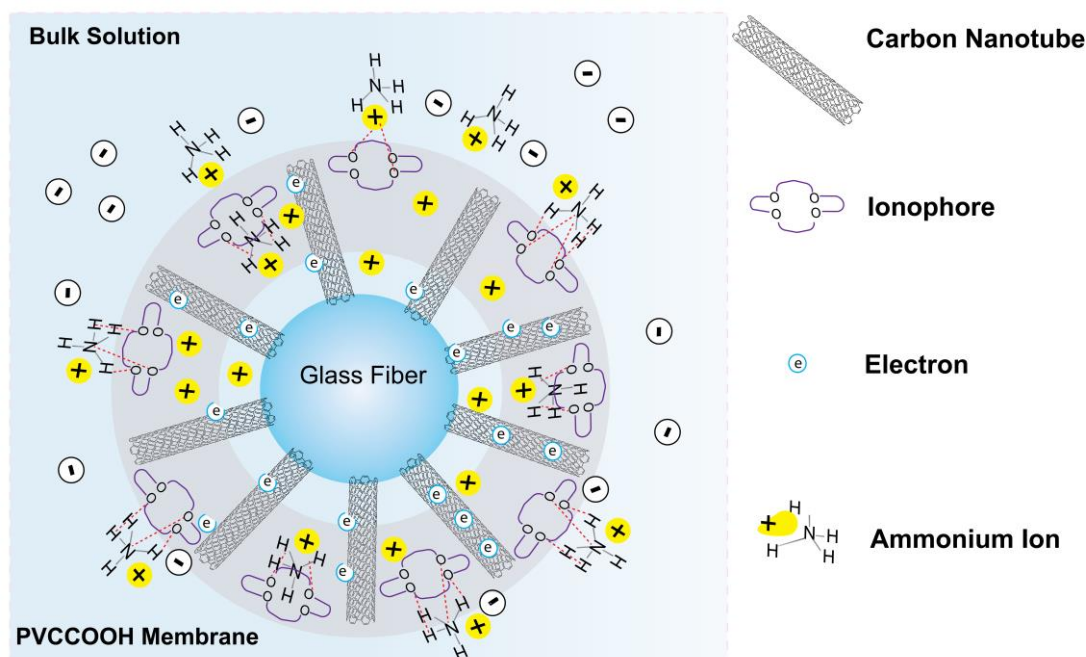


Figure 4.5 Potentiometric Sensing mechanism of r-ISE

As shown in Figure 4.5, the sensing mechanism of the NH_4^+ r-ISE, which utilizes radially aligned carbon nanotube glass fiber composites as a solid contact, can be described as follows: The membrane matrix typically includes polyvinyl chloride functionalized with carboxyl groups, enhancing both mechanical stability and ionic exchange properties (counter ions NO_3^- , as indicated by “ \ominus ” in Fig. 4.5). Nonactin, known for its high selectivity towards ammonium ions, is incorporated to target these specific ions. Importantly, the presence of carboxyl groups introduces fixed negative charges within the membrane, which plays a critical role in establishing the Donnan equilibrium at the membrane-solution interface. This equilibrium affects the distribution of both co-ions (NO_3^-) and counterions (NH_4^+) across the membrane, thereby influencing the overall ion selectivity and response of the electrode. The Donnan potential, established due to the differential ion distribution, contributes to the observed potential response, and must be considered when interpreting the r-ISE performance. The RACNT-GF serves as the solid contact layer within the r-ISE. This composite structure consists of radially aligned carbon nanotubes embedded within a glass fiber

substrate. The alignment and high surface area of the carbon nanotubes provide excellent conductivity and facilitate efficient electron transfer between the membrane and the electrode interface. The high conductivity and electron transfer efficiency of the radially aligned carbon nanotubes ensure minimal resistance, resulting in a stable baseline potential. The utilization of RACNT as a solid contact material ensures efficient electron transfer as compared to planar graphite electrodes (PGE) with a planar carbon morphology (Fig. 4.8 and 4.9). The design, when combined with the ion-selective properties influenced by Donnan equilibrium, minimizes potential interferences from other ions and environmental factors, thereby improving both the selectivity and sensitivity of the electrode.

4.3. Potentiometric Performance Characteristics of r-ISE

To assess the response of r-ISE to ammonium ions, potentiometric measurements were conducted using a series of standard solutions. These solutions were prepared by diluting a 1.0×10^{-1} M ammonium stock solution with appropriate amounts of deionized water. The potential values recorded in response to varying ammonium concentrations are depicted in Figure 4.6.

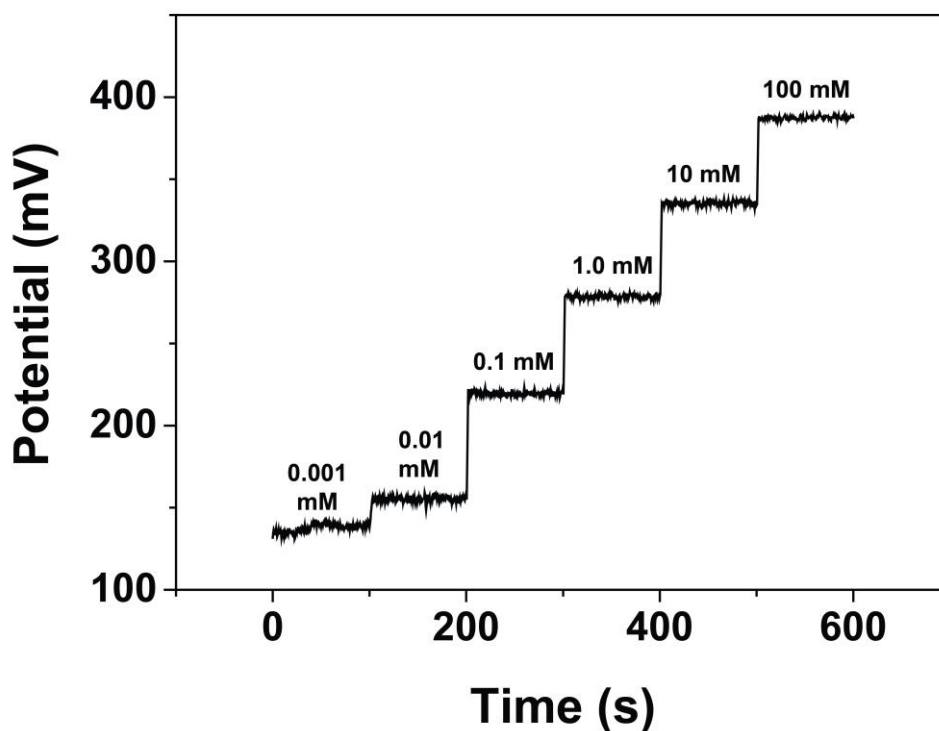


Figure 4.6 Potentiometric response of r-ISE in ammonium solutions at various concentrations

4.3.1. Forming the r-ISE Calibration Curve: Determining Slope, LOD, and LRR

The potential versus log concentration (potential-log C) graph, derived from the potential and concentration data presented in Figure 4.6, is also shown in Figure 4.7. This graph illustrates the relationship between electrode potential and the logarithm of ammonium ion concentration, providing further insights into the potentiometric response of the r-ISE.

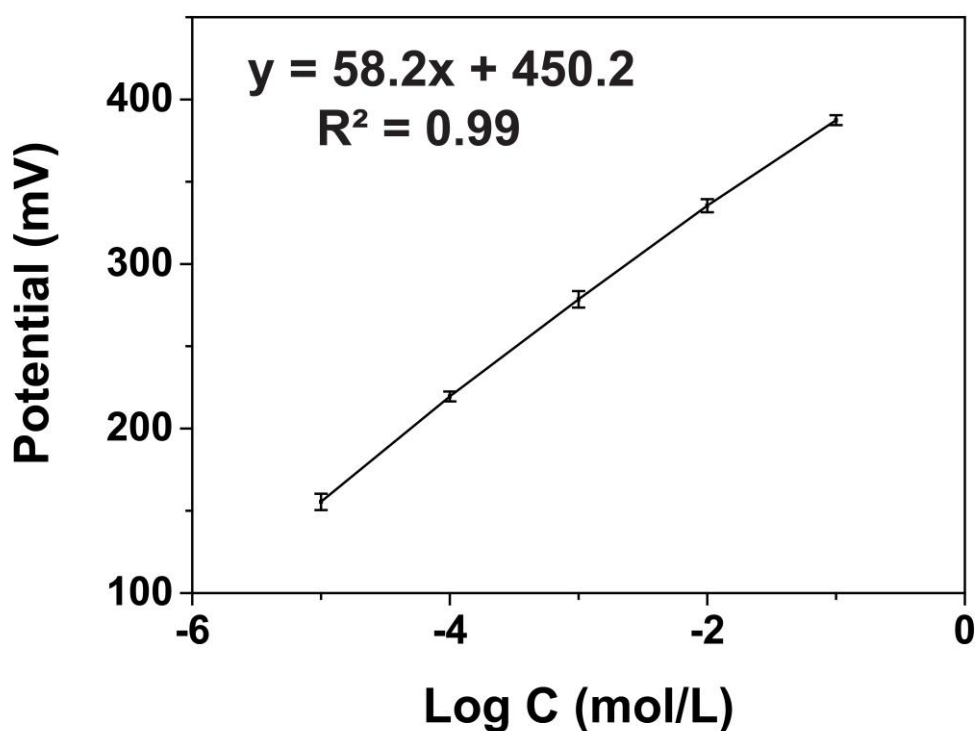


Figure 4.7 Linear calibration plot for NH_4^+ detection

Figure 4.6 presents the time-dependent potentiometric response of the r-ISE to NH_4^+ ions in aqueous solutions with concentrations ranging from 1.0×10^{-6} to 1.0×10^{-1} M. The potential-log C plot (Figure 4.7) demonstrates that the r-ISE exhibited a linear response within the concentration range of 1.0×10^{-5} to 1.0×10^{-1} M, with a correlation coefficient (R^2) of 0.99 and a slope of 58 ± 0.6 mV per decade of concentration. In accordance with IUPAC recommendations (Buck and Lindner 1994b), the limit of detection (LOD) for the r-ISE was determined to be 7.5×10^{-6} M, calculated from the intersection of the two extrapolated segments of the calibration curve.

4.3.2. Determination of r-ISE Selectivity

The potentiometric selectivity of an ion-selective electrode is crucial as it indicates the electrode's relative response to the primary ion in the presence of interfering ions. Typically, selectivity coefficients are determined using the methods specified in the IUPAC protocol, with the separate solution method employed to calculate these coefficients for various interfering ions. (Yoshio Umezawa et al. 2000)

The procedure involves creating a calibration curve with primary ion (NH_4^+ , denoted as " a_A ") solutions at concentrations ranging from 1.0×10^{-6} to 1.0×10^{-1} M. The r-ISE is then tested in individual interfering ion solutions with a concentration of 1.0×10^{-2} M (denoted as " a_B "), and the corresponding potential values for each interfering ion are recorded. These potential values are subsequently used to determine the activity of the primary ion using the calibration plot. The selectivity coefficient values ($K_{A,B}^{pot}$) listed in Table 4.4 were obtained by substituting the calculated primary ion activity (a_A) and the corresponding interfering ion activity (a_B) into the relevant equation.

$$K_{A,B}^{pot} = a_A / (a_B)^{Z_A/Z_B} \quad (4.1)$$

Where Z_A and Z_B represent the net charges of the primary and interfering ions, respectively. Table 4.4 indicates that the tested cations do not significantly interfere with the r-ISE's performance. The electrode maintains a selectivity of at least 100-fold, even in the presence of the most interfering ion, K^+ , in the assay solution.

Table 4.4 Selectivity coefficients of ammonium-selective r-ISE to various cationic species calculated using the separate solution method

Interferents	Log K
K^+	1.8
Na^+	2.8
Li^+	4.2
Ca^{2+}	4.5

4.4. Comparison of r-ISE with Pencil Graphite Electrode

The potentiometric responses of electrodes utilizing RACNT, and pencil graphite as solid contact materials were compared against several common cations. As illustrated in Figure 4.8, the electrode prepared with RACNT demonstrates superior potentiometric performance, notably in terms of slope and selectivity, compared to the one with pencil graphite.

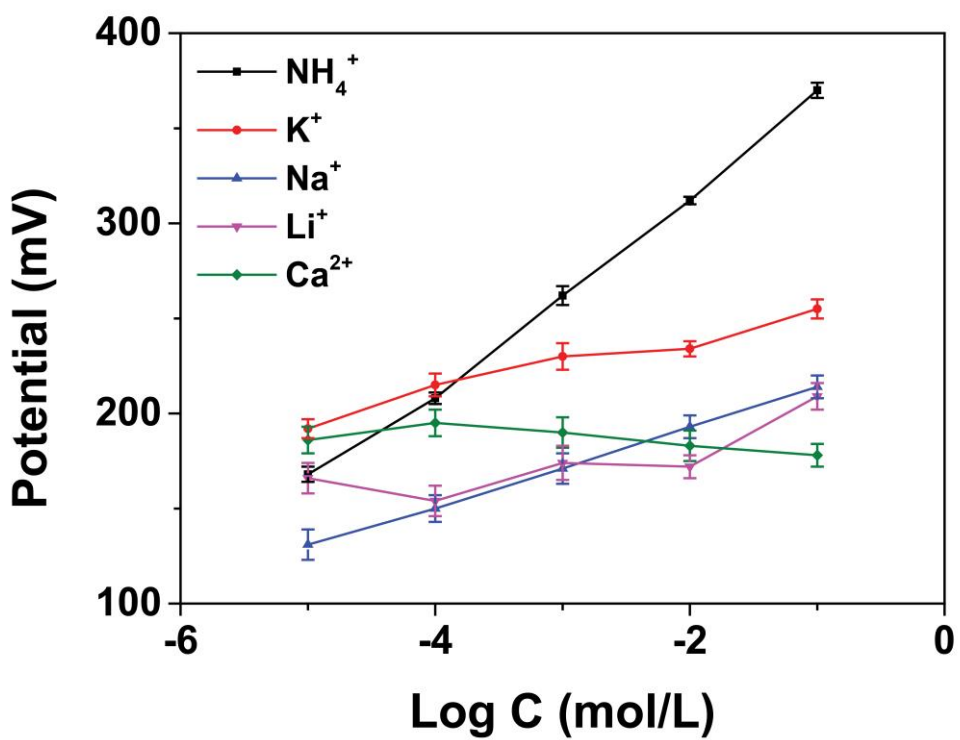


Figure 4.8 Potentiometric response of r-ISE for varying concentrations of cations.

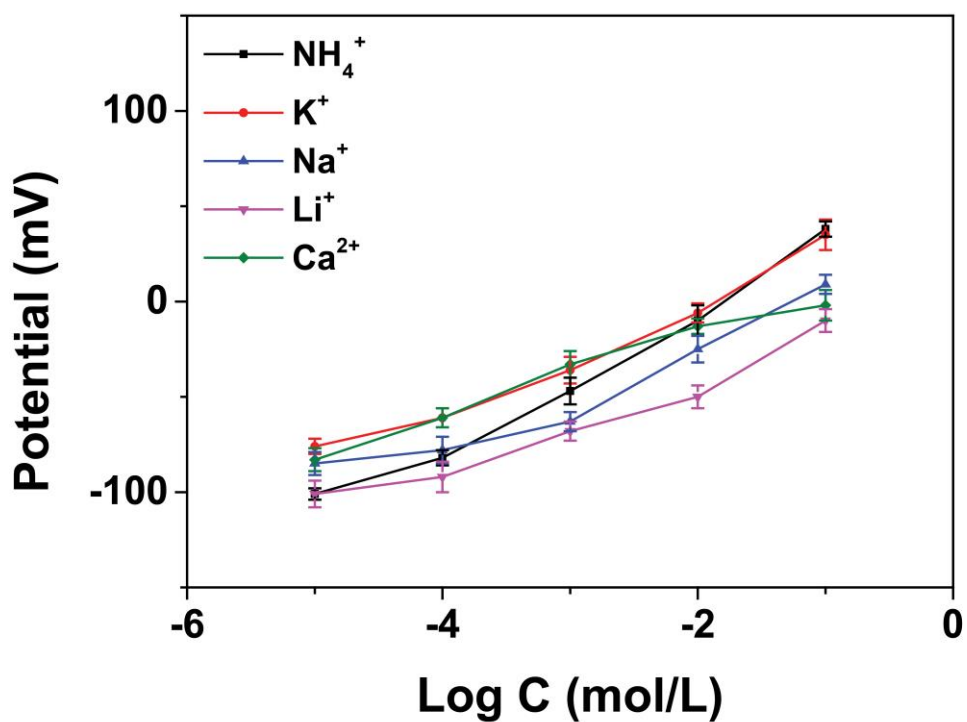


Figure 4.9 Potentiometric response of pencil graphite electrode for varying concentrations of cations.

The use of RACNT as a solid contact material markedly enhances the diffusion of NH_4^+ , as demonstrated by the superior potentiometric performance of the r-ISE compared to the pencil graphite electrode (PGE) with a planar carbon morphology (Figures 4.8 and 4.9). This observation confirms that the RACNT network, with its high surface area and the fibrous morphology of GF, collectively improves the capture of NH_4^+ , enabling effective signal transduction even at lower concentrations compared to conventional ISEs with planar morphologies.

4.5. Comparison of the lifetime of r-ISE with PGE

For the potential stability of the ammonium-selective RACNT and PGE, the slope was measured at regular intervals over 6 h. The change in slope per hour (slope/h) was recorded to evaluate the stability of both electrodes over time. Over the 6-hour period, the RACNT electrode exhibited a consistent decline in slope, with an average change of -1.4 mV/h , indicating relatively stable potential behaviour with a gradual decrease in sensitivity. In comparison, the PGE showed a more pronounced decline, with an average change of -3.8 mV/h , suggesting a faster loss of sensitivity over the same period.

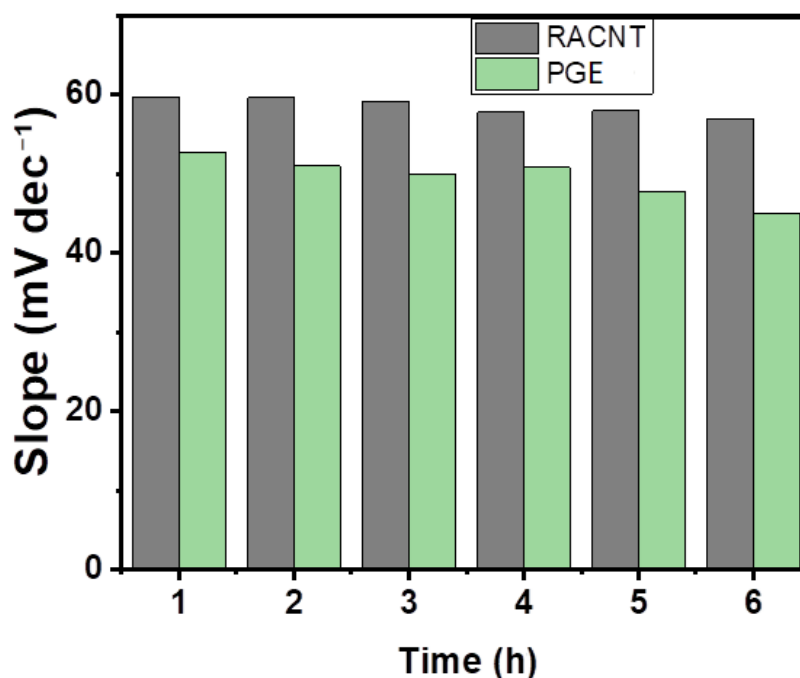


Figure 4.10 Change in the slope of the ammonium-selective electrodes with time (hour)

To determine the lifetime of the electrodes utilizing both RACNT and PGE, calibration curves were created by taking measurements on different days in ammonium solutions within the concentration range of 1.0×10^{-5} to 1.0×10^{-1} M, where both electrodes exhibited a linear response. Figure 4.11 reveals a decline in the slope of both the RACNT and PGE around the fifteenth day. For commercial electrodes, the lifespan is defined as the time taken for the electrode's slope to decrease to ~70% of its initial value. Accordingly, for the r-ISE the initial slope value (58.2 mV per decade concentration change) should decrease to 40.7 mV per decade concentration change by the end of its usage period. It was observed that after 15 days of use, the slope of the electrode reduced to ~38.7 mV per decade concentration change. As a result, the lifespan of both the RACNT and PGE could be estimated to be ~15 days. Before measurements were taken, the electrodes were conditioned in a 1.0×10^{-2} M NH_4^+ solution for 30 min. When not in use, the electrodes were stored in a closed and dark environment at room conditions.

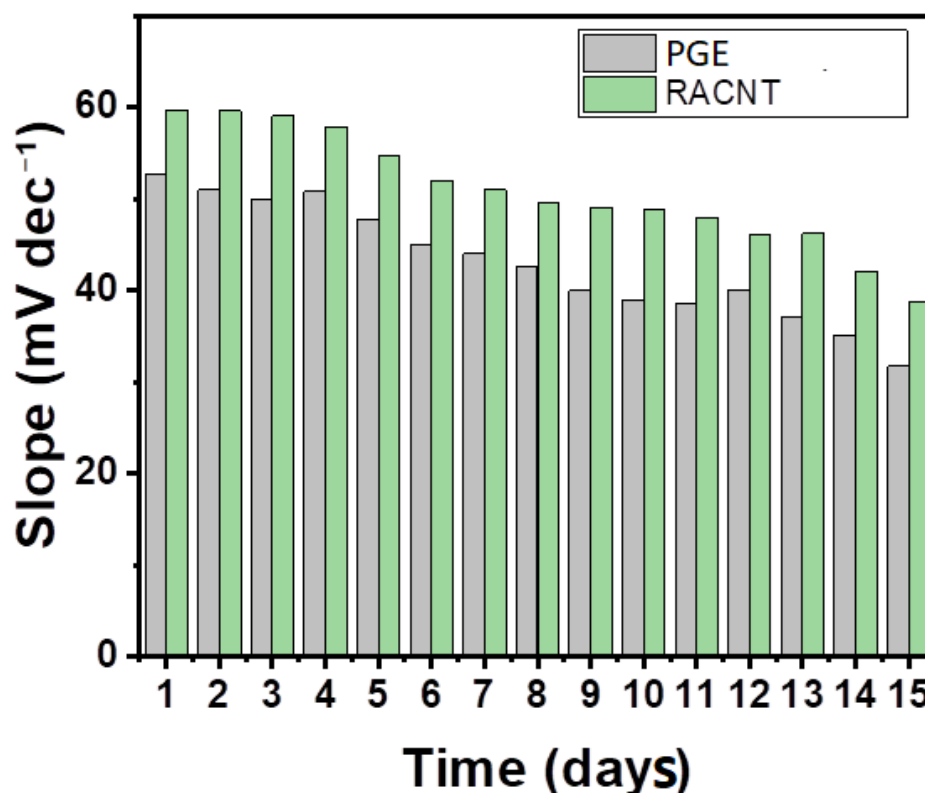


Figure 4.11 Change in the slope of the ammonium-selective electrodes with time (day)

4.6. Determination of ISME Assay Performance

Figure 4.12 depicts the typical flow injection responses of the r-ISE for repeated injections of standard ammonium solutions. The potentiometric assay's consistency and the high reproducibility of the ISE fabricated with the RACNT-GF composite are evident from the triplicate injections of NH_4^+ at all test concentrations. An increase in peak width was observed at higher concentrations, likely due to the reduced diffusion rate of NH_4^+ within the PVCCOOH membrane. This can be optimized by adjusting the injection flow rate of the assay solution. When operated in the flow injection analysis (FIA) mode with a 1 mM sodium nitrate carrier solution, a near-Nernstian response with a slope of 54.2 ± 1.2 mV/decade was achieved.

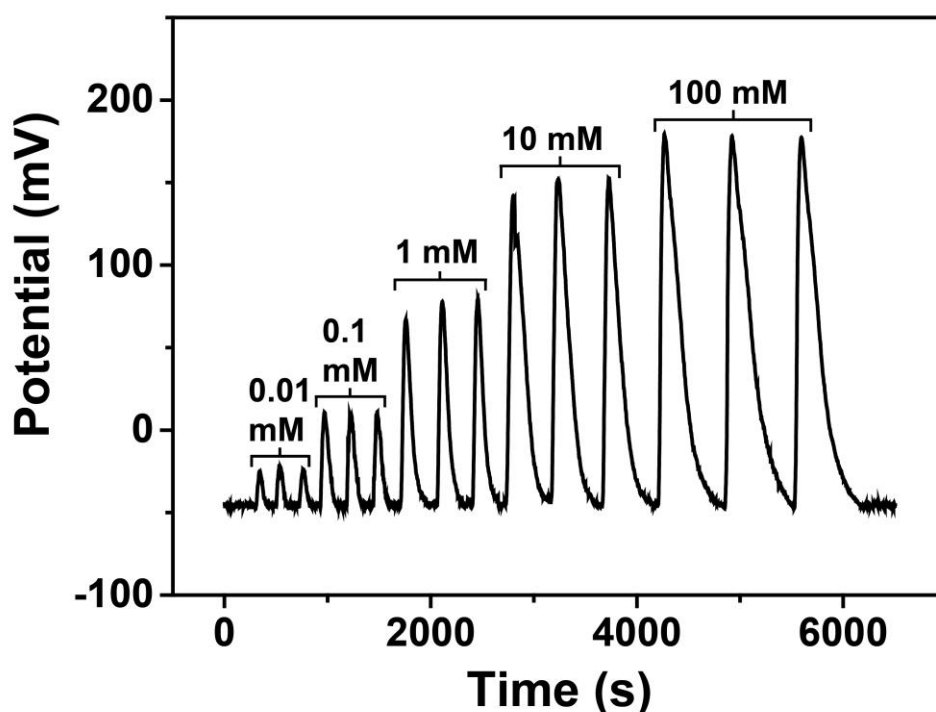


Figure 4.12 Potentiometric response of r-ISE in the FIA system

The calibration curve presented in Figure 4.13 was constructed from the flow injection potentiometric responses shown in Figure 4.10 by averaging the responses obtained from triplicate injections. The linearity of the calibration curve indicates that the effects of diffusion limitations and carrier phase interference are minimal. Although the r-ISE incorporates RACNT with transduction materials on the nanometer scale, their

density and homogeneity effectively mitigate diffusion-specific limitations in confined flow settings. Consequently, the slope of the ISME's potentiometric response in flow injection mode is consistent with that obtained under steady-state conditions. Therefore, the RACNT-GF composite is a promising material for fabricating ISMEs with miniaturized dimensions and robustness for ion assays in microfluidic environments.

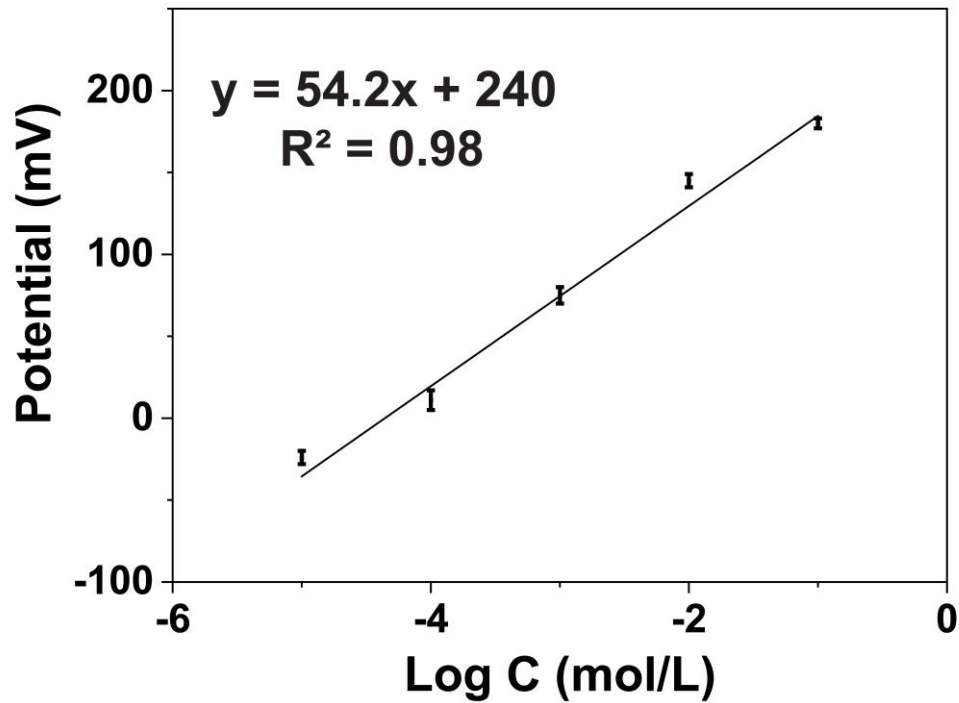


Figure 4.13 Calibration curve of r-ISE in the FIA system

4.7.Synthesis and Analysis of Cage-based Ionophores

The cage compounds were analyzed using Fourier transform infrared spectroscopy (FT-IR), nuclear magnetic resonance spectroscopy (NMR), and mass spectrometry (MS). Initially, the chemical structure of the cage compounds was confirmed through FT-IR (Figure 4.14-C). The presence of characteristic triazine stretching bands at 1500 and 1350 cm^{-1} indicates that the cage units' structure is preserved. Additionally, the disappearance of the chlorine groups' (C-Cl) stretching band at 750 cm^{-1} , along with the emergence of distinct aliphatic stretching (C-H) bands from dimethylamine moieties, signifies the conversion of CAGE-0 and CAGE-1 into aCAGE-0 and aCAGE-1, respectively. The formation of the cage structures was further verified using ^1H NMR spectroscopy (Figure 4.14-A and B).

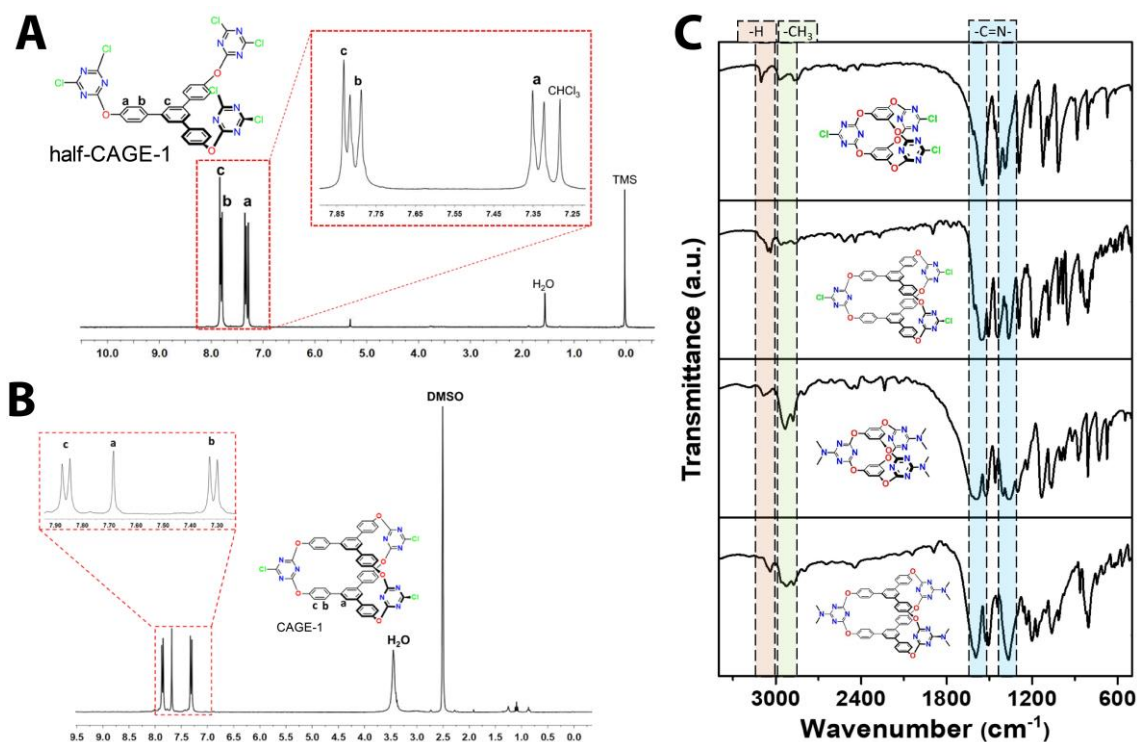


Figure 4.14 ^1H NMR spectra of half-CAGE-1(A), ^1H NMR spectra of CAGE-1 (B), and FT-IR spectra of cage molecules(C).

The proton signals linked to the central benzene ring of the 1,3,5-tri(p-hydroxyphenyl)benzene unit shifted upfield after reacting with an equimolar amount of 1,3,5-tri(p-hydroxyphenyl)benzene and Half-CAGE-1. This shift in the spectrum confirms the formation of CAGE-1. Additionally, nucleophilic substitution reactions on

CAGE-0 and CAGE-1 with dimethylamine resulted in a significant downfield shift for all the protons, along with the emergence of a distinct C-H signal.

4.8. Morphological Characterization of CAGE Incorporated ISE

Incorporation of ion-selective CAGE molecules onto the electrodes was achieved via the dip-coating technique. The morphological characteristics of the electrodes were examined using Scanning Electron Microscopy (SEM). The SEM images are presented in Figure 4.15, with Figure 4.15-A illustrating the electrode without CAGE ionophores and Figure 4.15-B showing the electrode after a single dip-coating step with CAGE ionophores. Higher magnification SEM images reveal the presence of graphite flakes prior to the incorporation of CAGE molecules (Figure 4.15-A). Post-incorporation, the surface features of the graphite flakes are less distinct, indicating the successful formation of a uniform layer of CAGE molecules (Figure 4.15-B).

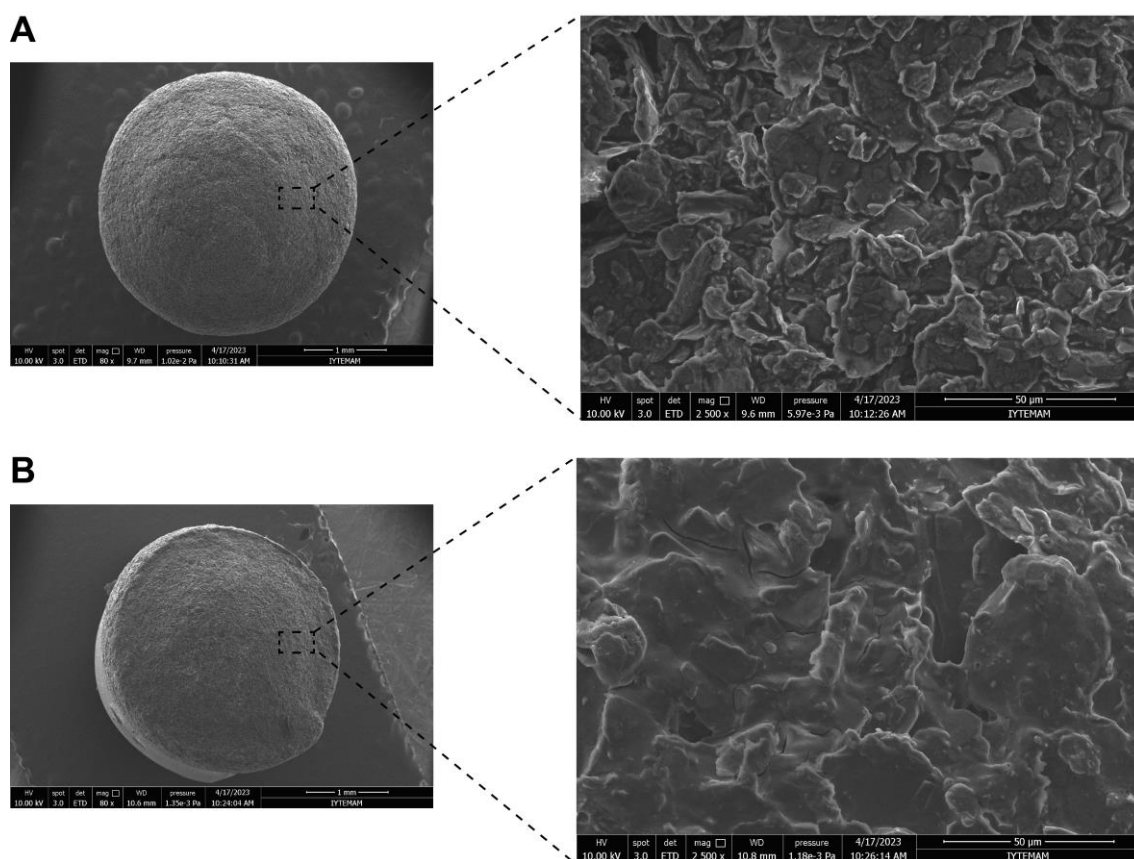


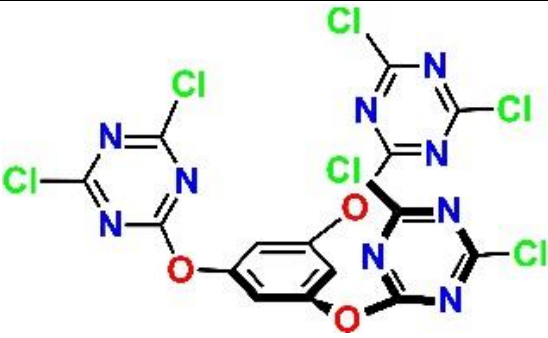
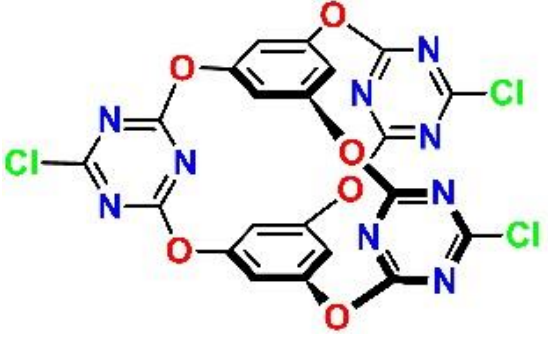
Figure 4.15 SEM Images of Electrodes Pre- (A) and Post- (B) CAGE Incorporation

4.9. Determination of Optimal CAGE and Composition

Systematic variations in the structure and size of the CAGE molecules significantly influence their interaction with NO_3^- ions. In this study, the optimal molecular CAGE structure for NO_3^- ion interaction was initially identified (Table 4.5). Subsequently, the coating thickness of this optimal structure was evaluated (Table 4.6).

Table 4.5 illustrates the impact of different CAGE structures on the potentiometric performance characteristics of electrodes in the presence of NO_3^- ions, within a concentration range of 1.0×10^{-1} to 1.0×10^{-5} M. The data in Table 4.5 reveal that electrode E4 (CAGE-1) exhibited the most pronounced slope and highest R^2 value within the specified linear range for NO_3^- ions. This underscores the critical role that systematic variations in the structure and size of CAGE molecules play in their interaction with NO_3^- ions.

Table 4.5 Impact of CAGE structure on the potentiometric performance characteristics of NO_3^- selective electrodes

Electrode Code	Cage type	Structure	Slope	R^2
B1	-	-	-10.9	0.7347
E1	Half-CAGE-0		-46.7	0.9613
E2	CAGE-0		-42.5	0.9635

(cont. on next page)

Table 4.5 (cont.)

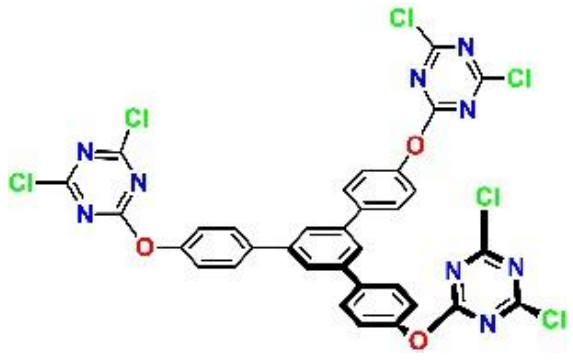
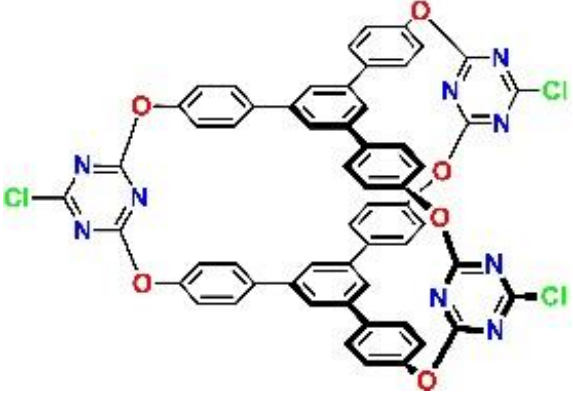
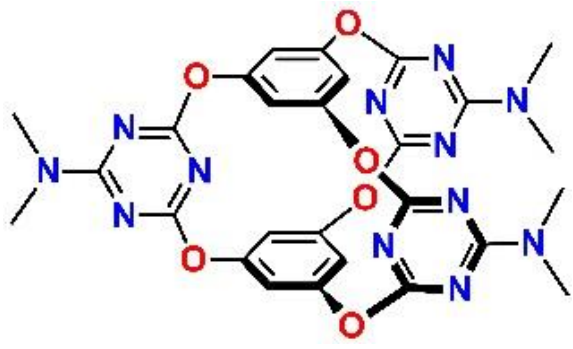
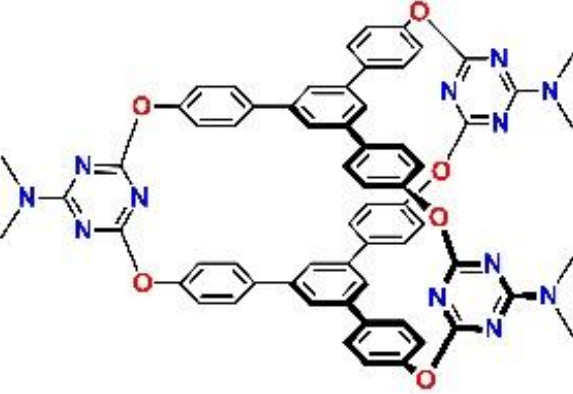
E3	Half-CAGE-1		-45.5	0.9798
E4	CAGE-1		-50.3	0.9956
E5	aCAGE-0		-29.8	0.9418
E6	aCAGE-1		-31.2	0.9069

Table 4.6 Impact of coating cycle on the potentiometric performance characteristics of NO₃⁻ selective electrodes

Electrode Code	Coating Cycle (5μL)	Slope	R ² value
E4.1	1 Cycle	-53.1	0,997
E4.2	2 Cycles	-50,3	0,996
E4.3	3 Cycles	-45,5	0,993
E4.4	4 Cycles	-42,5	0,974

To assess the significance of CAGE structure in the detection of NO₃⁻ ions, electrodes E1 and E3 were intentionally designed with an open geometry, termed Half-CAGEs, which are anticipated to interact less effectively with NO₃⁻ ions compared to electrodes E2 and E4, which possess a CAGE geometry favourable for NO₃⁻ ion encapsulation. Electrodes E1 and E3, prepared using Half-CAGE-1 and Half-CAGE-3 respectively, exhibited similar slopes (dV/dC) over the concentration range of 1.0×10⁻¹ to 1.0×10⁻⁵ M. However, these electrodes did not demonstrate a fully reversible exchange of NO₃⁻ ions between the electrodes and the solution. This finding indicates that Half-CAGEs do not facilitate reversible NO₃⁻ ion binding as ionophores under the tested conditions. Subsequently, the CAGE structures of electrodes E2 and E4 were evaluated under the same conditions, yielding slopes (dV/dC) of -42.5 and -50.3 mV, respectively. Despite both CAGE structures exhibiting the same symmetry and functionality, the response of electrode E4, which has a larger CAGE size, demonstrated a higher level of reversible interaction compared to electrode E2 with a smaller CAGE size. The reversible response observed in electrode E4, as opposed to the non-reversible response in electrode E2, can be attributed to the differing sizes of the CAGE structures incorporated into each electrode. Electrode E4 possesses a CAGE size specifically designed to effectively accommodate NO₃⁻ ions, resulting in a more stable and reversible interaction between the electrode and the ions in solution. Consequently, electrode E4 exhibits a more pronounced and consistent response across the tested concentration range, reflecting its capability to effectively capture and release NO₃⁻ ions in a reversible manner. In contrast, electrode E2 demonstrated a non-reversible response, implying that the CAGE structure integrated into this electrode may not be as suitable for facilitating reversible ion binding.

These observations may be attributed to factors such as steric hindrance, insufficient ion binding sites, or the limited structural flexibility of the CAGE molecules. Additionally, we investigated the influence of the electronic structures of the CAGE molecules on NO_3^- binding by adjusting the electron density of triazine units with dimethyl amine groups. The results showed a significant reduction in NO_3^- binding ability for electrodes E5 and E6, which incorporated dimethyl amine-substituted CAGE structures. These findings are consistent with our design principles: increasing the electron density of the CAGE molecules with electron-donating units, such as amine groups, diminishes the anion- π interactions between NO_3^- ions and the host molecules, resulting in weaker interactions. In contrast, the presence of electron-withdrawing groups enhances NO_3^- binding by decreasing the electron density of the CAGEs and increasing anion- π interactions.

4.10. Potentiometric Performance Characteristics of CAGE Incorporated ISE

To evaluate the response of CAGE-incorporated ion-selective electrodes (ISE) to nitrate ions, potentiometric measurements were performed using a series of standard solutions at pH 7.0. These solutions were prepared by diluting a 1.0×10^{-1} M nitrate stock solution with appropriate volumes of deionized water. The recorded potential values in response to varying nitrate concentrations are presented in Figure 4.16.

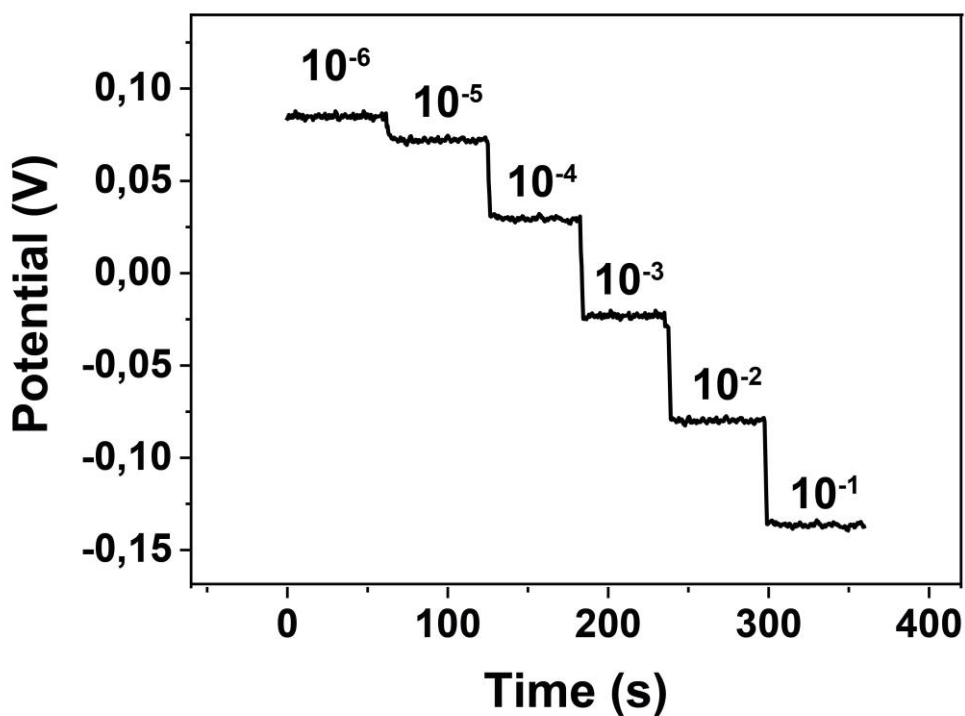


Figure 4.16 Potentiometric response of CAGE-incorporated-ISE in nitrate solutions at various concentrations

4.10.1. Forming the CAGE Incorporated ISE Calibration Curve: Determining Slope, LOD, and LRR

The potential versus log concentration (potential-log C) graph, derived from the data presented in Figure 4.17, is shown in Figure 4.18. This graph illustrates the relationship between electrode potential and the logarithm of nitrate ion concentration, offering additional insights into the potentiometric response of the CAGE-incorporated ISE.

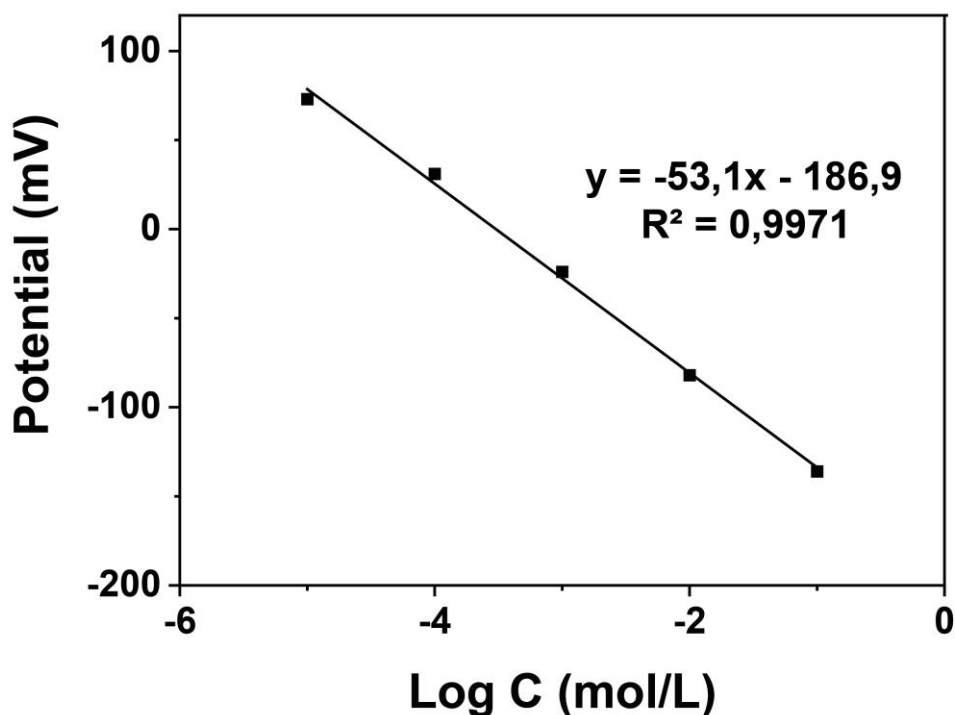


Figure 4.17 Linear calibration plot for NO_3^- detection

Figure 4.16 depicts the time-dependent potentiometric response of the CAGE-incorporated ISE to NO_3^- ions in aqueous solutions with concentrations ranging from 1.0×10^{-6} to 1.0×10^{-1} M at pH 7.0. The potential-log C plot (Figure 4.17) shows that the CAGE-incorporated ISE exhibited a linear response within the concentration range of 1.0×10^{-5} to 1.0×10^{-1} M, with a correlation coefficient (R^2) of 0.9971 and a slope of -53.1 ± 1.4 mV per decade of concentration. Following IUPAC recommendations (Buck and Lindner 1994b), the limit of detection for the CAGE-incorporated ISE was determined to be 7.5×10^{-6} M, calculated from the intersection of the two extrapolated segments of the calibration curve. This sensitivity threshold highlights the electrode's ability to detect trace amounts of NO_3^- ions, demonstrating its effectiveness and precision in analytical applications.

4.10.2. Determination of the Repeatability of CAGE Incorporated ISE

To evaluate the repeatability of the ion-selective electrode, real-time potentials were recorded for solutions at concentrations of 1.0×10^{-3} , 1.0×10^{-2} , and 1.0×10^{-1} M (pH=7.0), as illustrated in Figure 4.18. Potentiometric measurements were performed in both ascending and descending concentration orders. The average potential values and their standard deviations were as follows: -138.3 ± 2.3 mV for 1.0×10^{-3} M, -80.6 ± 1.3 mV for 1.0×10^{-2} M, and -23.1 ± 1.0 mV for 1.0×10^{-1} M. The minimal standard deviation values indicate the exceptional reproducibility of the NO_3^- selective electrode. This consistency in recorded potential values underscores the electrode's reliability and its capacity to provide consistent measurements across different concentrations, making it a dependable tool for analytical tasks where precision and repeatability are critical.

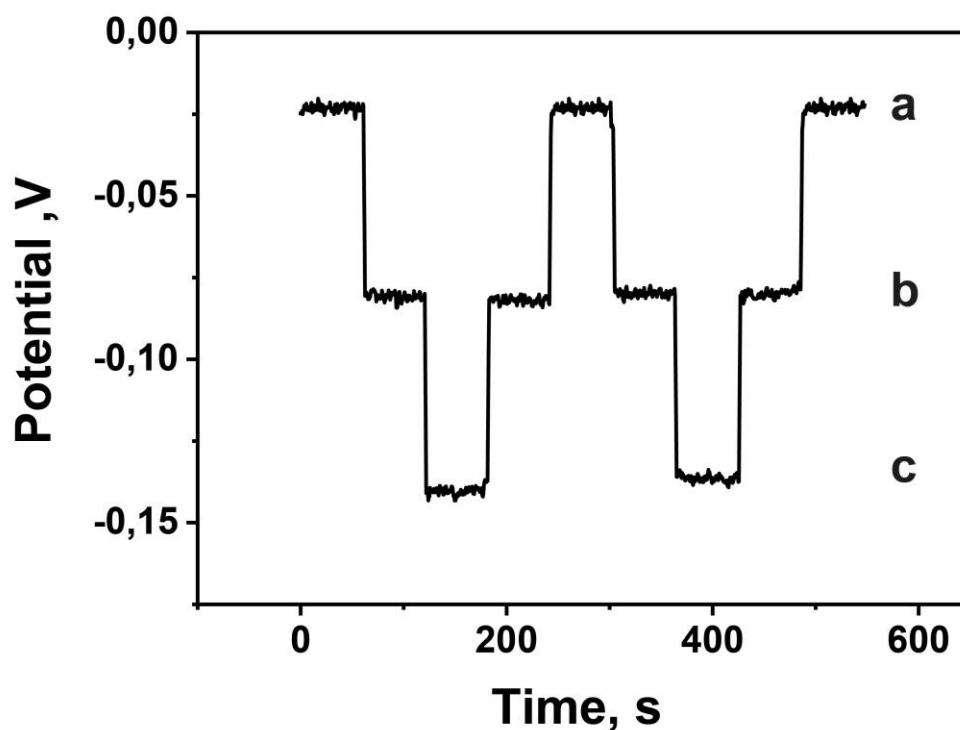


Figure 4.18 Repeatability of the CAGE-incorporated ISE a: 1.0×10^{-3} M; b: 1.0×10^{-2} M; c: 1.0×10^{-1} M NO_3^- (pH:7.0)

4.10.3. Determination of the Response Time of CAGE Incorporated ISE

The response time of an ion-selective electrode can be determined using various methods established by the International Union of Pure and Applied Chemistry (IUPAC). One such method, described by Buck and Lindner in 1994, defines response time as the duration (t_{95}) required for 95% of the potential change to reach equilibrium. (Buck and Lindner 1994b) According to IUPAC guidelines, response time is the period needed for the potential to stabilize after immersing the ion-selective working electrode and reference electrode into a solution containing the analyte. In Figure 4.19, the response time of the NO_3^- selective electrode was assessed using NO_3^- solutions at different standard concentrations. Following this method, the average response time was determined to be approximately 10 seconds.

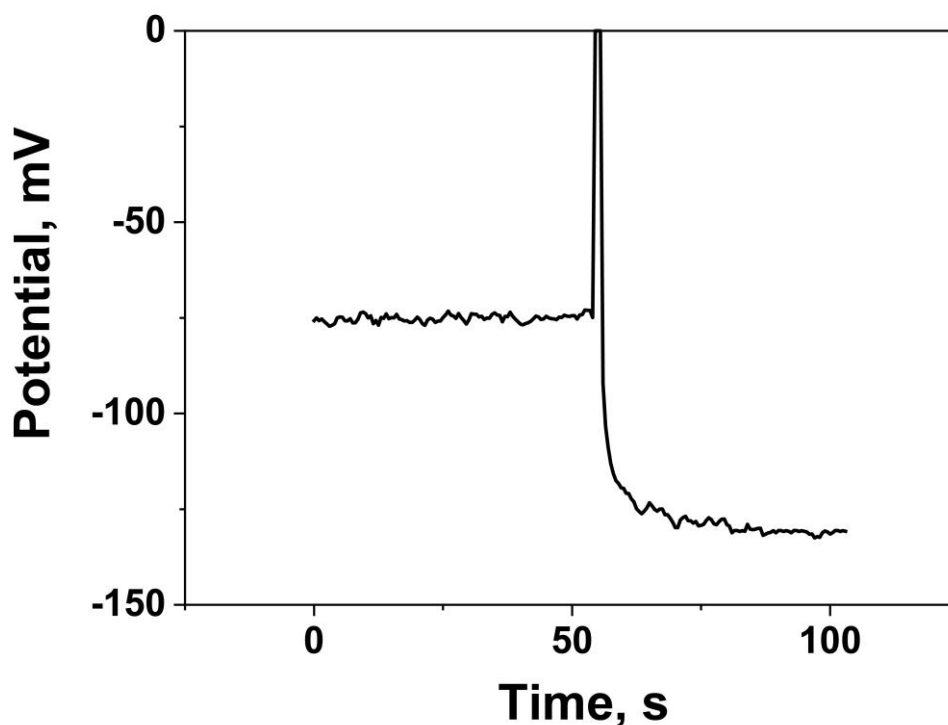


Figure 4.19 Response time of the CAGE-incorporated ISE

4.10.4. Determination of the pH Range of CAGE Incorporated ISE

To determine the pH working range of the electrode, 250 mL of 1.0×10^{-2} M and 1.0×10^{-3} M nitrate solutions were prepared. First, 250 mL of the 1.0×10^{-3} M nitrate solution was stirred using a magnetic stirrer at a constant speed. The reference electrode, CAGE incorporated ISE, and a combined pH electrode were immersed in the solution to monitor its pH. The pH was adjusted by incrementally adding concentrated HCl. With each addition, the pH and the corresponding potential values from the incorporated ISE were recorded. The same procedure was repeated by incrementally adding NaOH to a fresh 250 mL aliquot of the 1.0×10^{-3} M nitrate solution, and the potential values were plotted against pH. These steps were also applied to 250 mL of the 1.0×10^{-2} M nitrate solution. The resulting potential values versus pH for both nitrate solutions (1.0×10^{-2} M and 1.0×10^{-3} M) are shown collectively in Figure 4.20.

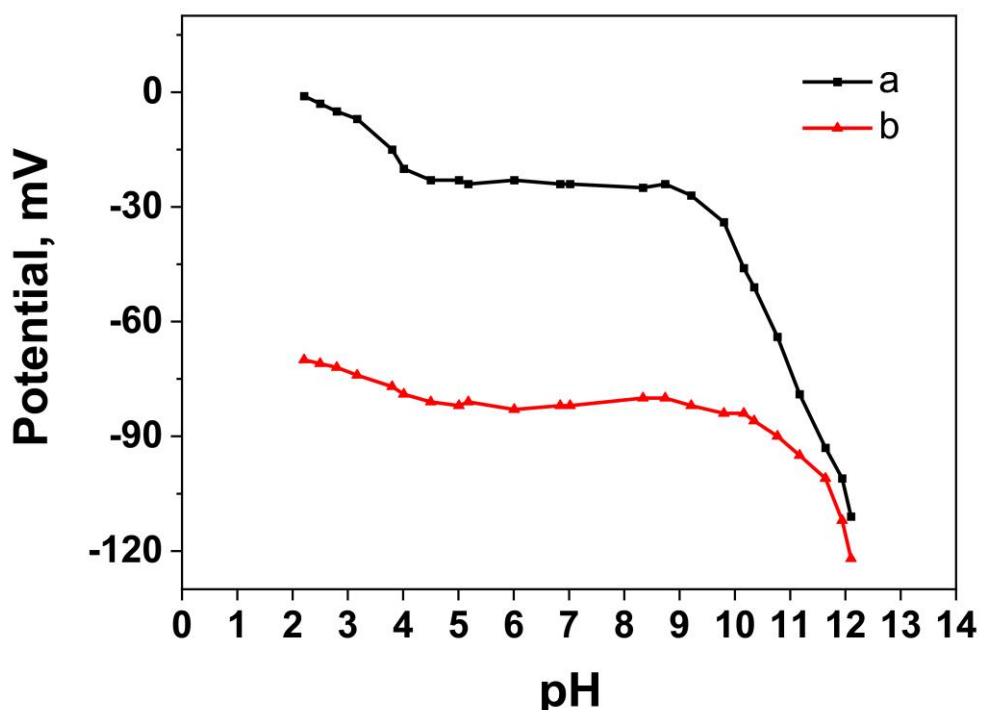


Figure 4.20 Variation in the response of the nitrate-selective electrode with pH: (a) 1.0×10^{-3} M nitrate solution, (b) 1.0×10^{-2} M nitrate solution

The changes in the CAGE incorporated ISE 's potential response due to pH variations are shown in Figure 4.20. As illustrated in Figure 4.20, significant OH⁻ ion

interference occurs at low NO_3^- concentrations, becoming evident above pH 9. In contrast, under acidic conditions, the potential stabilizes significantly after pH 4. This suggests an optimal performance range for the NO_3^- selective electrode between pH 4 and 9. These findings highlight the electrode's sensitivity to pH variations and its potential applicability across different pH levels.

4.10.5. Determination of CAGE Incorporated ISE Selectivity

The potentiometric selectivity of an ion-selective electrode is essential, as it measures the electrode's relative response to the primary ion when other interfering ions are present. Selectivity coefficients are generally determined following the methods outlined in the IUPAC protocol, specifically using the separate solution method to calculate these coefficients for various interfering ions. (Yoshio Umezawa et al. 2000) This procedure involves creating a calibration curve with primary ion (NO_3^- , denoted as " a_A ") solutions at concentrations ranging from 1.0×10^{-6} to 1.0×10^{-1} M. The CAGE incorporated ISE is then tested in solutions of individual interfering ions at a concentration of 1.0×10^{-2} M (denoted as " a_B "), and the corresponding potential values for each interfering ion are recorded. These potential values are then used to determine the activity of the primary ion using the calibration plot. The selectivity coefficient values ($K_{A,B}^{pot}$) listed in Table 4.7 are obtained by substituting the calculated primary ion activity (" a_A ") and the corresponding interfering ion activity (" a_B ") into the relevant equation (4.1).

Table 4.7 Selectivity coefficients of nitrate-selective CAGE incorporated ISE to various anionic species calculated using the separate solution method

Interferents	Log K
Cl ⁻	1.65
F ⁻	3.24
HCO ₃ ⁻	3.02
ClO ₃ ⁻	2.53
HPO ₄ ²⁻	3.11
S ₂ O ₃ ²⁻	3.57
CO ₃ ²⁻	3.55
SO ₄ ²⁻	3.82

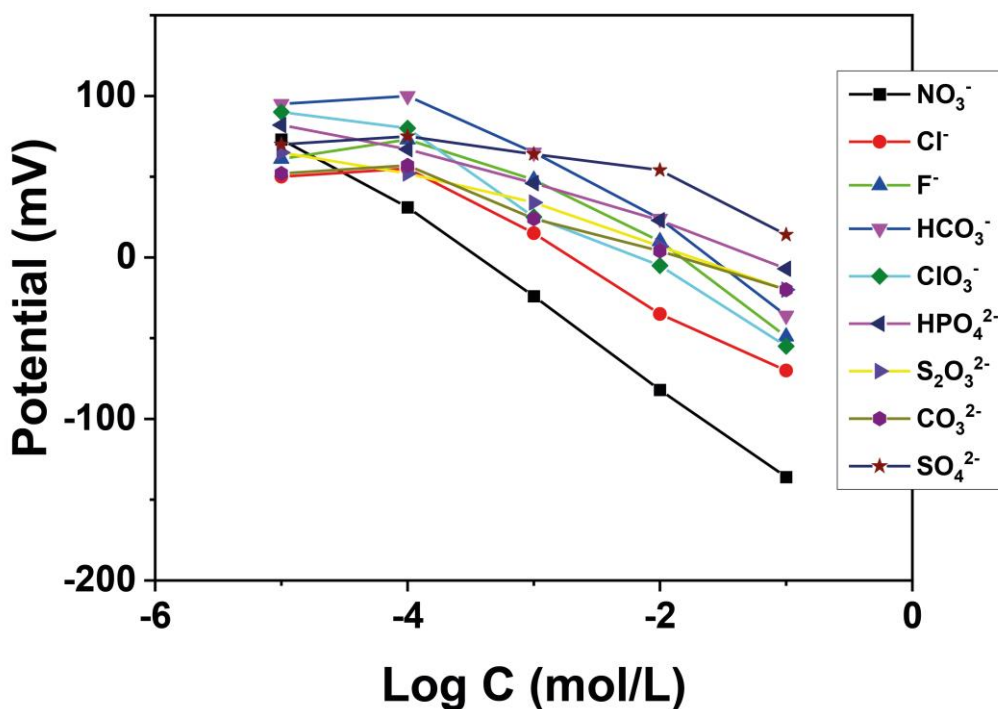


Figure 4.21 Potentiometric responses of NO₃⁻ selective electrode CAGE incorporated ISE for varying concentrations of anions

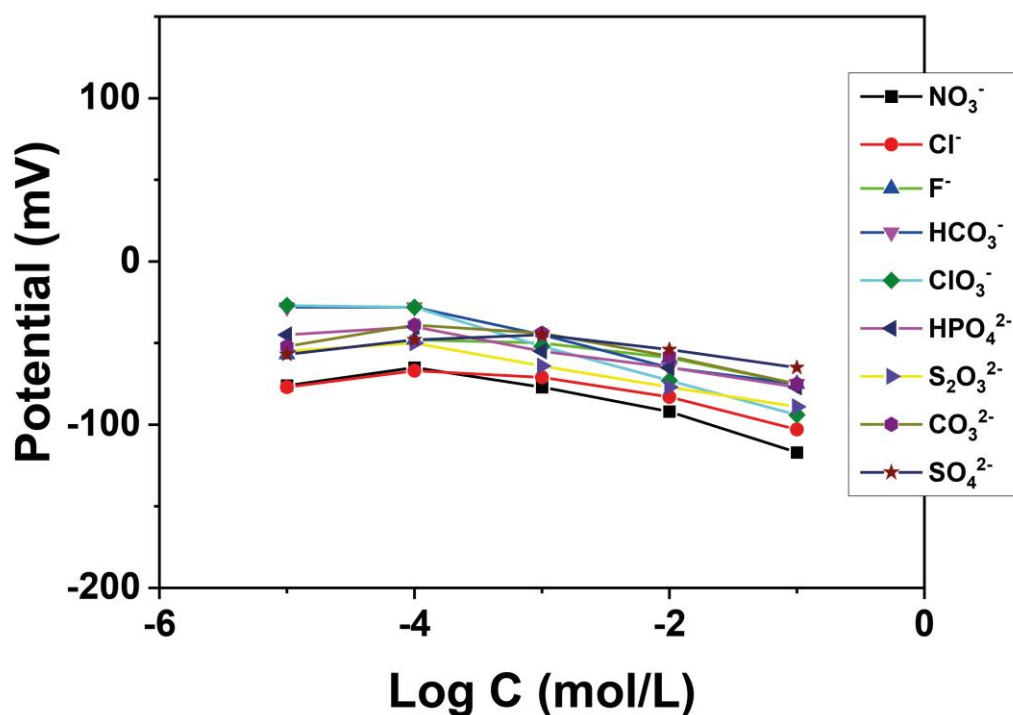


Figure 4.22 Potentiometric responses of cage-free electrode for varying concentrations of anions

The use of molecular CAGE-1 (E4) as an ionophore greatly enhances the diffusion and reversible binding of NO_3^- , as shown by the superior potentiometric performance characteristics of the ISE compared to the cage-free electrode (Figure 4.21 and 4.22). This finding confirms that molecular CAGE-1 (E4) provides a more pronounced and consistent response at the tested concentration of NO_3^- , demonstrating its ability to efficiently capture and release NO_3^- ions in a reversible manner.

4.11. Morphological Characterization of NH_4^+ -SPE

Coating was accomplished by applying 10 μl of the nonactin-based ammonium-selective membrane, optimized in Section 4.2, onto the working electrode part of the commercial Metrohm DropSens Screen-Printed Carbon Electrodes. The morphological characteristics of the electrodes were analyzed using a Scanning Electron Microscope.

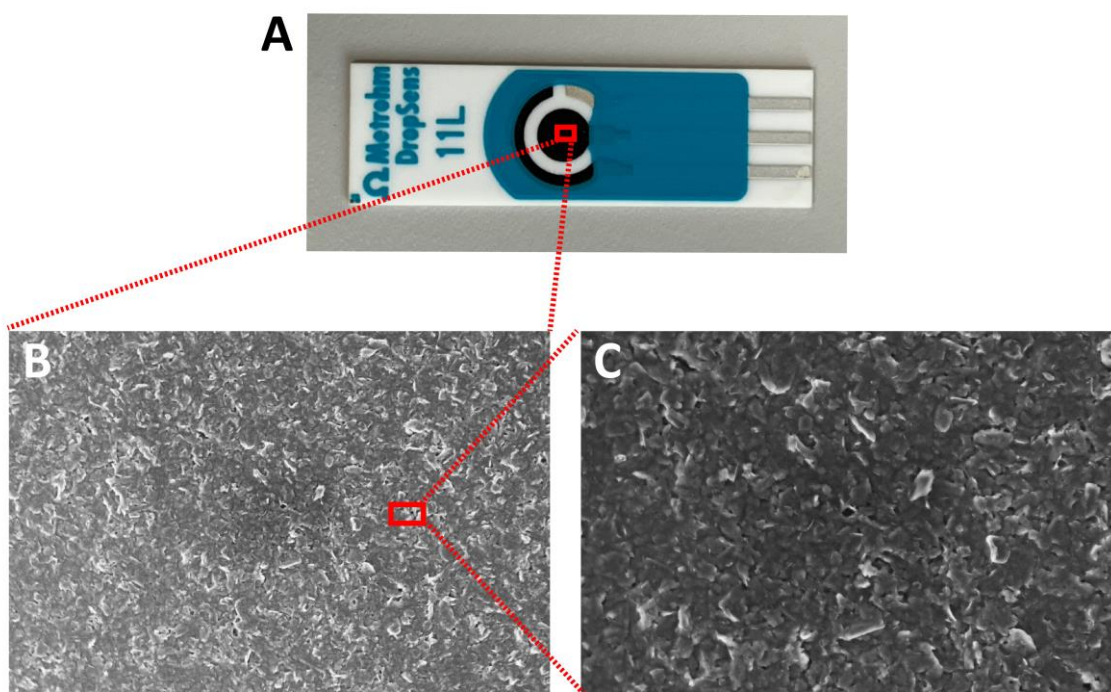


Figure 4.23 Screen-Printed Carbon Electrodes (A), SEM images of Screen-Printed Carbon Electrodes (B), 2x magnification (C).

The SEM images are displayed in Figure 4.23 and 4.24; Figures 4.23-B and 4.23-C show the electrode without membrane coating, while Figure 4.24-F depicts the SPE coated with 10 μl of the ammonium-selective membrane. Figure 4.24-G illustrates both conditions. SEM images at higher magnification reveal the presence of graphite flakes in the uncoated SPE (Figure 4.23-C). After coating, the surface features of the graphite flakes are almost obscured, indicating successful application of the PCV membrane on the surface (Figure 4.24-F).

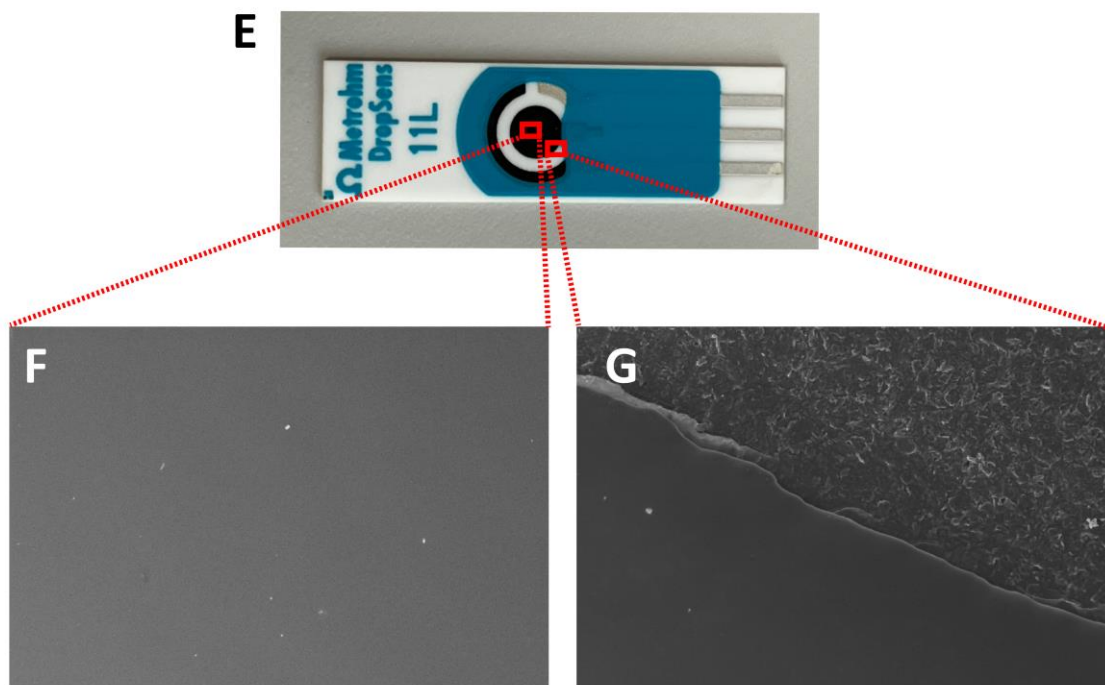


Figure 4.24 PVC coated Screen-Printed Carbon Electrodes (E), SEM images of PVC coated Screen-Printed Carbon Electrodes (F), both conditions (bare and coated) (G).

4.12. Forming the NH_4^+ -SPE Calibration Curve: Determining Slope, LOD, and LRR

To evaluate the response of SPE to ammonium ions, potentiometric measurements were performed with a range of standard solutions. These solutions were created by diluting a 1.0×10^{-1} M ammonium stock solution with deionized water. The recorded potential values corresponding to water and different ammonium concentrations are illustrated in Figure 4.25.

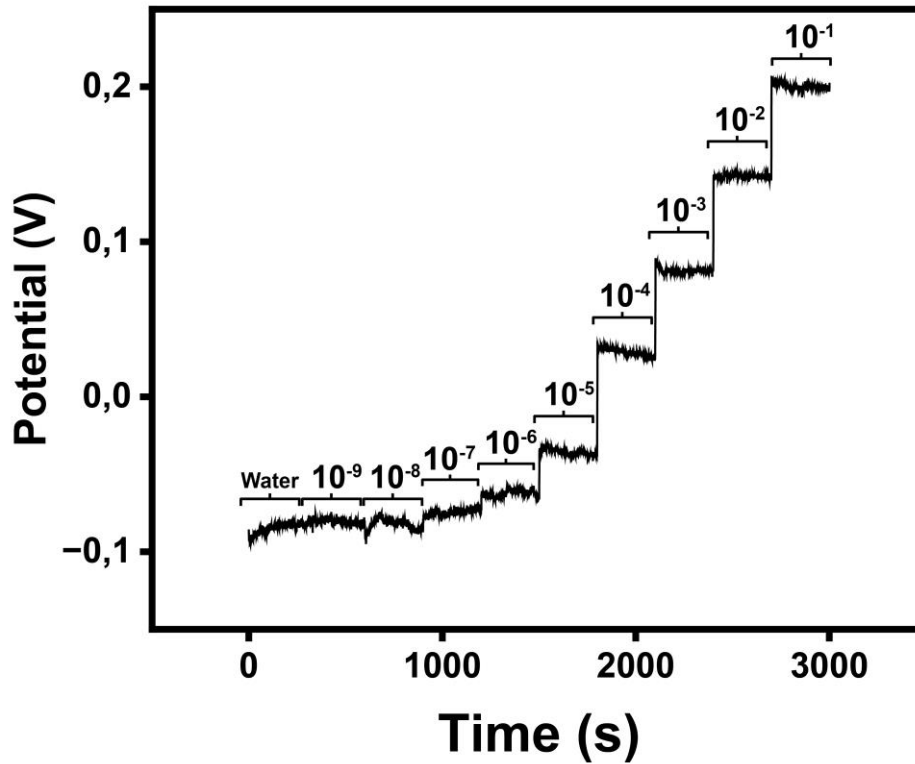


Figure 4.25 Potentiometric response of SPE in water and ammonium solutions at various concentrations

The potential versus log concentration (potential-log C) graph, generated from the potential and concentration data in Figure 4.25, is displayed in Figure 4.26. This graph demonstrates the relationship between electrode potential and the logarithm of ammonium ion concentration, offering additional insights into the potentiometric behavior of the SPE.

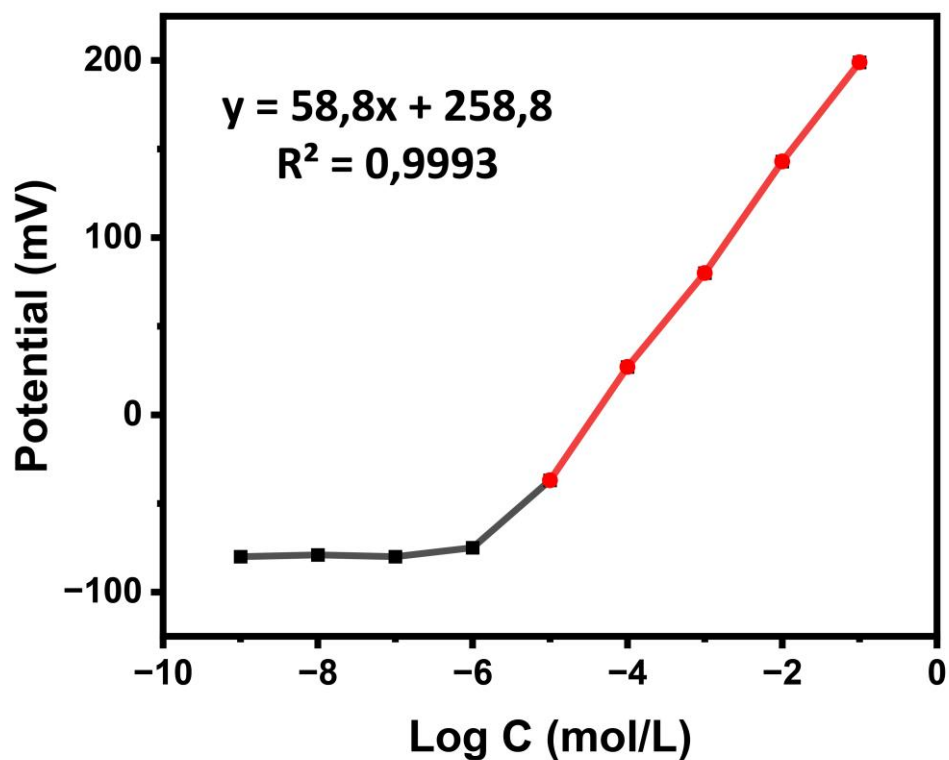


Figure 4.26 Linear calibration plot of SPE for NH_4^+ detection

Figure 4.25 shows the time-dependent potentiometric response of the SPE to water and NH_4^+ ions in aqueous solutions with concentrations ranging from 1.0×10^{-9} to 1.0×10^{-1} M. The potential-log C plot in Figure 4.26 (red line) indicates that the SPE exhibited a linear response within the concentration range of 1.0×10^{-5} to 1.0×10^{-1} M, with a correlation coefficient (R^2) of 0.9993 and a slope of 58.8 ± 0.3 mV per decade of concentration. Following IUPAC recommendations (Buck and Lindner 1994b), the limit of detection (LOD) for the SPE was calculated to be 3.0×10^{-6} M, determined from the intersection of the two extrapolated segments of the calibration curve.

4.13. Improving the Detection Limit of the NH_4^+ -SPE

F. De Angelis et al. (2011) introduce an innovative method to improve the detection of highly diluted molecules by combining super-hydrophobic surfaces with plasmonic nanostructures. This approach aims to overcome the inherent limitations of nanosensors, which are often hindered by diffusion limits, making the detection of

molecules in femto- or attomolar solutions impractically slow. The super-hydrophobic surfaces ensure that droplets retain a quasi-spherical shape during evaporation, thereby concentrating the solute into a small area (Figure 4.27).

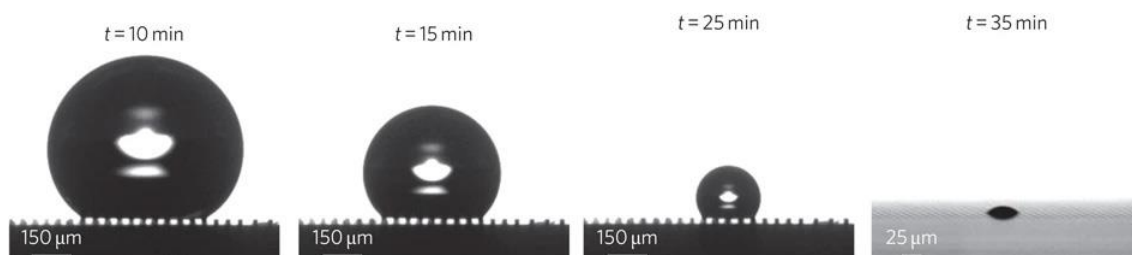


Figure 4.27 Contact angle measurements during evaporation at four different times (Source: De Angelis et al. 2011).

Plasmonic nanostructures generate "hot spots" that amplify the electromagnetic field, allowing for sensitive detection using Raman and fluorescence spectroscopy. The devices detected rhodamine at concentrations below 1 femtomolar and lambda DNA at attomolar concentrations. For protein detection, lysozyme molecules were effectively identified using an advanced plasmonic device featuring a nanocone structure. This study offers a promising approach to enhance the sensitivity and functionality of nanosensors for detecting minute quantities of molecules across various fields, potentially leading to significant improvements in diagnostic capabilities and environmental monitoring. (De Angelis et al. 2011)

In this context, drop evaporation was carried out with the help of a holder integrated into the SPE. To obtain steady-state measurements, a volume of 200 μL of test solution was dropped into contact with both the working and reference electrodes (Figure 4.28). Before each measurement sequence, both the reference and working electrodes were rinsed with distilled deionized water and carefully dried using a soft absorbent tissue.

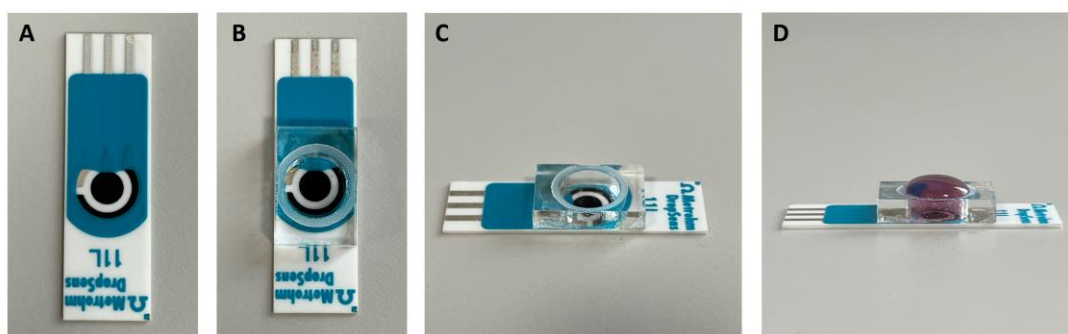


Figure 4.28 Photographs of the Screen-Printed Carbon Electrodes (A), SPE with a reservoir that can hold a drop of 200 μL volume (B and C), and with a sample solution drop (D).

To evaluate the response of SPE to ammonium ions, potentiometric Steady-state measurements were carried out by dropping a 200 μL volume of water and ammonium solutions from 1.0×10^{-9} to 1.0×10^{-4} M in contact with both the working and reference electrodes (Figure 4.28).

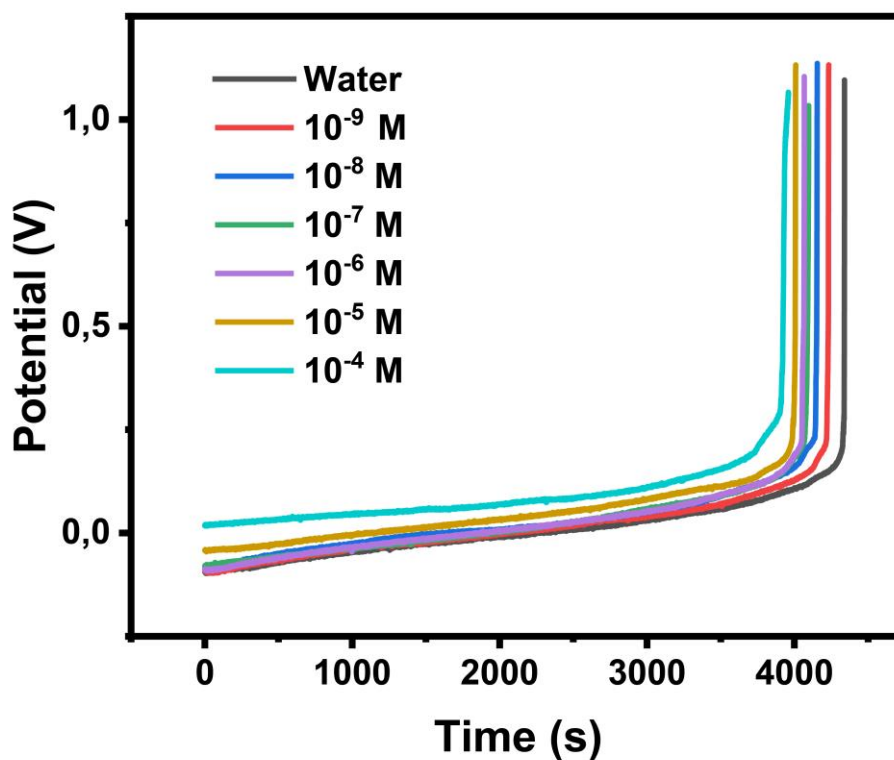


Figure 4.29 Potentiometric response of NH_4^+ -SPE until drop evaporated

Upon examining Figure 4.29, it is evident that as the concentration of ammonium decreases, the evaporation time of the drop increases. Notably, ionized water exhibits the longest evaporation time. As drops of ammonium solution of increasing concentrations from 1.0×10^{-9} to 1.0×10^{-4} M evaporated, the measured potential values increased. This suggests that the concentration of the drops increases over time, eventually reaching a potential that falls within the linear range. It is feasible to measure concentrations outside of the linear range using the suggested approach, provided that the air flow, temperature, pressure, and relative humidity of the environment in which the measurement is conducted are optimized. According to Figure 2.29, the drop with a concentration of 1.0×10^{-9} M ammonium achieved the same potential as the drop with a concentration of 1.0×10^{-5} M ammonium during the 3020th second of measurement. The mathematical demonstration of the relationship between evaporation time and concentrations is still pending. This is due to the continuing optimization studies. Preliminary results indicate that this approach will be efficacious in enhancing the detection limit.

CHAPTER 5

CONCLUSION

In the initial part of this thesis, the development of an NH_4^+ selective ion-selective electrode utilized RACNT directly grown on glass fiber via chemical vapor deposition. For the fabrication of the r-ISE, the RACNT-GF composite surface was modified by coating it with a PVC-COOH/DOS plasticized membrane containing nonactin at optimal stoichiometric ratios. This r-ISE demonstrated potentiometric responses that were superior to conventional ISEs fabricated using planar interface materials such as graphite. The potentiometric characteristics of the r-ISE included a slope of approximately 58.2 ± 0.6 mV per decade, a limit of detection of 7.5×10^{-6} M, and a linear response range from 1.0×10^{-5} to 1.0×10^{-1} M. Additionally, the feasibility of using the r-ISE as an ion-selective microelectrode was demonstrated through assays performed in a microfluidic cell. In the flow injection analysis system, the r-ISE exhibited a near-Nernstian response with a slope of 54.2 ± 1.2 mV per decade, an LOD of 1.0×10^{-5} M, and a rapid response time of 10 seconds with good reproducibility. The r-ISE can be easily fabricated in various shapes and sizes, which facilitates miniaturization and the construction of microfluidic devices for the multiplexed detection of various ions. Moreover, a 10 cm x 10 cm GF fabric has the potential to yield a large number of ISEs in a single CVD growth process, enabling mass production and significantly reducing the fabrication costs per ISE.

In conclusion, the widespread presence of nitrate ions as pollutants in water and soil underscores the critical need for effective monitoring methods to protect both human health and the environment. Electrochemical analysis, especially through the use of potentiometric ion-selective electrodes, has proven to be a highly effective technique for the accurate and sensitive detection of nitrate levels. Traditional ionophores derived from natural sources, however, often face limitations in terms of selectivity and modifiability. In contrast, synthetic ionophores provide greater flexibility and specificity for targeting specific ions. The second part of this thesis demonstrates the successful application of a molecular cage as an ionophore for nitrate ions. This molecular cage exhibited a linear response over a broad concentration range and achieved a low limit of

detection. The effectiveness of this approach was contingent upon optimizing the interaction between the cage molecules and nitrate ions. This optimization was accomplished by adjusting the internal dimensions and electron density of the cage molecule to create an environment conducive to the selective binding of nitrate ions. The resulting nitrate-selective cage-electrode displayed potentiometric characteristics with a slope of approximately 53.1 ± 1.4 mV per decade, a limit of detection of 7.5×10^{-6} M, and a linear response range from 1.0×10^{-5} to 1.0×10^{-1} M. This innovative development represents a significant advancement in the field of electrochemical analysis, offering a practical and effective solution for monitoring nitrate pollution.

In the third study, attempts were undertaken to improve the detection limit of ammonium electrodes crafted with Screen Printed Carbon Electrodes through the use of the drop evaporation technique, all while keeping the electrode material and membrane composition unchanged. For this purpose, potentiometric measurements were carried out on SPEs modified with a chamber designed to hold a 200 μ L drop. In the potentiometric measurements of NH_4^+ -SPE, the drop with an ammonium concentration of 1.0×10^{-9} M reached the same potential as the drop with an ammonium concentration of 1.0×10^{-5} M at the 3020th second of the measurement. This makes it possible to include concentrations outside the linear range into the linear range by evaporation. Preliminary results show that this approach will be effective in increasing the detection limit.

REFERENCES

- Abdel-Ghany, Maha F., Lobna A. Hussein, and Noha F. El Azab. 2017. "Novel Potentiometric Sensors for the Determination of the Dinotefuran Insecticide Residue Levels in Cucumber and Soil Samples." *Talanta* 164 (March):518–28. <https://doi.org/10.1016/j.talanta.2016.12.019>.
- Akyüz, Mehmet, and Şevket Ata. 2009. "Determination of Low Level Nitrite and Nitrate in Biological, Food and Environmental Samples by Gas Chromatography–Mass Spectrometry and Liquid Chromatography with Fluorescence Detection." *Talanta* 79 (3): 900–904. <https://doi.org/10.1016/j.talanta.2009.05.016>.
- Alahi, Md. Eshrat E., and Subhas Chandra Mukhopadhyay. 2018. "Detection Methods of Nitrate in Water: A Review." *Sensors and Actuators A: Physical* 280 (September):210–21. <https://doi.org/10.1016/j.sna.2018.07.026>.
- Alizadeh, Taher, Sahar Nayeri, and Sahar Mirzaee. 2019. "A High Performance Potentiometric Sensor for Lactic Acid Determination Based on Molecularly Imprinted Polymer/MWCNTs/PVC Nanocomposite Film Covered Carbon Rod Electrode." *Talanta* 192 (January):103–11. <https://doi.org/10.1016/j.talanta.2018.08.027>.
- Angelis, F. De, F. Gentile, F. Mecarini, G. Das, M. Moretti, P. Candeloro, M. L. Coluccio, et al. 2011. "Breaking the Diffusion Limit with Super-Hydrophobic Delivery of Molecules to Plasmonic Nanofocusing SERS Structures." *Nature Photonics* 5 (11): 682–87. <https://doi.org/10.1038/nphoton.2011.222>.
- Annu, Swati Sharma, Rajeev Jain, and Antony Nitin Raja. 2020. "Review—Pencil Graphite Electrode: An Emerging Sensing Material." *Journal of The Electrochemical Society* 167 (3): 037501. <https://doi.org/10.1149/2.0012003JES>.
- Anupriya, Jeyaraman, Sethupathi Velmurugan, Shen-Ming Chen, and Yoon-Bong Hahn. 2022. "Enhanced Electrochemical Performance of In-Situ Synthesized Cu Nanoparticle/C Spheres Composite for Highly Sensitive Sensing of Azathioprine

- Immunosuppressive Drug." *Composites Part B: Engineering* 242 (August):110079. <https://doi.org/10.1016/j.compositesb.2022.110079>.
- Bakker, Eric. 2016. "Electroanalysis with Membrane Electrodes and Liquid-Liquid Interfaces." *Analytical Chemistry* 88 (1): 395–413. <https://doi.org/10.1021/acs.analchem.5b04034>.
- Bakker, Eric, Philippe Bühlmann, and Ernő Pretsch. 1997. "Carrier-Based Ion-Selective Electrodes and Bulk Optodes. 1. General Characteristics." *Chemical Reviews* 97 (8): 3083–3132. <https://doi.org/10.1021/cr940394a>.
- Bakker, Eric, and Ernő Pretsch. 2005. "Potentiometric Sensors for Trace-Level Analysis." *TrAC Trends in Analytical Chemistry* 24 (3): 199–207. <https://doi.org/10.1016/j.trac.2005.01.003>.
- Bakker, Eric, and Martin Telting-Diaz. 2002. "Electrochemical Sensors." *Analytical Chemistry* 74 (12): 2781–2800. <https://doi.org/10.1021/ac0202278>.
- Bard, A. J., & Faulkner, L. R. 2001. *Electrochemical Methods: Fundamentals and "*
- Baumbauer, Carol L., Payton J. Goodrich, Margaret E. Payne, Tyler Anthony, Claire Beckstoffer, Anju Toor, Whendee Silver, and Ana Claudia Arias. 2022. "Printed Potentiometric Nitrate Sensors for Use in Soil." *Sensors* 22 (11): 4095. <https://doi.org/10.3390/s22114095>.
- Bhandari, Pallab, and Partha Sarathi Mukherjee. 2023. "Covalent Organic Cages in Catalysis." *ACS Catalysis* 13 (9): 6126–43. <https://doi.org/10.1021/acscatal.3c01080>.
- Bisson, Adrian P., Vincent M. Lynch, Mary-Katherine C. Monahan, and Eric V. Anslyn. 1997a. "Recognition of Anions through NH π Hydrogen Bonds in a Bicyclic Cyclophane—Selectivity for Nitrate." *Angewandte Chemie International Edition in English* 36 (21): 2340–42. <https://doi.org/10.1002/anie.199723401>.
- Bobacka, Johan, Ari Ivaska, and Andrzej Lewenstam. 2008a. "Potentiometric Ion Sensors." *Chemical Reviews* 108 (2): 329–51. <https://doi.org/10.1021/cr068100w>.

- Bomar, Ellen, George Owens, and George Murray. 2017. "Nitrate Ion Selective Electrode Based on Ion Imprinted Poly(N-Methylpyrrole)." *Chemosensors* 5 (1): 2. <https://doi.org/10.3390/chemosensors5010002>.
- Borrelli, Pasquale, Panos Panagos, Cristiano Ballabio, Emanuele Lugato, Melanie Weynants, and Luca Montanarella. 2016. "Towards a Pan-European Assessment of Land Susceptibility to Wind Erosion." *Land Degradation & Development* 27 (4): 1093–1105. <https://doi.org/10.1002/ldr.2318>.
- Buck, R. P., and E. Lindner. 1994a. "Recommendations for Nomenclature of Ionselective Electrodes (IUPAC Recommendations 1994)." *Pure and Applied Chemistry* 66 (12): 2527–36. <https://doi.org/10.1351/pac199466122527>.
- Buyukcakir, Onur, Yongbeom Seo, and Ali Coskun. 2015. "Thinking Outside the Cage: Controlling the Extrinsic Porosity and Gas Uptake Properties of Shape-Persistent Molecular Cages in Nanoporous Polymers." *Chemistry of Materials* 27 (11): 4149–55. <https://doi.org/10.1021/acs.chemmater.5b01346>.
- Carey, Jesse L., Akira Hirao, Kenji Sugiyama, and Philippe Bühlmann. 2017. "Semifluorinated Polymers as Ion-selective Electrode Membrane Matrixes." *Electroanalysis* 29 (3): 739–47. <https://doi.org/10.1002/elan.201600586>.
- Chen, Lijun, Stuart N. Berry, Xin Wu, Ethan N.W. Howe, and Philip A. Gale. 2020. "Advances in Anion Receptor Chemistry." *Chem* 6 (1): 61–141. <https://doi.org/10.1016/j.chempr.2019.12.002>.
- Colaço, A. F., and J. P. Molin. 2017. "Variable Rate Fertilization in Citrus: A Long Term Study." *Precision Agriculture* 18 (2): 169–91. <https://doi.org/10.1007/s11119-016-9454-9>.
- Crespo, Gastón A., Santiago Macho, and F. Xavier Rius. 2008. "Ion-Selective Electrodes Using Carbon Nanotubes as Ion-to-Electron Transducers." *Analytical Chemistry* 80 (4): 1316–22. <https://doi.org/10.1021/ac071156l>.
- Cuartero, Maria, Josiah Bishop, Raymart Walker, Robert G. Acres, Eric Bakker, Roland De Marco, and Gaston A. Crespo. 2016. "Evidence of Double Layer/Capacitive

- Charging in Carbon Nanomaterial-Based Solid Contact Polymeric Ion-Selective Electrodes." *Chemical Communications* 52 (62): 9703–6. <https://doi.org/10.1039/C6CC04876E>.
- Cuartero, María, Noemi Colozza, Bibiana M. Fernández-Pérez, and Gastón A. Crespo. 2020. "Why Ammonium Detection Is Particularly Challenging but Insightful with Ionophore-Based Potentiometric Sensors – an Overview of the Progress in the Last 20 Years." *The Analyst* 145 (9): 3188–3210. <https://doi.org/10.1039/D0AN00327A>.
- Cui, Meng, Lihua Zeng, Wei Qin, and Juan Feng. 2020. "Measures for Reducing Nitrate Leaching in Orchards:A Review." *Environmental Pollution* 263 (August):114553. <https://doi.org/10.1016/j.envpol.2020.114553>.
- Dinnes, Dana L., Douglas L. Karlen, Dan B. Jaynes, Thomas C. Kaspar, Jerry L. Hatfield, Thomas S. Colvin, and Cynthia A. Cambardella. 2002. "Nitrogen Management Strategies to Reduce Nitrate Leaching in Tile-Drained Midwestern Soils." *Agronomy Journal* 94 (1): 153–71. <https://doi.org/10.2134/agronj2002.1530>.
- Dubey, Rama, Dhiraj Dutta, Arpan Sarkar, and Pronobesh Chattopadhyay. 2021a. "Functionalized Carbon Nanotubes: Synthesis, Properties and Applications in Water Purification, Drug Delivery, and Material and Biomedical Sciences." *Nanoscale Advances* 3 (20): 5722–44. <https://doi.org/10.1039/D1NA00293G>.
- Evans, Nicholas H., and Paul D. Beer. 2014. "Advances in Anion Supramolecular Chemistry: From Recognition to Chemical Applications." *Angewandte Chemie International Edition* 53 (44): 11716–54. <https://doi.org/10.1002/anie.201309937>.
- Fan, Yingzheng, Yuankai Huang, Will Linthicum, Fangyuan Liu, André O'Reilly Beringhs, Yanliu Dang, Zhiheng Xu, et al. 2020. "Toward Long-Term Accurate and Continuous Monitoring of Nitrate in Wastewater Using Poly(Tetrafluoroethylene) (PTFE)–Solid-State Ion-Selective Electrodes (S-ISEs)." *ACS Sensors* 5 (10): 3182–93. <https://doi.org/10.1021/acssensors.0c01422>.

- Faraji, Masoud, and Hossein Mohammadzadeh Aydisheh. 2019. "Facile and Scalable Preparation of Highly Porous Polyvinyl Chloride-Multi Walled Carbon Nanotubes-Polyaniline Composite Film for Solid-State Flexible Supercapacitor." *Composites Part B: Engineering* 168 (July):432–41. <https://doi.org/10.1016/j.compositesb.2019.03.060>.
- Fayose, T., L. Mendecki, S. Ullah, and A. Radu. 2017. "Single Strip Solid Contact Ion Selective Electrodes on a Pencil-Drawn Electrode Substrate." *Analytical Methods* 9 (7): 1213–20. <https://doi.org/10.1039/C6AY02860H>.
- Fozia, Guangyao Zhao, Yanhong Nie, Jianrong Jiang, Qian Chen, Chaogang Wang, Xu Xu, Ming Ying, Zhangli Hu, and Hong Xu. 2023. "Preparation of Nitrate Bilayer Membrane Ion-Selective Electrode Modified by Pericarpium Granati-Derived Biochar and Its Application in Practical Samples." *Electrocatalysis* 14 (4): 534–45. <https://doi.org/10.1007/s12678-023-00812-3>.
- Gallardo-Gonzalez, J., A. Baraket, S. Boudjaoui, T. Metzner, F. Hauser, T. Rößler, S. Krause, et al. 2019. "A Fully Integrated Passive Microfluidic Lab-on-a-Chip for Real-Time Electrochemical Detection of Ammonium: Sewage Applications." *Science of The Total Environment* 653 (February):1223–30. <https://doi.org/10.1016/j.scitotenv.2018.11.002>.
- Guzinski, Marcin, Jennifer M. Jarvis, Felio Perez, Bradford D. Pendley, Ernő Lindner, Roland De Marco, Gaston A. Crespo, Robert G. Acres, Raymart Walker, and Josiah Bishop. 2017. "PEDOT(PSS) as Solid Contact for Ion-Selective Electrodes: The Influence of the PEDOT(PSS) Film Thickness on the Equilibration Times." *Analytical Chemistry* 89 (6): 3508–16. <https://doi.org/10.1021/acs.analchem.6b04625>.
- Hasell, Tom, Marcin Miklitz, Andrew Stephenson, Marc A. Little, Samantha Y. Chong, Rob Clowes, Linjiang Chen, et al. 2016. "Porous Organic Cages for Sulfur Hexafluoride Separation." *Journal of the American Chemical Society* 138 (5): 1653–59. <https://doi.org/10.1021/jacs.5b11797>.

- He, Ning, Soma Papp, Tom Lindfors, Lajos Höfler, Rose-Marie Latonen, and Róbert E. Gyurcsányi. 2017. "Pre-Polarized Hydrophobic Conducting Polymer Solid-Contact Ion-Selective Electrodes with Improved Potential Reproducibility." *Analytical Chemistry* 89 (4): 2598–2605. <https://doi.org/10.1021/acs.analchem.6b04885>.
- Hjort, Robert G., Raquel R. A. Soares, Jingzhe Li, Dapeng Jing, Lindsey Hartfiel, Bolin Chen, Bryan Van Belle, et al. 2022. "Hydrophobic Laser-Induced Graphene Potentiometric Ion-Selective Electrodes for Nitrate Sensing." *Microchimica Acta* 189 (3): 122. <https://doi.org/10.1007/s00604-022-05233-5>.
- Hu, Jinbo, Andreas Stein, and Philippe Bühlmann. 2016. "A Disposable Planar Paper-Based Potentiometric Ion-Sensing Platform." *Angewandte Chemie* 128 (26): 7670–73. <https://doi.org/10.1002/ange.201603017>.
- Hu, Jinbo, Xu U. Zou, Andreas Stein, and Philippe Bühlmann. 2014. "Ion-Selective Electrodes with Colloid-Imprinted Mesoporous Carbon as Solid Contact." *Analytical Chemistry* 86 (14): 7111–18. <https://doi.org/10.1021/ac501633r>.
- Hulanicki, A., S. Glab, and F. Ingman. 1991a. "Chemical Sensors: Definitions and Classification." *Pure and Applied Chemistry* 63 (9): 1247–50. <https://doi.org/10.1351/pac199163091247>.
- Hyusein, Chiydem, and Vessela Tsakova. 2023. "Nitrate Detection at Pd-Cu-Modified Carbon Screen Printed Electrodes." *Journal of Electroanalytical Chemistry* 930 (February):117172. <https://doi.org/10.1016/j.jelechem.2023.117172>.
- Jarvis, Jennifer M., Marcin Guzinski, Bradford D. Pendley, and Erno Lindner. 2016. "Poly(3-Octylthiophene) as Solid Contact for Ion-Selective Electrodes: Contradictions and Possibilities." *Journal of Solid State Electrochemistry* 20 (11): 3033–41. <https://doi.org/10.1007/s10008-016-3340-2>.
- Jaworska, Ewa, Krzysztof Maksymiuk, and Agata Michalska. 2016. "Optimizing Carbon Nanotubes Dispersing Agents from the Point of View of Ion-selective Membrane Based Sensors Performance – Introducing Carboxymethylcellulose as

- Dispersing Agent for Carbon Nanotubes Based Solid Contacts." *Electroanalysis* 28 (5): 947–53. <https://doi.org/10.1002/elan.201500609>.
- Jaworska, Ewa, Mario L. Naitana, Emilia Stelmach, Giuseppe Pomarico, Marcin Wojciechowski, Ewa Bulska, Krzysztof Maksymiuk, Roberto Paolesse, and Agata Michalska. 2017. "Introducing Cobalt(II) Porphyrin/Cobalt(III) Corrole Containing Transducers for Improved Potential Reproducibility and Performance of All-Solid-State Ion-Selective Electrodes." *Analytical Chemistry* 89 (13): 7107–14. <https://doi.org/10.1021/acs.analchem.7b01027>.
- Jiang, Chengmei, Yao Yao, Yalu Cai, and Jianfeng Ping. 2019. "All-Solid-State Potentiometric Sensor Using Single-Walled Carbon Nanohorns as Transducer." *Sensors and Actuators B: Chemical* 283 (March):284–89. <https://doi.org/10.1016/j.snb.2018.12.040>.
- Jiao, Tianyu, Liang Chen, Dong Yang, Xin Li, Guangcheng Wu, Pingmei Zeng, Ankun Zhou, et al. 2017. "Trapping White Phosphorus within a Purely Organic Molecular Container Produced by Imine Condensation." *Angewandte Chemie International Edition* 56 (46): 14545–50. <https://doi.org/10.1002/anie.201708246>.
- Jordan, Jack W., William J. V. Townsend, Lee R. Johnson, Darren A. Walsh, Graham N. Newton, and Andrei N. Khlobystov. 2021. "Electrochemistry of Redox-Active Molecules Confined within Narrow Carbon Nanotubes." *Chemical Society Reviews* 50 (19): 10895–916. <https://doi.org/10.1039/D1CS00478F>.
- Kang, Sung Ok, José M. Llinares, Victor W. Day, and Kristin Bowman-James. 2010. "Cryptand-like Anion Receptors." *Chemical Society Reviews* 39 (10): 3980. <https://doi.org/10.1039/c0cs00083c>.
- Karimi, Mojtaba, and Kosar Moradi. 2018. "The Response of Stevia (*Stevia Rebaudiana* Bertoni) to Nitrogen Supply under Greenhouse Condition." *Journal of Plant Nutrition* 41 (13): 1695–1704. <https://doi.org/10.1080/01904167.2018.1459692>.

- Kharton, Vladislav V., and Ekaterina V. Tsipis. 2013. "Reference Electrodes for Solid-Electrolyte Devices." In *Handbook of Reference Electrodes*, 243–78. Berlin, Heidelberg: Springer Berlin Heidelberg. https://doi.org/10.1007/978-3-642-36188-3_9.
- Kim, Min-Yeong, Jong-Won Lee, Da Jung Park, Joo-Yul Lee, Nosang Vincent Myung, Se Hun Kwon, and Kyu Hwan Lee. 2021. "Highly Stable Potentiometric Sensor with Reduced Graphene Oxide Aerogel as a Solid Contact for Detection of Nitrate and Calcium Ions." *Journal of Electroanalytical Chemistry* 897 (September):115553. <https://doi.org/10.1016/j.jelechem.2021.115553>.
- Klink, Stefan, Yu Ishige, and Wolfgang Schuhmann. 2017. "Prussian Blue Analogues: A Versatile Framework for Solid-Contact Ion-Selective Electrodes with Tunable Potentials." *ChemElectroChem* 4 (3): 490–94. <https://doi.org/10.1002/celc.201700091>.
- Komaba, Shinichi, Tatsuya Akatsuka, Kohei Ohura, Chihiro Suzuki, Naoaki Yabuuchi, Shintaro Kanazawa, Kazuhiko Tsuchiya, and Taku Hasegawa. 2017. "All-Solid-State Ion-Selective Electrodes with Redox-Active Lithium, Sodium, and Potassium Insertion Materials as the Inner Solid-Contact Layer." *The Analyst* 142 (20): 3857–66. <https://doi.org/10.1039/C7AN01068K>.
- Kupis-Rozmystowicz, Justyna, Michał Wagner, Johan Bobacka, Andrzej Lewenstam, and Jan Migdalski. 2016. "Biomimetic Membranes Based on Molecularly Imprinted Conducting Polymers as a Sensing Element for Determination of Taurine." *Electrochimica Acta* 188 (January):537–44. <https://doi.org/10.1016/j.electacta.2015.12.007>.
- Langton, Matthew J., Christopher J. Serpell, and Paul D. Beer. 2016. "Anion Recognition in Water: Recent Advances from a Supramolecular and Macromolecular Perspective." *Angewandte Chemie International Edition* 55 (6): 1974–87. <https://doi.org/10.1002/anie.201506589>.
- Lauer, Jochen C., Avinash S. Bhat, Chantal Barwig, Nathalie Fritz, Tobias Kirschbaum, Frank Rominger, and Michael Mastalerz. 2022. "[2+3] Amide Cages by Oxidation

- of [2+3] Imine Cages – Revisiting Molecular Hosts for Highly Efficient Nitrate Binding.” *Chemistry – A European Journal* 28 (51). <https://doi.org/10.1002/chem.202201527>.
- Li, Long, Haitao Liu, Jing Tang, Peidong Zhang, and Yi Qian. 2022. “Anchoring H-Bond Donating/Accepting Pyrrolic Derivatives on Preorganized Scaffolds: Conformationally Switchable Bipedal/Tripodal and Locked Molecular Cage Ionophores for Potentiometric Sensing of Phosphate and Fluoride.” *Analytical Chemistry* 94 (40): 13762–69. <https://doi.org/10.1021/acs.analchem.2c02024>.
- Li, Pengjuan, Rongning Liang, Xiaofeng Yang, and Wei Qin. 2018. “Imprinted Nanobead-Based Disposable Screen-Printed Potentiometric Sensor for Highly Sensitive Detection of 2-Naphthoic Acid.” *Materials Letters* 225 (August):138–41. <https://doi.org/10.1016/j.matlet.2018.04.119>.
- Li, Yang, Juanqi Li, Lihong Gao, and Yongqiang Tian. 2018. “Irrigation Has More Influence than Fertilization on Leaching Water Quality and the Potential Environmental Risk in Excessively Fertilized Vegetable Soils.” *PLOS ONE* 13 (9): e0204570. <https://doi.org/10.1371/journal.pone.0204570>.
- Liu, Chenchen, Xiaohui Jiang, Yunyan Zhao, Wenwen Jiang, Zhiming Zhang, and Liangmin Yu. 2017. “A Solid-Contact Pb 2+ - Selective Electrode Based on Electrospun Polyaniline Microfibers Film as Ion-to-Electron Transducer.” *Electrochimica Acta* 231 (March):53–60. <https://doi.org/10.1016/j.electacta.2017.01.162>.
- Liu, Cheng-Wei, Yu Sung, Bo-Ching Chen, and Hung-Yu Lai. 2014. “Effects of Nitrogen Fertilizers on the Growth and Nitrate Content of Lettuce (*Lactuca Sativa* L.)” *International Journal of Environmental Research and Public Health* 11 (4): 4427–40. <https://doi.org/10.3390/ijerph110404427>.
- Liu, Ming, Linda Zhang, Marc A. Little, Venkat Kapil, Michele Ceriotti, Siyuan Yang, Lifeng Ding, et al. 2019. “Barely Porous Organic Cages for Hydrogen Isotope Separation.” *Science* 366 (6465): 613–20. <https://doi.org/10.1126/science.aax7427>.

- Liu, Yueling, Yunzhong Liu, Zhen Meng, Yu Qin, Dechen Jiang, Kai Xi, and Ping Wang. 2020. "Thiol-Functionalized Reduced Graphene Oxide as Self-Assembled Ion-to-Electron Transducer for Durable Solid-Contact Ion-Selective Electrodes." *Talanta* 208 (February):120374. <https://doi.org/10.1016/j.talanta.2019.120374>.
- Liu, Yun, Wei Zhao, Chun-Hsing Chen, and Amar H. Flood. 2019. "Chloride Capture Using a C–H Hydrogen-Bonding Cage." *Science* 365 (6449): 159–61. <https://doi.org/10.1126/science.aaw5145>.
- Lugert-Thom, Elizabeth C., John A. Gladysz, József Rábai, and Philippe Bühlmann. 2018. "Cleaning of PH Selective Electrodes with Ionophore-doped Fluorous Membranes in NaOH Solution at 90 °C." *Electroanalysis* 30 (4): 611–18. <https://doi.org/10.1002/elan.201700228>.
- Luo, Na, Yu-Fei Ao, De-Xian Wang, and Qi-Qiang Wang. 2021a. "Exploiting Anion– π Interactions for Efficient and Selective Catalysis with Chiral Molecular Cages." *Angewandte Chemie International Edition* 60 (38): 20650–55. <https://doi.org/10.1002/anie.202106509>.
- . 2021b. " π -Face Promoted Catalysis in Water: From Electron-deficient Molecular Cages to Single Aromatic Slides." *Chemistry – An Asian Journal* 16 (22): 3599–3603. <https://doi.org/10.1002/asia.202100920>.
- Lv, Enguang, Jiawang Ding, and Wei Qin. 2018. "Potentiometric Aptasensing of Small Molecules Based on Surface Charge Change." *Sensors and Actuators B: Chemical* 259 (April):463–66. <https://doi.org/10.1016/j.snb.2017.12.067>.
- Lyu, Yan, Shiyu Gan, Yu Bao, Lijie Zhong, Jianan Xu, Wei Wang, Zhenbang Liu, Yingming Ma, Guifu Yang, and Li Niu. 2020. "Solid-Contact Ion-Selective Electrodes: Response Mechanisms, Transducer Materials and Wearable Sensors." *Membranes* 10 (6): 128. <https://doi.org/10.3390/membranes10060128>.
- Makra, István, Alexandra Brajnovits, Gyula Jágerszki, Péter Fürjes, and Róbert E. Gyurcsányi. 2017. "Potentiometric Sensing of Nucleic Acids Using Chemically

- Modified Nanopores." *Nanoscale* 9 (2): 739–47.
<https://doi.org/10.1039/C6NR05886H>.
- Mendecki, Lukasz, Nicole Callan, Meghan Ahern, Benjamin Schazmann, and Aleksandar Radu. 2016. "Influence of Ionic Liquids on the Selectivity of Ion Exchange-Based Polymer Membrane Sensing Layers." *Sensors* 16 (7): 1106.
<https://doi.org/10.3390/s16071106>.
- Niedzielski, Przemysław, Iwona Kurzyca, and Jerzy Siepak. 2006. "A New Tool for Inorganic Nitrogen Speciation Study: Simultaneous Determination of Ammonium Ion, Nitrite and Nitrate by Ion Chromatography with Post-Column Ammonium Derivatization by Nessler Reagent and Diode-Array Detection in Rain Water Samples." *Analytica Chimica Acta* 577 (2): 220–24.
<https://doi.org/10.1016/j.aca.2006.06.057>.
- "Noticeboard." 2006. *TrAC Trends in Analytical Chemistry* 25 (11): I.
<https://doi.org/10.1016/j.trac.2006.11.001>.
- Ogawara, Shogo, Jesse L. Carey, Xu U. Zou, and Philippe Bühlmann. 2016. "Donnan Failure of Ion-Selective Electrodes with Hydrophilic High-Capacity Ion-Exchanger Membranes." *ACS Sensors* 1 (1): 95–101.
<https://doi.org/10.1021/acssensors.5b00128>.
- Onder, Ahmet, Cihan Topcu, and Fatih Coldur. 2018. "Construction of a Novel Highly Selective Potentiometric Perchlorate Sensor Based on Neocuproine–Cu(II) Complex Formed in Situ during the Conditioning Period." *Chemija* 29 (1).
<https://doi.org/10.6001/chemija.v29i1.3644>.
- Paczosa-Bator, Beata, Robert Piech, Cecylia Wardak, and Leszek Cabaj. 2018. "Application of Graphene Supporting Platinum Nanoparticles Layer in Electrochemical Sensors with Potentiometric and Voltammetric Detection." *Ionics* 24 (8): 2455–64. <https://doi.org/10.1007/s11581-017-2356-7>.
- Papp, Soma, Gyula Jágerszki, and Róbert E. Gyurcsányi. 2018. "Ion-Selective Electrodes Based on Hydrophilic Ionophore-Modified Nanopores." *Angewandte*

Chemie International Edition 57 (17): 4752–55.
<https://doi.org/10.1002/anie.201800954>.

Paré, Franc, Aida Visús, Gemma Gabriel, and Mireia Baeza. 2023. “Novel Nitrate Ion-Selective Microsensor Fabricated by Means of Direct Ink Writing.” *Chemosensors* 11 (3): 174. <https://doi.org/10.3390/chemosensors11030174>.

Parrilla, Marc, Jordi Ferré, Tomàs Guinovart, and Francisco J. Andrade. 2016. “Wearable Potentiometric Sensors Based on Commercial Carbon Fibres for Monitoring Sodium in Sweat.” *Electroanalysis* 28 (6): 1267–75. <https://doi.org/10.1002/elan.201600070>.

Patel, Amit Kumar, Piyush Sindhu Sharma, and Bhim Bali Prasad. 2008. “Development of a Creatinine Sensor Based on a Molecularly Imprinted Polymer-Modified Sol-Gel Film on Graphite Electrode.” *Electroanalysis* 20 (19): 2102–12. <https://doi.org/10.1002/elan.200804294>.

Pięk, Magdalena, Robert Piech, and Beata Paczosa-Bator. 2016. “All-Solid-State Nitrate Selective Electrode with Graphene/Tetrathiafulvalene Nanocomposite as High Redox and Double Layer Capacitance Solid Contact.” *Electrochimica Acta* 210 (August):407–14. <https://doi.org/10.1016/j.electacta.2016.05.170>.

———. 2018. “TTF-TCNQ Solid Contact Layer in All-Solid-State Ion-Selective Electrodes for Potassium or Nitrate Determination.” *Journal of The Electrochemical Society* 165 (2): B60–65. <https://doi.org/10.1149/2.0161803jes>.

Pietrzak, Karolina, Cecylia Wardak, and Renata Łyszczek. 2020. “Solid Contact Nitrate Ion-selective Electrode Based on Cobalt(II) Complex with 4,7-Diphenyl-1,10-phenanthroline.” *Electroanalysis* 32 (4): 724–31. <https://doi.org/10.1002/elan.201900462>.

Ping, Jianfeng, Yixian Wang, Jian Wu, and Yibin Ying. 2011. “Development of an All-Solid-State Potassium Ion-Selective Electrode Using Graphene as the Solid-Contact Transducer.” *Electrochemistry Communications* 13 (12): 1529–32. <https://doi.org/10.1016/j.elecom.2011.10.018>.

- Pławińska, Żaneta, Agata Michalska, and Krzysztof Maksymiuk. 2016. "Optimization of Capacitance of Conducting Polymer Solid Contact in Ion-Selective Electrodes." *Electrochimica Acta* 187 (January):397–405. <https://doi.org/10.1016/j.electacta.2015.11.050>.
- Priego-López, E, and M.D Luque de Castro. 2004. "Superheated Water Extraction of Linear Alkylbenzene Sulfonates from Sediments with On-Line Preconcentration/Derivatization/Detection." *Analytica Chimica Acta* 511 (2): 249–54. <https://doi.org/10.1016/j.aca.2004.02.005>.
- Qin, Hongmei, Jing Jiang, Xiaoxu Sun, Na Lin, Pengfei Yang, and Yin Chen. 2023. "Anion- π Interaction Powered Perrhenate Recognition and Extraction in Aqueous Media." *Inorganic Chemistry* 62 (16): 6458–66. <https://doi.org/10.1021/acs.inorgchem.3c00471>.
- Sacramento, Ana S., Felismina T.C. Moreira, Joana L. Guerreiro, Ana P. Tavares, and M. Goreti F. Sales. 2017. "Novel Biomimetic Composite Material for Potentiometric Screening of Acetylcholine, a Neurotransmitter in Alzheimer's Disease." *Materials Science and Engineering: C* 79 (October):541–49. <https://doi.org/10.1016/j.msec.2017.05.098>.
- Sadik, Omowunmi A, and Gordon G. Wallace. 1994. "Detection of Electroinactive Ions Using Conducting Polymer Microelectrodes." *Electroanalysis* 6 (10): 860–64. <https://doi.org/10.1002/elan.1140061009>.
- Sakurai, Shunsuke, Hidekazu Nishino, Don N. Futaba, Satoshi Yasuda, Takeo Yamada, Alan Maigne, Yutaka Matsuo, Eiichi Nakamura, Motoo Yumura, and Kenji Hata. 2012. "Role of Subsurface Diffusion and Ostwald Ripening in Catalyst Formation for Single-Walled Carbon Nanotube Forest Growth." *Journal of the American Chemical Society* 134 (4): 2148–53. <https://doi.org/10.1021/ja208706c>.
- Salve, Mary, Khairunnisa Amreen, Prasant Kumar Pattnaik, and Sanket Goel. 2022. "Integrated Microfluidic Device With Carbon-Thread Microelectrodes for Electrochemical DNA Elemental Analysis." *IEEE Transactions on NanoBioscience* 21 (3): 322–29. <https://doi.org/10.1109/TNB.2021.3121659>.

- Santhiago, Murilo, and Lauro T. Kubota. 2013. "A New Approach for Paper-Based Analytical Devices with Electrochemical Detection Based on Graphite Pencil Electrodes." *Sensors and Actuators B: Chemical* 177 (February):224–30. <https://doi.org/10.1016/j.snb.2012.11.002>.
- Schazmann, B., S. Demey, Z. Waqar Ali, M-S. Plissart, E. Brennan, and A. Radu. 2018. "Robust, Bridge-less Ion-selective Electrodes with Significantly Reduced Need for Pre- and Post-application Handling." *Electroanalysis* 30 (4): 740–47. <https://doi.org/10.1002/elan.201700716>.
- Shamsipur, Mojtaba, Mohammad Yousefi, Morteza Hosseini, Mohammad Reza Ganjali, Hashem Sharghi, and Hossein Naeimi. 2001. "A Schiff Base Complex of Zn(II) as a Neutral Carrier for Highly Selective PVC Membrane Sensors for the Sulfate Ion." *Analytical Chemistry* 73 (13): 2869–74. <https://doi.org/10.1021/ac001449d>.
- Shao, Yuzhou, Yibin Ying, and Jianfeng Ping. 2020. "Recent Advances in Solid-Contact Ion-Selective Electrodes: Functional Materials, Transduction Mechanisms, and Development Trends." *Chemical Society Reviews* 49 (13): 4405–65. <https://doi.org/10.1039/C9CS00587K>.
- Song, Qilei, Shan Jiang, Tom Hasell, Ming Liu, Shijing Sun, Anthony K. Cheetham, Easan Sivaniah, and Andrew I. Cooper. 2016. "Porous Organic Cage Thin Films and Molecular-Sieving Membranes." *Advanced Materials* 28 (13): 2629–37. <https://doi.org/10.1002/adma.201505688>.
- Suriyaprakash, Jagadeesh, Lianwei Shan, Neeraj Gupta, Hao Wang, and Lijun Wu. 2022. "Janus 2D-Carbon Nanocomposite-Based Ascorbic Acid Sensing Device: Experimental and Theoretical Approaches." *Composites Part B: Engineering* 245 (October):110233. <https://doi.org/10.1016/j.compositesb.2022.110233>.
- Takahashi, Kosuke, Kensuke Namiki, Takahiro Fujimura, Eun-Beom Jeon, and Hak-Sung Kim. 2015. "Instant Electrode Fabrication on Carbon-Fiber-Reinforced Plastic Structures Using Metal Nano-Ink via Flash Light Sintering for Smart

- Sensing." *Composites Part B: Engineering* 76 (July):167–73.
<https://doi.org/10.1016/j.compositesb.2015.02.012>.
- Telting-Diaz, Martin, and Yu Qin. 2006. "Chapter 18a Potentiometry." In , 625–59.
[https://doi.org/10.1016/S0166-526X\(06\)47027-6](https://doi.org/10.1016/S0166-526X(06)47027-6).
- Thuy, Nguyen Thi Dieu, Xiaochan Wang, Guo Zhao, Tingyu Liang, and Zaihan Zou. 2022. "A Co₃O₄ Nanoparticle-Modified Screen-Printed Electrode Sensor for the Detection of Nitrate Ions in Aquaponic Systems." *Sensors* 22 (24): 9730.
<https://doi.org/10.3390/s22249730>.
- Tian, Ke, Sven M. Elbert, Xin-Yue Hu, Tobias Kirschbaum, Wen-Shan Zhang, Frank Rominger, Rasmus R. Schröder, and Michael Mastalerz. 2022. "Highly Selective Adsorption of Perfluorinated Greenhouse Gases by Porous Organic Cages." *Advanced Materials* 34 (31). <https://doi.org/10.1002/adma.202202290>.
- Toczyłowska-Mamińska, Renata, Monika Kloch, Anna Zawistowska-Deniziak, and Agnieszka Bala. 2016. "Design and Characterization of Novel All-Solid-State Potentiometric Sensor Array Dedicated to Physiological Measurements." *Talanta* 159 (October):7–13. <https://doi.org/10.1016/j.talanta.2016.06.001>.
- Topcu, Cihan, Bulent Caglar, Ahmet Onder, Fatih Coldur, Sema Caglar, Eda Keles Guner, Osman Cubuk, and Ahmet Tabak. 2018. "Structural Characterization of Chitosan-Smectite Nanocomposite and Its Application in the Development of a Novel Potentiometric Monohydrogen Phosphate-Selective Sensor." *Materials Research Bulletin* 98 (February):288–99.
<https://doi.org/10.1016/j.materresbull.2017.09.068>.
- Triroj, Napat, Rattanakorn Saensak, Supanit Porntheeraphat, Boonchoat Paosawatyanong, and Vittaya Amornkitbamrung. 2020. "Diamond-Like Carbon Thin Film Electrodes for Microfluidic Bioelectrochemical Sensing Platforms." *Analytical Chemistry* 92 (5): 3650–57.
<https://doi.org/10.1021/acs.analchem.9b04689>.

- Umezawa, Y., K. Umezawa, and H. Sato. 1995. "Selectivity Coefficients for Ion-Selective Electrodes: Recommended Methods for Reporting $K_{A,B}^{pot}$ Values (Technical Report)." *Pure and Applied Chemistry* 67 (3): 507–18. <https://doi.org/10.1351/pac199567030507>.
- Umezawa, Yoshio, Philippe Bühlmann, Kayoko Umezawa, Koji Tohda, and Shigeru Amemiya. 2000. "Potentiometric Selectivity Coefficients of Ion-Selective Electrodes. Part I. Inorganic Cations (Technical Report)." *Pure and Applied Chemistry* 72 (10): 1851–2082. <https://doi.org/10.1351/pac200072101851>.
- Uria, Naroa, Natalia Abramova, Andrey Bratov, Francesc-Xavier Muñoz-Pascual, and Eva Baldrich. 2016. "Miniaturized Metal Oxide PH Sensors for Bacteria Detection." *Talanta* 147 (January):364–69. <https://doi.org/10.1016/j.talanta.2015.10.011>.
- Volkov, Alexander G., and Vladislav S. Markin. 2002. "Electrochemical Double Layers: Liquid–Liquid Interfaces." In *Encyclopedia of Electrochemistry*. Wiley. <https://doi.org/10.1002/9783527610426.bard010203>.
- Wang, Chan, Longbin Qi, Rongning Liang, and Wei Qin. 2022. "Multifunctional Molecularly Imprinted Receptor-Based Polymeric Membrane Potentiometric Sensor for Sensitive Detection of Bisphenol A." *Analytical Chemistry* 94 (22): 7795–7803. <https://doi.org/10.1021/acs.analchem.1c05444>.
- Wang, De-Xian, and Mei-Xiang Wang. 2020. "Exploring Anion– π Interactions and Their Applications in Supramolecular Chemistry." *Accounts of Chemical Research* 53 (7): 1364–80. <https://doi.org/10.1021/acs.accounts.0c00243>.
- Wang, De-Xian, Qi-Qiang Wang, Yuchun Han, Yilin Wang, Zhi-Tang Huang, and Mei-Xiang Wang. 2010. "Versatile Anion– π Interactions between Halides and a Conformationally Rigid Bis(Tetraoxacalix[2]Arene[2]Triazine) Cage and Their Directing Effect on Molecular Assembly." *Chemistry – A European Journal* 16 (44): 13053–57. <https://doi.org/10.1002/chem.201002307>.

- Wang, Enju, Lin Zhu, Leanne Ma, and Hema Patel. 1997. "Optical Sensors for Sodium, Potassium and Ammonium Ions Based on Lipophilic Fluorescein Anionic Dye and Neutral Carriers." *Analytica Chimica Acta* 357 (1–2): 85–90. [https://doi.org/10.1016/S0003-2670\(97\)00532-1](https://doi.org/10.1016/S0003-2670(97)00532-1).
- Wang, Shuqi, Yongjin Wu, Yang Gu, Tie Li, Hui Luo, Lian-Hui Li, Yuanyuan Bai, et al. 2017. "Wearable Sweatband Sensor Platform Based on Gold Nanodendrite Array as Efficient Solid Contact of Ion-Selective Electrode." *Analytical Chemistry* 89 (19): 10224–31. <https://doi.org/10.1021/acs.analchem.7b01560>.
- Wang, Xue-Yuan, Jun Zhu, Qi-Qiang Wang, Yu-Fei Ao, and De-Xian Wang. 2019. "Anion- π -Directed Self-Assembly between Di- and Trisulfonates and a Rigid Molecular Cage with Three Electron-Deficient V-Clefts." *Inorganic Chemistry* 58 (9): 5980–87. <https://doi.org/10.1021/acs.inorgchem.9b00295>.
- Willner, Marjorie R., and Peter J. Vikesland. 2018. "Nanomaterial Enabled Sensors for Environmental Contaminants." *Journal of Nanobiotechnology* 16 (1): 95. <https://doi.org/10.1186/s12951-018-0419-1>.
- Xie, Han, Tyler J. Finnegan, Vageesha W. Liyana Gunawardana, Radoslav Z. Pavlović, Curtis E. Moore, and Jovica D. Badjić. 2021. "A Hexapodal Capsule for the Recognition of Anions." *Journal of the American Chemical Society* 143 (10): 3874–80. <https://doi.org/10.1021/jacs.0c12329>.
- Xiong, Chuanyin, Tiehu Li, Tingkai Zhao, Alei Dang, Hao Li, Xianglin Ji, Wenbo Jin, Shasha Jiao, Yudong Shang, and Yonggang Zhang. 2017. "Reduced Graphene Oxide-Carbon Nanotube Grown on Carbon Fiber as Binder-Free Electrode for Flexible High-Performance Fiber Supercapacitors." *Composites Part B: Engineering* 116 (May):7–15. <https://doi.org/10.1016/j.compositesb.2017.02.028>.
- Xu, Yun, Wei Huang, Yan Zhang, Hongwei Duan, and Fei Xiao. 2022. "Electrochemical Microfluidic Multiplexed Bioanalysis by a Highly Active Bottlebrush-like Nanocarbon Microelectrode." *Analytical Chemistry* 94 (10): 4463–73. <https://doi.org/10.1021/acs.analchem.1c05544>.

- Yin, Tanji, Jinghui Li, and Wei Qin. 2017. "An All-solid-state Polymeric Membrane Ca²⁺-selective Electrode Based on Hydrophobic Alkyl-chain-functionalized Graphene Oxide." *Electroanalysis* 29 (3): 821–27. <https://doi.org/10.1002/elan.201600383>.
- Zdrachek, Elena, and Eric Bakker. 2019. "Potentiometric Sensing." *Analytical Chemistry* 91 (1): 2–26. <https://doi.org/10.1021/acs.analchem.8b04681>.
- Zeng, Xianzhong, and Wei Qin. 2017. "A Solid-Contact Potassium-Selective Electrode with MoO₂ Microspheres as Ion-to-Electron Transducer." *Analytica Chimica Acta* 982 (August):72–77. <https://doi.org/10.1016/j.aca.2017.05.032>.
- Zhang, Huan, Ruiqing Yao, Ning Wang, Rongning Liang, and Wei Qin. 2018. "Soluble Molecularly Imprinted Polymer-Based Potentiometric Sensor for Determination of Bisphenol AF." *Analytical Chemistry* 90 (1): 657–62. <https://doi.org/10.1021/acs.analchem.7b03432>.
- Zhang, Lei, Zhengying Wei, and Pengcheng Liu. 2020. "An All-Solid-State NO₃- Ion-Selective Electrode with Gold Nanoparticles Solid Contact Layer and Molecularly Imprinted Polymer Membrane." *PLOS ONE* 15 (10): e0240173. <https://doi.org/10.1371/journal.pone.0240173>.
- Zhang, Yan, Jian Xiao, Yimin Sun, Lu Wang, Xulin Dong, Jinghua Ren, Wenshan He, and Fei Xiao. 2018. "Flexible Nanohybrid Microelectrode Based on Carbon Fiber Wrapped by Gold Nanoparticles Decorated Nitrogen Doped Carbon Nanotube Arrays: In Situ Electrochemical Detection in Live Cancer Cells." *Biosensors and Bioelectronics* 100 (February):453–61. <https://doi.org/10.1016/j.bios.2017.09.038>.
- Zhao, Anshun, Tao Lin, Yun Xu, Weiguo Zhang, Muhammad Asif, Yimin Sun, and Fei Xiao. 2022. "Integrated Electrochemical Microfluidic Sensor with Hierarchically Porous Nanoarrays Modified Graphene Fiber Microelectrode for Bioassay." *Biosensors and Bioelectronics* 205 (June):114095. <https://doi.org/10.1016/j.bios.2022.114095>.

- Zhao, Changzhi, Yi Meng, Changli Shao, Li Wan, and Kui Jiao. 2008. "Unadulterated Glucose Biosensor Based on Direct Electron Transfer of Glucose Oxidase Encapsulated Chitosan Modified Glassy Carbon Electrode." *Electroanalysis* 20 (5): 520–26. <https://doi.org/10.1002/elan.200704086>.
- Zhuo, Kelei, Xueli Ma, Yujuan Chen, Congyue Wang, Aoqi Li, and Changling Yan. 2016. "Molecularly Imprinted Polymer Based Potentiometric Sensor for the Determination of 1-Hexyl-3-Methylimidazolium Cation in Aqueous Solution." *Ionics* 22 (10): 1947–55. <https://doi.org/10.1007/s11581-016-1708-z>.
- Zuo, Yuegang, Chengjun Wang, and Thuan Van. 2006. "Simultaneous Determination of Nitrite and Nitrate in Dew, Rain, Snow and Lake Water Samples by Ion-Pair High-Performance Liquid Chromatography." *Talanta* 70 (2): 281–85. <https://doi.org/10.1016/j.talanta.2006.02.034>.

VITA

EDUCATION

Ph.D. in Chemistry, Izmir Institute of Technology (2024)

M.Sc. in Chemistry, Erzincan University (2016)

B.Sc. in Chemistry, Nevşehir University (2013)

PUBLICATIONS

1. Önder, Ahmet. (2016) *Neokuproin temelli perklorat-seçici potansiyometrik PVC membran sensör*. MS thesis. Fen Bilimleri Enstitüsü.
2. Çoldur, Fatih, Hakan Boz, and Ahmet Önder. "Bütünüyle katı hal PVC membran izoniazid-seçici potansiyometrik sensör." *Erzincan University Journal of Science and Technology* 9.1 (2015): 29-39.
3. Çoldur, Fatih, Müberra Andaç, and Ahmet Önder. "Metiltrioktilamonyum Klorür Temelli Potansiyometrik Perklorat-Seçici PVC-Membran Sensör." *Erciyes Üniversitesi Fen Bilimleri Enstitüsü Fen Bilimleri Dergisi* 33.1 (2017): 1-9.
4. Topcu, C., Caglar, B., Onder, A., Coldur, F., Caglar, S., Guner, E. K., & Tabak, A. (2018). Structural characterization of chitosan-smectite nanocomposite and its application in the development of a novel potentiometric monohydrogen phosphate-selective sensor. *Materials Research Bulletin*, 98, 288-299.
5. Onder, Ahmet, Cihan Topcu, and Fatih Coldur. "Construction of a novel highly selective potentiometric perchlorate sensor based on neocuproine–Cu (II) complex formed in situ during the conditioning period." *Chemija* 29.1 (2018).
6. Yeasmin, S., Ammanath, G., Onder, A., Yan, E., Yildiz, U. H., Palaniappan, A., & Liedberg, B. (2022). Current trends and challenges in point-of-care urinalysis of biomarkers in trace amounts. *TrAC Trends in Analytical Chemistry*, 157, 116786.